BMC Genomics

https://doi.org/10.1186/s12864-026-12823-7

Article in Press

New approaches to discovering epigenetic rules of homeostasis in diverse mammal species

Received: 25 January 2026

Accepted: 31 March 2026

Published online: 10 April 2026

Cite this article as: Gonzalez J., Genereux D.P., Crouse K. *et al.* New approaches to discovering epigenetic rules of homeostasis in diverse mammal species. *BMC Genomics* (2026). https://doi.org/10.1186/s12864-026-12823-7

Jorge Gonzalez, Diane P. Genereux, Kristin Crouse, Bradley Frishman, Allyson G. Hindle, Elinor Karlsson, Carla B. Madelaire, Lucas Moreira & Valery Forbes

New approaches to discovering epigenetic rules of homeostasis in diverse mammal species

Jorge Gonzalez (corresponding author) * Diane P. Genereux † Kristin Crouse ‡
Bradley Frishman § Allyson Hindle ¶
Elinor Karlsson ‖ Carla Madelaire ** Lucas Moreira †† Valery Forbes ‡‡

Abstract

Background: While the cells of some mammals, such as humans, maintain their internal temperature within tightly controlled ranges, the cells of others, such as dromedary camels, experience wide ranges of temperature variation. In order to understand these differences, it is critical to identify differentially expressed genes (DEGs) and their interactions; however, the data available are often insufficient to obtain statistically significant results.

Results: We develop an explanatory model to understand the mechanisms of response of mammalian species to environmental perturbation on the basis of empirical gene expression data. Our approach is motivated by the novel idea that approximately *preserved or reduced inter-individual variability* of expression levels upon environmental change is an indicator that a given gene contributes to a homeostasis-preserving mechanism for the species. To identify such genes, we use a simple non-statistical criterion that is suitable even when the number of replicates is limited. We then identify four extreme subgroups of the DEGs, and from these construct an intuitive neural network architecture that *best* interpolates the data and describes the principal response rules of the considered species. Finally, we propose measures of the robustness of homeostasis (*well-being*) from these networks based on perturbation analysis and entropy computations. The data used to develop the model were collected from homogeneous cell cultures of skin fibroblasts.

Conclusions: Even with data available for just a few individuals, our model identifies extreme response sets of genes, using inter-individual variability to provide a faithful representation of the response of the species to environmental perturbations. Sets of genes identified as relevant in individual species are useful for comparing responses across species. All the measures of cellular well-being introduced in this work rank camels higher than humans for both the 32° and 41° treatments.

Keywords: inter-individual variability of genes, differential expression, stress response model

1 Background

A central goal of genomics is to identify genes differentially expressed between tissues or treatment conditions. Most existing approaches, such as those implemented by De Anoy et al 2024 ([7]) and Huang et al. 2019 ([10]), achieve this by calculating mean fold change—the ratio of

*Florida Atlantic University, Embry-Riddle Aeronautical University, gonzj211@erau.edu
†Broad Institute, genereux@broadinstitute.org
‡University of Minnesota, crou0048@umn.edu
§University of Florida, frishmanbradley@ufl.edu
¶University of Nevada, allyson.hindle@unlv.edu
‖Broad Institute, elinor@broadinstitute.org
**San Diego Zoo Wildlife Alliance, carlamadelaire@gmail.com
††Broad Institute, Colossal Biosciences, lucas@colossal.com
‡‡Florida Atlantic University, veforbes@fau.edu

gene expression values between two states for each of several biological replicates— and then asking whether the change observed for a given gene is larger than expected under the null assumption that the expression level for that gene does not differ between the two conditions.

While such statistical approaches can be highly effective for identifying genes whose expression levels differ between cell types or are altered in disease states ([13]), they may be less powerful for identifying genes whose expression changes are essential to a species' response to environmental change. Consider, for example, a case in which three individuals of the same species have expression levels for a given gene that differ greatly under baseline conditions but are nearly identical under some biological stressor. The change in expression of this gene might well meet the threshold for detecting a statistically significant difference between the two conditions. However, methods focused on the magnitude of change could fail to capture an even more impressive feature of the data: the shift from high to minimal variation among individuals under the altered conditions.

We argue that the extent of change in expression variance among individuals has large—and underutilized—power for identifying genes essential to a species' response to environmental change. The underlying premise is rooted in evolution: if, for a given species, some level of expression of a given gene is essential for survival under a given environmental condition, then purifying selection should tend to reduce its variation among individuals.

Here, we develop a new mathematical approach that uses changes in expression variance, rather than changes in expression magnitude, to identify genes that are essential to how a species responds to environmental change. Our approach can distinguish, for example, genes for which inter-individual variability is small both before and after the treatment, suggesting essentiality under both conditions, from genes that have relatively large inter-individual variability before treatment but small inter-individual variability after treatment, suggesting that their expression level is essential specifically , and perhaps exclusively, under the altered conditions. We can also identify genes that have small inter-individual variability before the treatment and very large inter-individual variability after treatment, possibly indicating cellular stress and a breakdown in cellular function. Finally, we identify genes that have relatively large inter-individual variability both before and after treatment, but that are also *very-well-regulated* suggesting that they may be involved in individual-specific responses to the treatment. Another possibility is that these genes are related to the so called house-keeping genes [22].

Our approach was developed from transcriptome data collected from cultured fibroblasts in five mammalian species exposed to increased or decreased temperature.Central to our approach is the biological concept of homeostasis, which describes the state of the internal dynamics of a biological entity changing in such a way that its function remains stable. Our variance-focused approach for classifying DEGs according to their response to environmental perturbations is focused on addressing a fundamental biological question: What are the genome-response mechanisms responsible for maintaining homeostasis in cells exposed to environmental change? We broadly refer to these mechanisms as the rules of homeostasis.

We first develop a robust criterion for identifying differentially expressed genes (DEGs) that does not rely on statistical significance tests. Our DEGs are selected based on a simple inequality in terms of the inter-individual variability at baseline. Then, from all DEGs, we define four groups of *extreme response genes* taking into account their inter-individual variability after treatment. This second filter ensures that we are modeling the genes responsible for the characteristic response of the species.

The rules of homeostasis are modeled using neural networks that capture the interactions among the most important genes. These networks are required to satisfy conditions to optimize their reliability as biological models. We use the neural networks to model the species response to a change in temperature, however, the method is general and can be applied to any perturbation of a stable system whose dynamics are unknown.

In what follows, we develop a definition of cellular homeostasis that is based on gene transcription dynamics. The underlying assumption is that differential gene expression is the direct result of a regulatory response. Specifically, upon environmental change, the "activity level" of the genes related to a response mechanism will change in a quantitatively measurable manner that can be detected numerically (See [15] for recent work on analyzing gene expression). We assume the cell is at homeostasis if the transcript dynamics are constrained to an attracting set, meaning that a "small" perturbation will cause the system to return to the previous state after some time. This assumption also reflects the stability over long periods of time in the absence of abrupt perturbations.

In Section 2.6 we describe the architecture of the model, which reduces the number of possible models to a finite number. This is important in order to validate the model with experimental data. In Section 2.7 we propose a method to rank the activity of the genes, which is then used to define the DEGs. The fundamental idea that a species mechanism should not significantly increase inter-individual variability in transcript counts is also introduced in this section as Proposition 2.4. Our definition of *very-well-regulated* genes is extended to a metric of cellular well-being. In (Section 3.2) we explore which *very-well-regulated* genes are common to all five of the studied species. We are particularly interested in two distinct *very-well-regulated* DEG groups; those for which the inter-individual variabilities are comparable before and after treatment, and those for which the inter-individual variability after treatment is considerably smaller than before treatment. We introduce four unique *extreme response sets* according to their inter-individual variability before and after treatment. Of these four subsets, the *Support* set of genes, defined as those DEGs that are *very-well-regulated* but have large inter-individual variability before and after treatment, contain the least amount of information about the species response; while the *Noisy* set of genes - those having low inter-individual variability before treatment, but high variability after - reflect a decline in cell well-being. In Section 2.9 we introduce a measure of well-being after treatment that is based upon the entropy in the system and suitable for comparison across species. In Section 2.10 we discuss the network model in more detail, and in Section 2.11 we present the predictions and errors for the network models. Finally, in Section 2.12 we compute a measure of the strength of the interactions among the genes in the model, which can be used to validate our approach. In section 3.6 we provide a brief comparison of our model using the extreme response genes with a network constructed using the same script but based on DEGs identified by the commonly used limma software [16]. We also provide enrichment analysis using the publicly available database https://string-db.org/ and https://www.proteinatlas.org/.

2 Methods

2.1 Cell Culture and Experimental Treatment

Dermal fibroblasts were established from skin biopsies as previously described (Madelaire et al. 2022) from 13-lined ground squirrel (Ictidomys tridecemlineatus, “squirrel”), Sprague Dawley rat (Rattus norvegicus, “rat”) and little brown bat (Myotis lucifugus, “bat”) under IACUC and biosafety authorizations from the University of Nevada Las Vegas. Cells from dromedary camel (Camelus dromedarius, “camel”) and southern white rhinoceros (Ceratotherium simum simum, “rhino”) were provided under MTA from the San Diego Frozen Zoo. Human fibroblasts were acquired from Lifeline Cell Technology.

Cells were proliferated under baseline conditions (37°C, 5% CO2) in a humidified incubator to establish a common garden framework. We exposed fibroblasts from n=5 individuals per species to either baseline (37°C), a high temperature stressor (41°C) or a low temperature stressor (32°C).

2.2 Cell Culture and Experimental Treatment

Following 24h exposure at each culture condition, cells were washed twice in ice-cold PBS, and RNA was extracted using a Trizol-chloroform protocol. Prior to sequencing, RNA was treated to eliminate any genomic DNA contamination and other impurities using a column-based method (Zymo RNA Clean & Concentrator-5). Samples were sent Azenta Biosciences for 150bp paired-end sequencing of polyA-enriched libraries, yielding an average of 20 million reads per sample.

2.3 Transcript alignment and quantification

Paired-end raw RNA-seq reads for each sample were inspected for quality using FastQC [18], trimmed for Illumina adapters using Trimmomatic [3], and aligned to their respective reference genomes assembly (NCBI Accessions: *Camelus dromedarius*: GCF000803125.2; *Ceratotherium simum*: GCF021442165.1; *Ictidomys tridecemlineatus*: GCF016881025.1; *Rattus norvegicus*: GCF015227675.2; *Homo sapiens*: GCA000001405) using the splicing-aware aligner HiSat2 [11] . We used [14] to identify transcript abundances were quantified for the set of one-to-one orthologs across all study species, identified using TOGA's 488 placental mammals alignment [12].

2.4 RNA-seq preprocessing

Our analysis uses the limma-voom framework, which explicitly models the mean–variance trend in log2-CPM data via LOESS smoothing and assigns precision weights to each observation accordingly (Law et al., 2014). These precision weights correct for mean-expression dependence prior to downstream analyses, yielding weighted residuals that are mean-variance stabilized. Therefore, the variability estimates derived from our voom-weighted analysis are not likely confounded by mean expression level.

2.5 Conceptual Framework

Our aim is to identify the cellular response of a species to an environmental perturbation from information on a few individuals. To do this, we first identify an equivalence relationship for the individuals' DEGs. Once an equivalence relationship is established we can construct the mechanism of response of the species as a map on the equivalence classes (the equivalence class containing a denoted by $[a]$ is defined as the collection of all individuals related to individual a, i.e $[a] := \{x : x \sim a\}$).

We propose as an adequate notion of equivalence relation for a species, at a given condition, that of membership to the same *minimal attractor*. Recall that each individual is represented as a list of RNA counts that changes in time. This concept is borrowed from dynamical systems theory. A minimal attractor is an attractor in which every trajectory is dense (any orbit eventually visits any state in the attractor). This is natural notion in this case because any member of the attractor gives an equally good representation of the minimal attractor (the equivalence class); and we precisely want individuals to be indistinguishable in our model.

Previous epigenetic modeling attempts assume that gene regulation follows a stochastic process that converges toward a single value (Ornstein-Uhlenbeck) ([15]). Recent work by Yang and collaborators used gene knockout (KO) experiments to infer the function of genes. Their mathematical model uses a neural network with one hidden layer subject to a rectilin- ear activation function (ReLu) ([20]). The DEGs were selected using the Scanpy software. These authors found that different methods with varying model assumptions and thresholds could not converge to a consensus set of DEGs. For this reason, as well as the limited amount of data available for individuals in our study, we develop a robust criterion for selecting DEGs that does not rely on statistical methods.

We assume that the gene transcript counts are subject to deterministic processes in the presence of internal and external noise. We do not formally characterize the type of noise in this paper. It is enough for us to note that the presence of noise results in a random deviation from a deterministic behavior. By the level of noise we refer to the magnitude of this deviation. The level of noise expressed in the system as related to the species mechanism can be detected from the genes acting inconsistently among individuals of the same species. We will denote the solutions of this model by $\mathcal{N}(T, t; N_0)$ (gene transcript state), where T is a set of parameters (temperature, oxygen level, glucose level, etc), t is the time variable, and $N_0 = \mathcal{N}(T, 0; N_0)$ is the initial condition of the stochastic differential equation characterizing the gene counts. The parameters at baseline and those after treatment are denoted by T_0 and T_1 respectively.

Definition 2.1. *An individual is at* ***homeostasis*** *under parameters T if its gene transcript counts are different from 0 and would remain constrained to a bounded region in transcript space for all times in the absence of external stress.*

We will denote by J_0 and J_1 the set of all states at homeostasis at baseline and after treatment, respectively. The following maps will help us frame the response to the treatment:

$$D_0 = \mathcal{N}(T_0, 1; J_0) \tag{1}$$
$$D_1 = \mathcal{N}(T_1, 1; J_1) \tag{2}$$
$$f = \mathcal{N}(T_1, 1; J_0) \tag{3}$$

D_0 describes the one time change in transcript amounts for all genes at baseline conditions restricted to homeostasis states; similarly D_1 denotes the one time change in transcript amounts for all genes after treatment, again restricted to homeostasis states. The map f denotes the transition from homeostasis at T_0 to homeostasis at T_1 after one unit of time. Hence we have $D_0(J_0) = J_0$ and $D_1(J_1) = J_1$. We do not assume that $f(J_0) = J_1$ but only that $f(J_0) \supseteq J_1$, meaning that not all homeostasis states at baseline necessarily reach homeostasis after treatment. In terms of probability distributions, if ${n_1}^0, ..., {n_N}^0$ denotes the distributions of counts for gene 1 through N at baseline for an individual at homeostasis, then:

$$D_0({n_1}^0, ..., {n_N}^0) = ({n_1}^0, ..., {n_N}^0);$$

similarly, if ${n_1}^1, ..., {n_N}^1$ denotes the distribution of the counts after treatment and the organism reaches a new homeostasis then:

$$D_1({n_1}^1, ..., {n_N}^1) = ({n_1}^1, ..., {n_N}^1).$$

The distributions of the transcript counts are fixed at homeostasis by the corresponding maps D_0 and D_1 i.e changes in these distributions are correlated to changes in gene expression which are correlated to changes in the environment); in accordance with the assumption that differential gene expression follows from regulating responses [15]. Since homeostasis depends on the environment, we would have a different homeostasis state (or none) for significantly different external conditions. Thus, we expect the distribution of transcript counts at a baseline temperature of 37°C to be different from the distribution in the 41°C treatment.

We assume that a system at homeostasis is able to return to the same state if the perturbation is of moderate magnitude. This means that there is a *domain of attraction* associated with a homeostasis state. We also assume that $I_0 \subseteq J_0$ and $I_1 \subseteq J_1$ are *good* approximations of the corresponding attractor. The rules of homeostasis are hence encoded by f and our main goal is to approximate and validate our computations.

The conceptual framework is shown in Figure 1 where the aim is to compute a transition map f that takes as input the transcript counts of the responding genes at baseline to the transcript counts after the treatment as output. We require that the function f not only interpolates the data collected, but also that it maps the intervals containing the transcript counts at baseline (I_0) to those after treatment (I_1) (i.e $f(I_0) = I_1$). This condition treats those intervals as a first pass approximation of J_0 and J_1 respectively; however, it is possible that some states (i.e., transcript counts) contained within the intervals are not actually in the attractor (i.e., not biologically realizable). In other words, the structure of the attractors in the state space could be very complicated. In practice the image of the intervals is computed by first partitioning all gene intervals into $\mathcal{K}$ (the number of individuals in the data) sub-intervals centered at each individual counts (except for the minimum and the maximum), then computing the image for each of these sub-intervals and finally taking their union. This method mitigates the wrapping effect which is unavoidable when working with interval arithmetic, and it is easily updated to more accurately cover the attractor. As mentioned above, it is very likely that some count profiles within the intervals are in fact not realizable at homeostasis. For example, an individual with all gene counts equal to the minimum of the intervals may not be at homeostasis. A more accurate cover of the attractor may include gaps in the product of the intervals.

The consequences of the assumptions above are represented in Figure 1. First $D_0(I_0)$ is close to I_0 since I_0 is a good approximation of J_0. It follows that $f \circ D_0(I_0)$ is also close to J_1. On the other hand, $D_1(I_1)$ is also close to J_1 which ultimately implies that $f \circ D_0(I_0) \approx D_1 \circ f(I_0)$. Here $f \circ g(x)$ denotes the composition function f of $g(x)$, $f(g(x))$ for any two functions f and g. This relation is important because it validates our assumption that the D_1 dynamics can be written as a perturbation of the D_0 dynamics, and it clarifies the role of the transition map f. In other words we can represent D_1 as:

$$D_1 = f \circ D_0 \circ f^{-1} + \epsilon g, \tag{4}$$

where ϵ is a parameter and g is a perturbation map. For small values of ϵ we expect many stable orbits at baseline to correspond to stable orbits after treatment; however, some may break down. This situation is typical in other applications, such as problems in Celestial Mechanics [5, 4].

The schematic can be made more precise by restricting f to a family of functions and assuming specific bounds on the size of I_0 and I_1 relative to their corresponding attractors.

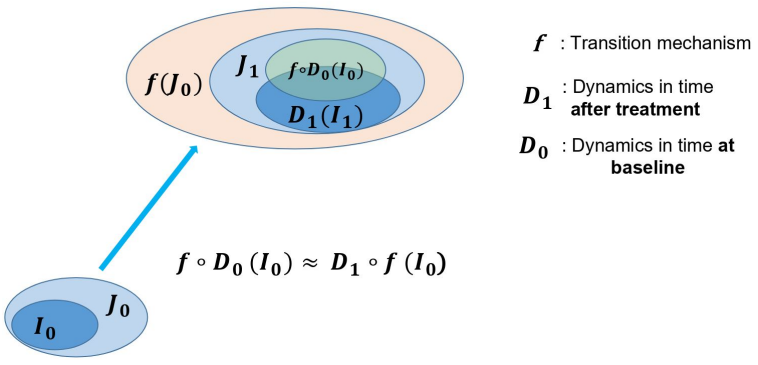

Figure 1: Diagram depicting the relation between the dynamics before and the dynamics after treatment. I_0 denotes the transcript counts for all individuals at baseline, J_0 is the set of homeostasis states, D_0 and D_1 are the homeostasis dynamics at the corresponding condition defined in (1) and f is the transition map also defined in (1).

2.6 The model

We will construct f as a neural network

$$f_{W_1,b_1,W_2,b_2}(x) = W_2 * (\sigma(W_1 * x + b_1)) + b_2 : \mathbb{R}^N \to \mathbb{R}, \tag{5}$$

where W_1 is an $N \times N$ real matrix, b_1 is a real N vector, W_2 is a $1 \times N$ real matrix, b_2 is a real number, and finally σ is a piece-wise linear function. In this format, the network has an intuitive biological interpretation; for example the weights W_1 and W_2 can be thought of as encoding the interactions among the genes (gene pathways), and the b_1 and b_2 biases are additional parameters affecting the pathways. See Figure 4 for a schematic representation.

One constraint of our study is that we only have data for 5 individuals per species, whereas the gene interactions for each species are complex, involving potentially several thousand genes. Nevertheless, it is feasible to compute networks that interpolate a given data point as it is well known by the universal approximation theorem ([6]) and due to readily available computational power and software. However, we are not merely interested in predicting epigenetic counts after a stress; our main goal is to shed light on the underlying biological mechanisms. It is then necessary to distinguish among a large number of possible networks the ones that indeed best capture the rules of homeostasis for each species.

Following the diagram in Figure 1, we require that f maps the N-ple of intervals of the available data for each gene before treatment (or best known **cover of the attractor containing the data**) to the interval containing the data of the considered gene after treatment (or best known **cover of the attractor containing the data**). We assume that the probability of sampling an individual of the species with gene counts outside of the collected interval is not large.

Under these assumptions and a few additional technical constraints, we compute a network that interpolates the data points and sends the intervals at baseline to good approximations of the intervals after treatment. We can not ensure that the network map is unique but with a fixed network topology we can at least reduce the search to a finite number of networks. To reiterate, we focus on obtaining coarse rules at the level of intervals for the species.

2.7 Differentially expressed genes (DEGs)

We exclude from our model genes that do not *considerably* respond to the treatment and focus only on modeling the most relevant genes for the treatment response. We will not rely on statistical tests to find these genes as mentioned in the Introduction.

In accordance with our goals of modeling *species rules*, two natural sets of genes to consider are the set of genes for which all individuals respond in the same direction (increase/decrease) after treatment with respect to a chosen tolerance.

This criterion is not convenient in the presence of noisy and limited data. For this reason we adopt a slightly different ranking to capture the DEGs which is more viable than the above when working with intervals. First we consider a measure of activity with respect to the treatment. We denote by $\mathcal{K}$ the total number of individuals available (in this case $\mathcal{K} = 5$). If $x_i^{(k)}$ represents the count for the ith gene for the kth individual at baseline and $y_i^{(k)}$ the count for the ith gene for the kth individual after treatment, then we define the **activity** of the ith gene denoted by α_i as:

$$\alpha_i := \sum_{k=1}^{\mathcal{K}} |x_i^{(k)} - y_i^{(k)}|. \tag{6}$$

More generally α_i could be defined in terms of a distance in $\mathbb{R}^{\mathcal{K}}$.

We rank the genes according to the following ratio:

$$r_i^0 := \frac{\alpha_i}{\Delta(N_i^0) + \epsilon}, \tag{7}$$

where $N_i{}^0$ is the approximation of the attractor containing the counts for the ith gene at baseline; respectively, $N_i{}^1$ is the approximation of the attractor containing the counts after treatment, and ϵ is a small tolerance number to avoid dividing by 0. The notation $\Delta(S)$ stands for the **diameter** of S. When S is just one interval containing the data, then $\Delta(S)$ is simply the length of the interval (or the inter-individual variability).

Definition 2.2. *The ith gene is considered to be a differentially expressed gene (DEG) if:*

$$\frac{1}{\mathcal{K}}(r_i^0 + r_i^1) > 2,$$

i.e, a gene is active only if its activity norm (α_i) is greater than the maximum net change that can be attributed to the inter-individual variabilities. Notice that this definition is symmetric.

Remark 2.3. *In this paper we used the simplified condition:*

$$\frac{r_i^0}{\mathcal{K}} > 1,$$

i.e, the activity is greater than the maximum activity that can be attributed to just the baseline inter-individual variability ($\Delta(N_i^0)$), i.e the gene average absolute response is greater than the inter-individual variability at baseline. We also discarded extreme values from the numerator and the denominator to safeguard the computations from typos in the data. Assuming that $X_i \sim Y_i$ (the distributions of $x_i^{(k)}$ and $y_i^{(k)}$ respectively we have results like:

- *Normal marginals:*
$$P(R > 2) \leq \exp(-c\,\mathcal{K}\log\mathcal{K}).$$
- *Log-normal marginals:*
$$P(R > 2) \sim \frac{1}{2\sigma^2\sqrt{\pi\log\mathcal{K}}}.$$
- *Regularly varying heavy tails with index $\alpha \in (0,1)$:*
$$P(R > 2) \asymp \mathcal{K}^{-\alpha}.$$
where $R := \frac{1}{\mathcal{K}}(r_i^0 + r_i^1)$ as in Definition 2.2

These results estimate the probability of a type I error. See the Tables in Section 7.1 in the SI. In particular, assuming the normal distributions leads to super exponential convergence to 0 w.r.t. $\mathcal{K}$.

On the other hand, for $X_i \sim N(0,1)$ and $Y_i = X_i + \epsilon Z_i$ where $\mathbb{E}|Z| < \infty$, and assuming that the range distributions of X_i does not dominate that of Y_i, then $1 - P(R > 2) = P(R \leq 2) \leq C_2\exp(-C_1\mathcal{K}^{2\beta})$. For some constants C_2 and C_1 when $\epsilon = \mathcal{K}^\beta$ with $\beta > 1$. i.e the convergence rate to 1 is super-exponential.

For Z_i regularly varying with unbounded expectation we have: $1-P(R > 2) \asymp \frac{(\log\mathcal{K})^{\alpha/2}}{\varepsilon^\alpha}\mathcal{K}^{-(1-\alpha)}$. These results help of understand the power of the DEG selection. See the Tables in Section 7.1 in the SI for informative Monte-Carlo simulations of the power.

The most common methods for selecting DEGs involve some type of statistical test. For example, the moderated t-statistic compares the groups' geometric means [21]:

$$\frac{n_1^{-1}\sum_j \log(x_{1j}) - n_2^{-1}\sum_j \log(x_{2j})}{s + s_0}.$$

Another popular tool is the limma package in the programming language R which first fits a linear model before running statistical tests [16]. For other applications of statistical methods

for determining DEGs see [1], [17]. Also see [13] for a comparative review of the statistical tools for finding DEGs. From now on the term DEG will refer exclusively to those genes obtained by definition 2.2.

We are also interested in those genes that do not increase inter-individual variability after treatment, with the rationale that genes (indexed by i) taking part in a mechanism present in the entire species should not have a large inter-individual variability ratio:

$$\frac{\Delta(N_i{}^1)}{\Delta(N_i{}^0)}. \tag{8}$$

An increase in variability for the species is associated with low reliability/low predictability/chaotic behavior. This assumption leads to a proposition that can be tested:

Proposition 2.4. *A species is resilient to an environmental perturbation if* ***most*** *DEGs have an inter-individual variability ratio that does not exceed 1* ***considerably****.*

Another way to express the proposition is to say that the number of genes for which the inter-individual variability ratio is badly preserved (noisy genes) is inversely related to how well the species as a whole responds to the environmental change. Proposition 2.4 as stated does not take into account the potential influence of noisy genes on the rest of the responding network, meaning that it will not be suitable for comparing the response to treatments on different network topologies. However, it could be useful to compare the response to different treatments in a given species. Specifically, we can validate it with species that are known to be more or less adapted to specific environments.

For example squirrels and bats which hibernate are considered to be better adapted to low temperature than to high temperature. One difficulty of applying Proposition 2.4 is to quantify the notion of "most genes". It is possible that some genes may have exceptionally high ratios, while the species itself is overall well adapted to the treatment. In other words, we do not know apriori what is a safe ratio for a given species.

Below (Figure 2) we present quantiles for the distribution of the ratios for squirrels and bats for the 32°C and 41°C treatments. The D and W reported in the boxplots refer to the Kolmogorov-Smirnov and Wilcoxon statistics (Mann-Whiteney U test) respectively. These are two widely used nonparametric tests to compare the distributions. We present the median and the 95% percentile of the log distributions of the ratios in order to establish the center and tail of the distributions respectively.

	Squirrels		Bats	
Temperature	50%	95%	50%	95%
32°	0.63	3.16	0.57	2.12
41°	0.68	3.58	0.49	2.35

Table 1: Log quantiles for the 32°C and 41°C treatments for all DEGs according to (7) for squirrels and bats. The upper quantiles provide bounds for the ratios of the inter-individual variability of the DEGs.

For squirrels, both the median and the 95th percentile for the 32°C treatment are smaller than for the 41°C treatment. Specifically, 95% of all DEGs at 32°C have a log ratio less than 3.16, while at 41°C, 95% of all DEGs have a ratio less than 3.58. This means that the tail of the former distribution is more shifted to the left than that of the latter distribution, suggesting that inter-individual variability is better preserved at the 32°C than the 41°C treatment. However, neither the Kolmogorov-Smirnov nor the Wilcoxon statistic is significant with respect to the

0.05 p-value standard. In the following sections we develop methods to compare the well-being of the species after treatment that do not rely on statistics.

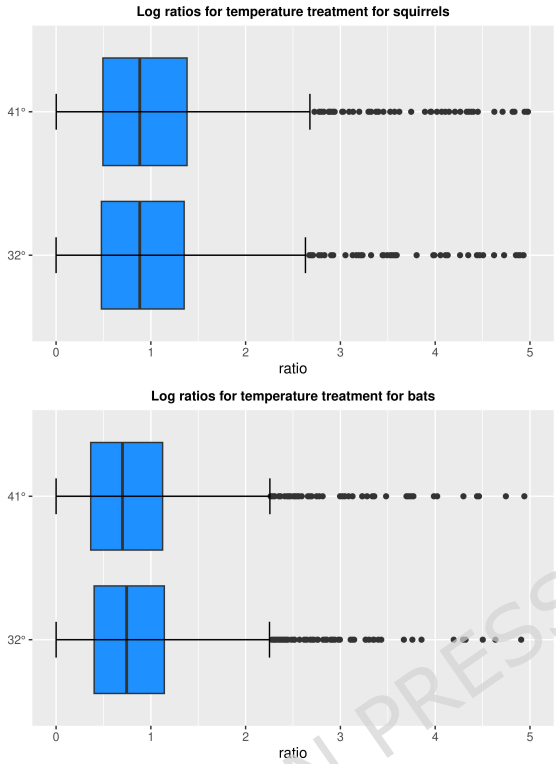

Figure 2: Top: Boxplots of log ratios of inter-individual variability before and after treatment for squirrels under the 32°C and 41°C treatments for all DEGs.
D = 0.0359, p-value = 0.19
W = 1612397, p-value = 0.056
Bottom: Boxplots of log ratios of inter-individual variability before and after treatment for bats under the 32° and 41° treatments for all DEGs.
D = 0.0492, p-value = 0.002
W = 4284104, p-value = 0.0054

The situation with bats is slightly different. In this case, the 50th percentile of the ratios is lower for the 41°C treatment, but the 95th percentile of the ratios is lower for the 32° treatment. We also show the computations for camels, humans, rats and rhinos in the SI, Section 7.

2.8 Extreme response genes: Genes modeling the primary cellular response

An important development of this paper is the identification of the extreme response genes in terms of inter-individual variability. In order to motivate the definition of these subsets of the DEGs we should mention that we are assuming that *the distributions of inter-individual variability for all DEGs genes with respect to a treatment at baseline and after-treatment, as well as the distributions of the inter-individual variability ratios are right skewed*. This assumption is motivated by the fact that these distributions refer to a single species, meaning that gene regulation for individuals will be similar and so the inter-individual variability will tend to be small rather than large. Also, all the individuals are able to reach homeostasis after treatment, so we expect that the ratio of inter-individual variability is maintained or reduced for most genes with the possible exception of a group of genes for which the response is noisy.

Given the right skewness assumption of the distributions, a suitable notion of small is "before the peak of the distributions"; however, due to the lack of a distinctive universal landmark for "large" in the distributions, we considered the 50th, 60th, 70th, 80th, and 90th percentiles but only show the median below for clarity in the presentation. The rest of the data can be found in the SI. It is also important to highlight that the following gene classes do not attempt to classify all the DEGs; but, as suggested by their names, these gene classes serve to focus the study of the response to stress in an efficient manner.

Definition 2.5. *A gene is called* ***very-well-regulated*** *under a given stress if its inter-individual variability after treatment is below the peak in the distribution; or its inter-individual variability ratio is before the peak in the distribution of inter-individual variability ratios for the species; i.e, its ratio is less than* $1+\gamma_s$ *for some relatively small number* γ_s *(can be positive or negative) that depends on the species and the stress.*

The following classification is in terms of the distributions of inter-individual variability before and after treatment.

Definition 2.6. *We will refer to the following sets of genes as the* ***extreme response sets****:*

1. ***Key Response genes (K-R-genes or G1):*** *The set of genes that have small inter-individual variability before the treatment and small inter-individual variability after the treatment. We assume that these are the most important genes for the species' reaction to the treatment. These genes can be captured by comparing the genes in the lower quantiles before treatments to those also in the lower quantiles after treatment. In terms of our adopted convention of small variability, these are genes that are before the peak at baseline and also before the peak after treatment. These genes allude to the central manifold or central direction in dynamical systems theory. These genes are very-well-regulated.*

2. ***Treatment-specific genes (T-S-genes or G2):*** *The set of genes that have a relatively large inter-individual variability before treatment but have a small inter-individual variability after treatment. These genes are also part of a common response to the treatment and should be included in the model. These genes can be identified by comparing the genes in the upper quantiles before treatment (above 50%, 60%, 70% 80% 90%) to those before the peak after treatment. These genes allude to the stable manifold in dynamical systems theory. These genes are very-well-regulated.*

3. ***Support genes (S-genes or G3):*** *The set of genes that have high inter-individual variability both before and after treatment; but that are very-well-regulated. These are genes that are in the upper quantiles before and after treatment (from above 50% to above 50% , from above 60% to above 60% etc), but are very-well-regulated according to the definition above. Since neither the baseline nor the after-treatment states are constrained for the species, we claim that these genes carry the least amount of information specific to the response of the species for this treatment. We suspect these are the so called housekeeping genes (see [22]) that are connected to many processes, and so their variability is high but they are still very-well-regulated.*

4. ***Noisy genes (N-genes or G4):*** *The genes for which variability increases drastically after treatment. These genes respond inconsistently among individuals. These would be genes that are located before the peak at baseline but have inter-individual variability in the upper quantiles after treatment, indicating that the treatment disrupts their regulation. These genes are constrained at baseline and stressed after treatment, in contrast to the Treatment-specific genes. They carry specific information about how regulation breaks down for a species for the given treatment. These genes allude to the unstable manifold in dynamical systems theory.*

Notice that the only extreme response set that is not *very-well-regulated* is the Noisy set of genes. Below we show a typical representation of the *extreme response groups* in the inter-individual variability at baseline and after treatment coordinate system.

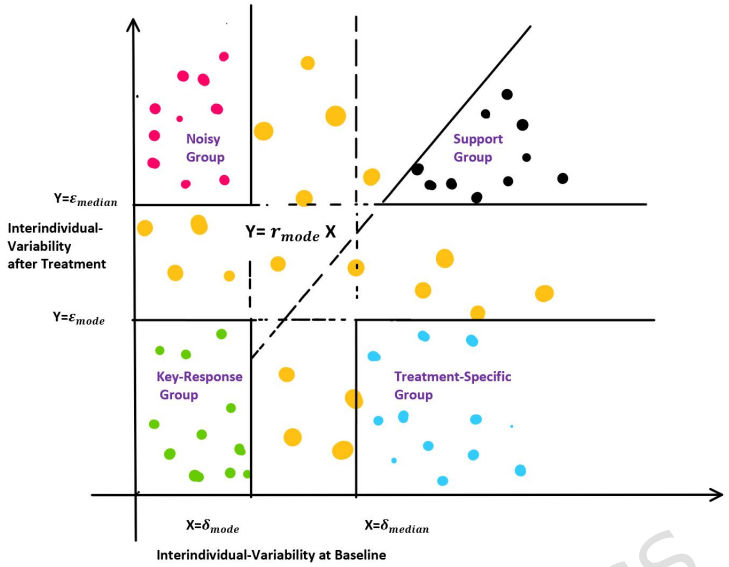

Figure 3: Diagram representation of the extreme response genes in the before and after treatment inter-individual variability coordinate systems.

2.9 Species comparison

As noted above, Proposition 2.4 is only viable for comparing the response after treatments for a given species since it does not account for the effect of genes in the Support and Noisy sets on genes in the Key-Response and Treatment-Specific sets (different network topologies for different species). The relevant comparison is: What is the impact on the species response of a small set of genes greatly increasing in inter-individual variability, whose role is important for the response to the stress (Noisy set) vs the impact of many genes increasing in inter-individual variability that are not so important for the survival of the species (uncategorized genes).

A reasonable comparison of the overall stress induced by a treatment on the species can be established by computing a net change in variability for all the DEGs. Using the same notation as in (8), consider the following average net sum of the change in inter-individual variability:

$$\frac{1}{|\mathrm{DEG}|}\sum_{k\in\ \mathrm{DEG}} \Delta({N_k}^1) - \Delta({N_k}^0). \tag{9}$$

The genes in the Key-Response and Support sets are expected to have a small contribution. The contribution of genes in the Treatment-Specific sets will be negative while the contribution of those in the Noisy set will be positive. The sum above is akin to a measure of entropy in the response. i.e the *disorder/disinformation* caused by the response to the treatment.

Notice that this table is not entirely consistent with our assumptions based on 2.4 (See Table 1). The main limitations of this metric are that it ignores the interactions between genes and weights the noise from each gene equally. In the next sections, we describe a measure of stress that overcomes these problems.

Table 2: Comparison of average net sum of the change in inter-individual variability across species at 32° and 41°.

Species	**Sum genes**	**32°**	**41°**
Camels	alls DEG	5.5	9.8
	$G1 \cup G2 \cup G3$	-7.3	-3.4
	$G4$	61.1	28.0
Humans	alls DEG	7.7	12.2
	$G1 \cup G2 \cup G3$	-14.8	-13.2
	$G4$	22.4	28.4
Rats	alls DEG	13.4	6.8
	$G1 \cup G2 \cup G3$	-4.3	-18.5
	$G4$	50.0	62.7
Rhinos	alls DEG	7.5	6.8
	$G1 \cup G2 \cup G3$	-11.9	-16.9
	$G4$	35.9	28.7
Squirrels	alls DEG	10.4	12.9
	$G1 \cup G2 \cup G3$	-6.5	-6.7
	$G4$	37.4	32.5
Bats	alls DEG	13.3	12.4
	$G1 \cup G2 \cup G3$	-1.5	-6.1
	$G4$	31.7	29.9

2.10 Network model

We have identified the extreme response genes as subsets of the DEGs that capture important features of the response (inter-individual behavior). In other words, we argue that the most important dynamics associated with the treatment involve these genes.

$$G1 \cup G2 \cup G3 \cup G4 \subset \text{DEG}$$

Out of these four subsets, the Support genes $G3$ contain the least amount of information common to the species; hence, we focus on understanding the rules of homeostasis on the other 3 extreme response subsets. That is, we only consider:

$$G1 \cup G2 \cup G3 \cup G4 \subset \text{DEG},$$

and build a network model to capture the interactions among these genes in each of these subsets. In mathematical terms, the dynamics are *projected* to these extreme response subsets.

In the model we will denote by N the number of genes to be considered and $\mathcal{K}$ the number of individuals available. The data collected are represented as points $x^{(k)}$ in $\mathbb{R}^N$ for $k = 1, ..., \mathcal{K}$ representing the transcript counts for each individual at baseline, and real values $y_i^{(k)}$ for $k = 1, ..., \mathcal{K}$ representing the transcript counts of the ith gene after treatment.

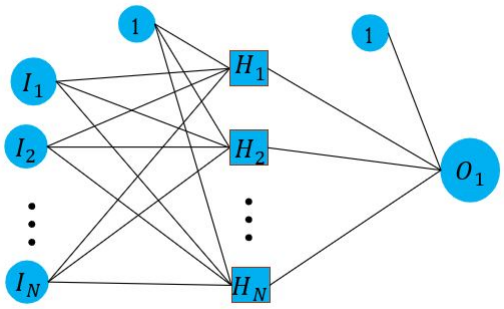

Figure 4: Picture representing the architecture of the network encoding the interactions of the genes. I_k represents the input for gene k. The intermediate stage value for gene k, denoted by H_k, is subject to an activation function σ. O_1 represents the output for gene 1. The two cells with value 1 represent the bias parameters collected in the vectors b_1 and b_2. The links encode weight values. H_1 is computed as follows: $H_1 = w^1_{11} * I_1 + ... + w^1_{1N} * I_N + b_{11}$ and then O_1 is computed: $O_1 = w^2_{11} * \sigma(H_1) + ... + w^2_{1N} * \sigma(H_N) + b_{21}$. In terms of (10), $x = (I_1, ..., I_N)'$, $(W_1)_{ij} = w^1_{ji}$, $b_1 = (b_{11}, ..., b_{1N})'$, $W_2 = (w^2_{11}, ..., w^2_{1N})$, and $b_2 = b_{21}$.

One innovation of the model is that it not only interpolates data points but it also approximates a transition between the attractors; which, along with the restrictions on the network architecture, reduces the number of possible suitable models to a finite number.

The function f describing the model for the output of the ith gene is of the form:

$$f_i(x) = f_{W_1^{(i)}, b_1^{(i)}, W_2^{(i)}, b_2^{(i)}}(x) := W_2^{(i)} * (\sigma^{(i)}(W_1^{(i)} * x + b_1^{(i)})) + b_2^{(i)} : \mathbb{R}^N \to \mathbb{R} \tag{10}$$

representing a neural network with one hidden layer subject to the piece-wise linear $\sigma^{(i)} : \mathbb{R} \to \mathbb{R}$ (σ is applied component-wise). See Figure 4. For the rest of the section we will drop the superscript referring to the network of the ith gene. Notice that we have used subscripts for indexing across genes and superscripts for indexing across individuals throughout the paper except in (10)

The data conditions are

$$f_i(x^{(k)}) = y_i^{(k)}$$

and

$$f_i([x^{(1)}, ..., x^{(\mathcal{K})}]) = [y_i^{(1)}, ..., y_i^{(\mathcal{K})}]$$

where $x^{(k)} = (x_1^{(k)}, ..., x_N^{(k)})$, and $[y_i^{(1)}, ..., y_i^{(\mathcal{K})}]$ denotes:

$$\bigcup_{k=1}^{\mathcal{K}} \text{int}(y_i^{(k)}),$$

with

$$\text{int}(y_i^{(k)}) := (y_i^{(k)} - r_k, y_i^{(k)} + r_k) \cap (\min(y_i^{(1)}, ..., y_i^{(\mathcal{K})}), \max(y_i^{(1)}, ..., y_i^{(\mathcal{K})})).$$

The intervals r_k are such that $(y_i^{(k)} - r_k, y_i^{(k)} + r_k)$ do not intersect. The notation $[x^{(1)}, ..., x^{(\mathcal{K})}]$ represents the set:

$$\bigcup_{k=1}^{\mathcal{K}} \Big(\bigotimes_{i=1}^{N} \text{int}(x_i^{(k)}) \Big).$$

Notice that the set $\bigotimes_{i=1}^{N} \text{int}(x_i^{(k)})$ is a neighborhood of the N-tuple genes collected for the kth individual.

The function:

$$\sigma^{(i)}(x) = \begin{cases} 0 & x \leq 0 \\ \frac{1}{a_i}x & 0 < x \leq a_i \\ 1 & x > a_i \end{cases},$$

is the activation function applied to the hidden layer, where a_i is a parameter to be optimized for each gene in the model for each species. Notice that the limit of $\sigma^{(i)}$ as alpha approaches 0 from the right exists and is the standard step function (denoted by σ_0). For convenience in later sections we also define the so called relu(x) function as equal to $x\sigma_0(x)$.

The activation function σ places $2N$ planes on $\mathbb{R}^N$ obtained by restricting each coordinate to 0 or α at the hidden layer, and results in at most 3^N regions in space. On each of these regions the model is linear.

The networks are optimized using a gradient descent algorithm where a loss function is minimized. For example, for each modeled DEG indexed by i we consider:

$$L(B_i) = \frac{1}{\mathcal{K}} \sum_{k=1}^{\mathcal{K}} (y_i^{(k)} - f_i(x^{(k)})^2.$$

Here, B_i denotes the complete set of parameters determining the network (10); that is, $B_i = \{W_1^{(i)}, b_1^{(i)}, W_2^{(i)}, b_2^{(i)}, \alpha_i\}$ for the *ith* gene.

Remark 2.7. *A gradient descent algorithm is a numerical approximation to the ODE:*

$$\dot{B}_i = -\nabla L(B_i).$$

The simplest algorithm comes from approximating the above ODE with the classical Euler's method.

2.11 Network predictions

After training the network subject to the constraints explained in the previous section, we compute errors for the test set and for the interval predictions. The error for the inter-individual variability intervals is computed using the following metric:

$$d(A, B) = |\inf(A) - \inf(B)| + |\sup(A) - \sup(B)|. \tag{11}$$

In this metric the magnitude of an interval is given by:

$$||A|| = d(A, 0) = |\inf(A)| + |\sup(A)|. \tag{12}$$

The error of the trained network on the ith gene is then computed by the following formula:

$$(\text{Response Error})_i = \frac{d([y_i^{(1)}, ..., y_i^{(\mathcal{K})}], f_i([x^{(1)}, ..., x^{(\mathcal{K})}])}{||[y_i^{(1)}, ..., y_i^{(\mathcal{K})}]||}. \tag{13}$$

We also compute the error of the output of the observations after treatment from the observations after treatment (Stability Error 2). This quantity captures how representative our intervals are of the corresponding states for the species, and also how well homeostasis is preserved. This is because we assume that:

$$\mathfrak{f}(J_1) = J_1$$

and the Stability Error measures:

$$(\text{Stability Error})_i = \frac{d([y_i^{(1)}, ..., y_i^{(\mathcal{K})}], f_i([y^{(1)}, ..., y^{(\mathcal{K})}])}{||[y_i^{(1)}, ..., y_i^{(\mathcal{K})}]||}, \tag{14}$$

where J_1 contains all possible states at homeostasis after treatment (the homeostasis attractor after treatment) as defined in Section 2, and $\mathfrak{f}$ is the exact homeostasis preserving response (without noise and approximations) of the species. Recall that $I_1 = [y^{(1)}, ..., y^{(\mathcal{K})}]$ approximates J_1 and that f_i approximates $\mathfrak{f}$ for the ith gene.

In the tables presented in SI Section 7.6 we show the results from training neural networks with the Key-Response group, the Treatment-Specific group, and the Noisy group for humans and camels for the 32° and 41° treatments. Humans and camels are chosen as representatives for the strict and flexible homeostasis mammals respectively, in order to compare their networks. The Response Prediction column shows the intervals containing the output of the trained networks with baseline conditions as input. The Stability Prediction column shows the intervals containing the output of the trained networks with observations after treatment used as the input conditions. The Response Prediction assesses how well the networks represent the response of the species, whereas the Stability Prediction measures how well homeostasis is approximated after treatment. In particular, in the case of the Treatment-Specific group and the Noisy group the Stability Prediction indicates whether the intervals continue to contract, expand, or are stable.

2.12 Strength of interactions

The networks computed in the previous section encode information about the strengths of the interactions between the genes in the response mechanism. First, we define the *net influence* of the kth gene on the jth gene:

$$(k \to j) = \sum_{i=1}^{N} (W_1^{(j)})_{i,k} \times (W_2^{(j)})_{k,i} \tag{15}$$

where the $(W_1^{(j)})_{i,k}$ and $(W_2^{(j)})_{k,i}$ are the network matrix parameters modeling the output of the jth gene (the jth network f_j).

This is the kth coordinate in the product:

$$(W_2) \times (W_1),$$

on the jth network, and it adds the net contributions of all the interactions for each gene output after treatment. We also define $(k \to j)^+$ as the sum of all positive terms in $(k \to j)$ and, similarly we define $(k \to j)^-$ as the absolute value of the sum of all the negative terms in $(k \to j)$. These quantities will be useful later in order to define a notion of well-being of the species based on a version of network entropy.

The absolute *influence* of the kth gene on the jth gene can be quantified by:

$$|k \to j| = (k \to j)^+ + (k \to j)^-.$$

We can visualize and compare the strengths of the interactions by graphing the directed interaction profile for all the DEGs. Explicitly, we compute the interaction for all genes on a fixed jth gene, order them from smallest to largest, and graph these values as a curve. To demonstrate how DEG interaction strengths vary among treatments and species, we plot curves for Key-Response genes for humans and camels at 32°C and 41°C. See Section 7.7 for the plots.

2.13 Network entropy

A more robust measure of entropy in the response can be defined in terms of the network models computed above. Since our models are signed graphs, we implement a modified Random Walker Shannon Entropy measure that accounts for the direction (sign) of the interactions.

For the kth gene we define the following probability distribution:

$$p_{ki}^{j+} = \frac{\text{relu}(W_{ik}^{(1)} W_{ki}^{(2)})}{(k \to j)^{+}}, \tag{16}$$

and define p_{ki}^{j-} similarly as:

$$p_{ki}^{j-} = \frac{\text{relu}(-W_{ik}^{(1)} W_{ki}^{(2)})}{(k \to j)^{-}}. \tag{17}$$

The *signed Shannon entropy* $\mathcal{H}$ of the model is defined by the following expressions:

$$S_k^{(j)} = S_k^{(j+)} + S_k^{(j-)} = -\sum_i p_{ki}^{j+} \ln p_{ki}^{j+} - \sum_i p_{ki}^{j-} \ln p_{ki}^{j-} \tag{18}$$

$$S^{(j)} = \frac{1}{N \ln(N)} \sum_k S_k^{(j)} \tag{19}$$

and finally:

$$\mathcal{H} = \frac{1}{N} \sum_j S^{(j)}. \tag{20}$$

Notice that in this notion of total entropy we add the contributions of the positive sub-network and the negative sub-network independently. The entropy for each subgraph can range from 0 to 1 as in the classical case; and hence, the total value of $\mathcal{H}$ will range from 0 to 2. It is not difficult to see that the maximum value of $S_k^{(j+)}$ and $S_k^{(j-)}$ is $\ln N$, so dividing by $N \ln(N)$ in (19) standardizes $S^{(j)}$.

The quantity $S_k^{(j)}$ in the computation of total entropy is the contribution of entropy from node k to node j. With this perspective, we define the entropy departing from the noisy genes, $S_{G4}^{G1 \cup G2}$, as:

$$S_{G4}^{G1 \cup G2} = \frac{1}{N^2 \ln(N)} \sum_{j \in G1 \cup G2} \sum_{k \in G4} S_k^{(j)}. \tag{21}$$

The notation $j \in G1 \cup G2$ means: the index j for genes in the list $G1 \cup G2$; which are genes in $G1$ together with genes in $G2$ ranked according to (7).

The computation of $S_{G4}^{G1 \cup G2}$ (the contribution to entropy coming from the Noisy genes), gives the adequate notion of connectivity of the Noisy genes to the rest of the network and is useful for accessing its influence on the response of the species under the treatment.

2.14 Software and data

I. **Project name** : bio_nnets

II. **Project home page** : https://github.com/joluigonza/bio_nnets

III. **Operating system(s)** : Platform independent

IV. **Programming languages** : Julia, R

V. **License** : MIT License

VI. **Data available at** : https://github.com/joluigonza/bio_nnets

3 Results

The data and the scripts used during the project are available at [9].

3.1 Extreme response genes: Genes modeling the primary cellular response

Below we present the numbers of genes in each of the extreme sets for Camels, Humans, Rats, Rhinos, and Squirrels. See Section 7 (SI) for the corresponding distributions showing the peaks.

	Camels	Humans	Rats	Rhinos	Squirrels
DEGs	2334	3144	2029	4178	1836
Key-Response	352	412	296	518	245
Treatment-Specific 50%	46	82	55	104	38
Support 50%	298	334	176	333	140
Noisy 50%	69	77	62	112	63

Table 3: Numbers of active genes belonging to the extreme response sets at 41° for camels, humans, rats, rhinos, and squirrels.

	Camels	Humans	Rats	Rhinos	Squirrels
DEGs	2991	3335	2021	4530	1823
Key-Response	406	426	264	548	149
Treatment-Specific 50%	73	97	42	136	52
Support 50%	234	266	167	330	100
Noisy 50%	98	102	68	129	72

Table 4: Numbers of active genes belonging to the extreme response sets at 32° for camels, humans, rats, rhinos, and squirrels.

We next argue that :
1. The principal coherent response that is common to the species and is specific to the treatment is represented by the dynamics of genes in the Key-Response and Treatment-Specific sets.
2. These two groups interact weakly with genes in the Support and Noisy sets.

Support genes are well regulated in a sense, but their response is independent of the treatment (see [19]. We suspect that these are typically ancient genes that are crucial to the survival of the cells and are hence always active. We reason that old genes are more likely to be related to many other genes for all species in which they are still present, which in turn contributes to their high variability at baseline and after treatment. However, since they are important to the survival of the cells of the species their inter-individual variability is conserved. The Noisy genes encode non-coherent responses and are correlated to the noise level associated with the treatment. The second argument above can be understood intuitively as the separation of uncertainty between different groups of genes, meaning that interpreting inter-individual variability in response to a treatment reflects noise in the response. Thus, the presence of a strong connection between genes in the Key-Response and Treatment-Specific sets with genes in the Support and Noisy sets would result in noise (variability) from the latter genes propagating to the former genes, contrary to observations.

We can support the above claims to some extent by computing the quantiles before and after treatment for genes found in the intersections among species. This will allow us to classify the genes in the intersection (or at least determine to which group they are closest to). For each DEG-by-treatment combination we compute its percentile placement in the distribution of inter-individual variability at baseline and after treatment in order to classify them.

583 Here are the percentile placements for the 41° treatment for genes in the intersection for all
584 5 species.

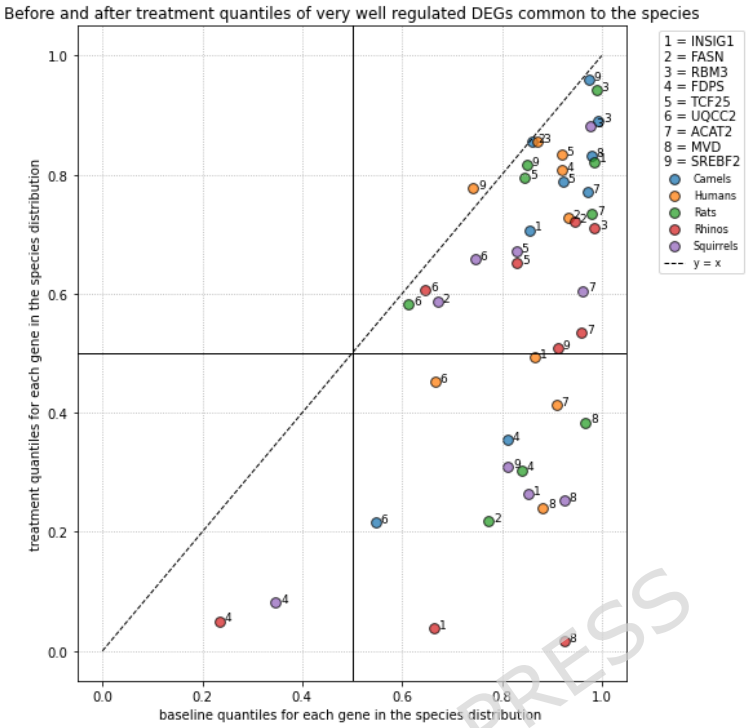

Figure 5: Percentiles for the inter-individual variability for *very-well-regulated* DEGs with respect to the 41° that are common for camels, humans, rats, rhinos, and squirrels in Figure 7. The x axis represents the percentiles at the baseline distributions of the species while the y axis shows the percentiles at the after treatment distributions.

585 Similarly, for the 32° treatment we have the following percentile tables for DEGs common
586 to all species:

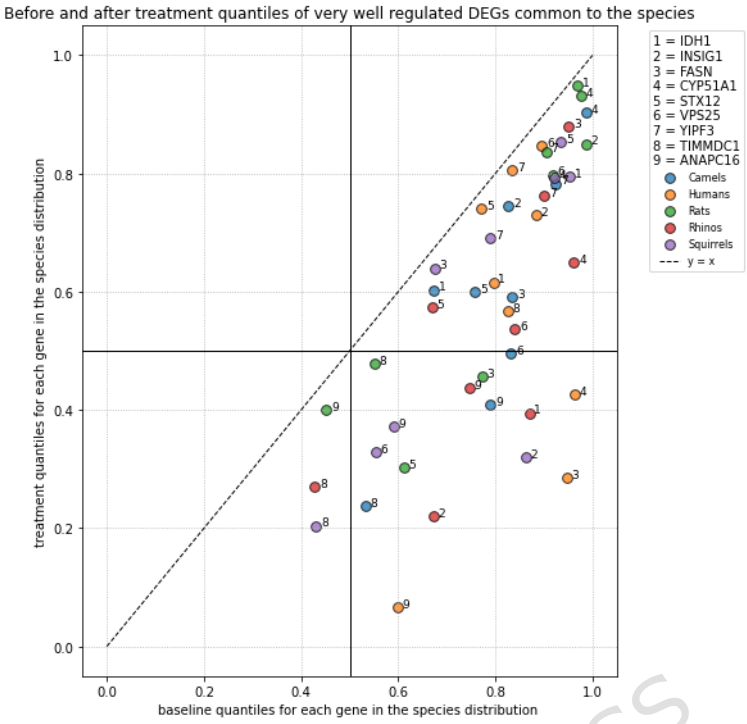

Figure 6: Percentiles for the inter-individual variability for *very-well-regulated* DEGs with respect to the 32° that are common for camels, humans, rats, rhinos, and squirrels in Figure 8. The x axis represents the percentiles at the baseline distributions of the species while the y axis shows the percentiles at the after treatment distributions.

Notice that the definition of the *extreme response genes* (Definition 2.6) depends on the treatment and the species.

3.2 Common very-well-regulated genes

Another fundamental question we wish to answer about the rules of homeostasis is which of the rules are common to mammals and which are species specific. A starting point is to discover which genes are active for the treatment, *very-well-regulated*, and common among species. With this information we can then investigate their roles in stress response mechanisms for the different species.

The following diagrams are constructed using the DEGs, according to their rank (7) for humans, that are also *very-well-regulated* as previously defined above with respect to (8).

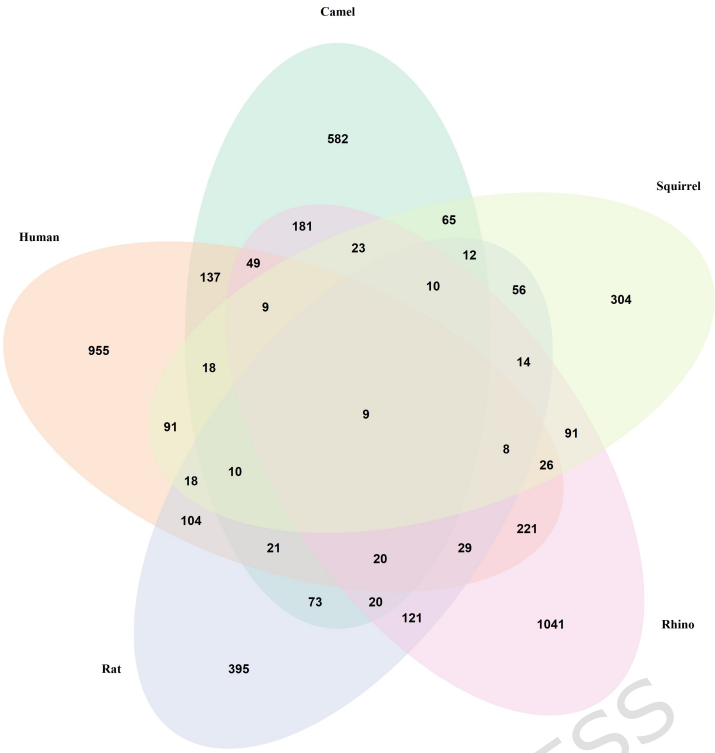

Figure 7: Diagram constructed from all DEG for which the inter-individual variability ratio (8) is less than $r_{mode} + \epsilon$, where ϵ is a small tolerance for the 41° treatment.

Genes in the intersection that are common to all species are listed below. Information on the gene functions was gathered from https://www.proteinatlas.org/ :

[1] INSIG1 (ENSG00000186480): This gene encodes an endoplasmic reticulum membrane protein that regulates cholesterol metabolism, lipogenesis, and glucose homeostasis. The encoded protein has six transmembrane helices which contain an effector protein binding site.

[2] FASN (ENSG00000169710): Fatty acid biosynthesis, Fatty acid metabolism, Lipid biosynthesis, Lipid metabolism.

[3] RBM3 (ENSG00000102317): Cold-inducible mRNA binding protein that enhances global protein synthesis at both physiological and mild hypothermic temperatures. Reduces the relative abundance of microRNAs, when overexpressed. Enhances phosphorylation of translation initiation factors and active polysome formation (By similarity).

[4] FDPS (ENSG00000160752): Cholesterol biosynthesis, Cholesterol metabolism, Host-virus interaction, Isoprene biosynthesis, Lipid biosynthesis, Lipid metabolism, Steroid biosynthesis, Steroid metabolism, Sterol biosynthesis, Sterol metabolism

[5] TCF25 (ENSG00000141002): May play a role in cell death control. Acts as a transcriptional repressor. Has been shown to repress transcription of SRF in vitro and so may play a role in heart development.

[6] UQCC2 (ENSG00000137288): Plays a role in the modulation of respiratory chain activities such as oxygen consumption and ATP production and via its modulation of the respiratory chain activity can regulate skeletal muscle differentiation and insulin secretion by pancreatic beta-cells. Involved in cytochrome b translation and/or stability.

[7] ACAT2 (ENSG00000120437): Involved in the biosynthetic pathway of cholesterol.

[8] MVD (ENSG00000167508): Catalyzes the ATP dependent decarboxylation of (R)-5-diphosphomevalonate to form isopentenyl diphosphate (IPP). Functions in the mevalonate (MVA) pathway leading to isopentenyl diphosphate (IPP), a key precursor for the biosynthesis of iso-

prenoids and sterol synthesis.

[9] SREBF2 (ENSG00000198911): This gene encodes a member of the a ubiquitously expressed transcription factor that controls cholesterol homeostasis by regulating transcription of sterol-regulated genes.

As in the case of 41°, the number DEGs that are *very-well-regulated* and found in the intersection is small (coincidentally also 9).

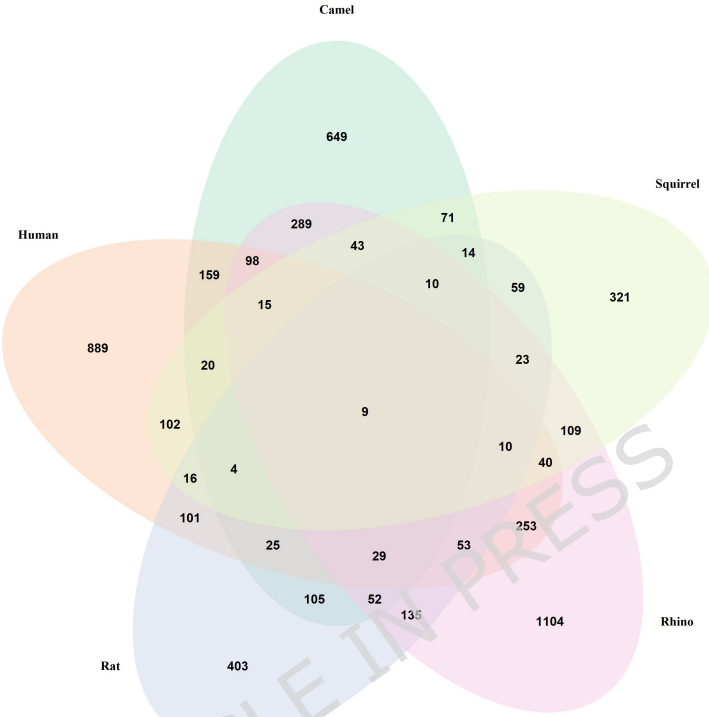

Figure 8: Diagram constructed from all DEG for which the inter-individual variability ratio (8) is less than $r_{mode} + \epsilon$, where ϵ is a small tolerance for the 32° treatment.

The only genes found in the intersection for all 5 species are :

[1] IDH1 (ENSG00000138413): Catalyzes the NADP(+)-dependent oxidative decarboxylation of isocitrate (D-threo-isocitrate) to 2-ketoglutarate (2-oxoglutarate), which is required by other enzymes such as the phytanoyl-CoA dioxygenase 1, 2. Plays a critical role in the generation of NADPH, an important cofactor in many biosynthesis pathways.

[2] INSIG1 (ENSG00000186480): This gene encodes an endoplasmic reticulum membrane protein that regulates cholesterol metabolism, lipogenesis, and glucose homeostasis.

[3] FASN (ENSG00000169710): Fatty acid biosynthesis, Fatty acid metabolism, Lipid biosynthesis, Lipid metabolism

[4] CYP51A1 (ENSG00000001630): This endoplasmic reticulum protein participates in the synthesis of cholesterol by catalyzing the removal of the 14alpha-methyl group from lanosterol. Homologous genes are found in all three eukaryotic phyla, fungi, plants, and animals, suggesting that this is one of the oldest cytochrome P450 genes.

[5] STX12 (ENSG00000117758): Predicted to enable SNAP receptor activity and SNARE binding activity. Involved in autophagosome assembly; cholesterol efflux; and protein stabilization.

[6] VPS25 (ENSG00000131475): Component of the ESCRT-II complex (endosomal sorting complex required for transport II), which is required for multivesicular body (MVB) formation

and sorting of endosomal cargo proteins into MVBs. The MVB pathway mediates delivery of transmembrane proteins into the lumen of the lysosome for degradation. The ESCRT-II complex is probably involved in the recruitment of the ESCRT-III complex. Protein transport, Transcription, Transcription regulation, Transport.

[7] YIPF3 (ENSG00000137207): Involved in the maintenance of the Golgi structure. May play a role in hematopoiesis.

[8] TIMMDC1 (ENSG00000113845): Chaperone protein involved in the assembly of the mitochondrial NADH:ubiquinone oxidoreductase complex (complex I). Participates in constructing the membrane arm of complex I.

[9] ANAPC16 (ENSG00000166295): Cell cycle, Cell division, Mitosis, Ubl conjugation pathway.

Several genes found in the intersection are indeed genes known to have been conserved through evolution and to (directly or indirectly) play a role in the well being and survival of the cell.

3.3 Network predictions

In the tables below we show the results from training neural networks with the Key-Response group, the Treatment-Specific group, and the Noisy group for humans and camels for the 32° and 41° treatments. Humans and camels are chosen as representatives for the strict and flexible homeostasis mammals respectively, in order to compare their networks. The Response Prediction column shows the intervals containing the output of the trained networks with baseline conditions as input. The Stability Prediction column shows the intervals containing the output of the trained networks with observations after treatment used as the input conditions. The interval arithmetic package *IntervalArithmetic.jl* is used for the computations involving intervals to guarantee enclosures [2]. Response Prediction assesses how well the networks represent the response of the species, whereas Stability Prediction measures how well homeostasis is approximated after treatment. In particular, in the case of the Treatment-Specific group and the Noisy group Stability Prediction indicates whether the intervals continue to contract, expand, or are stable.

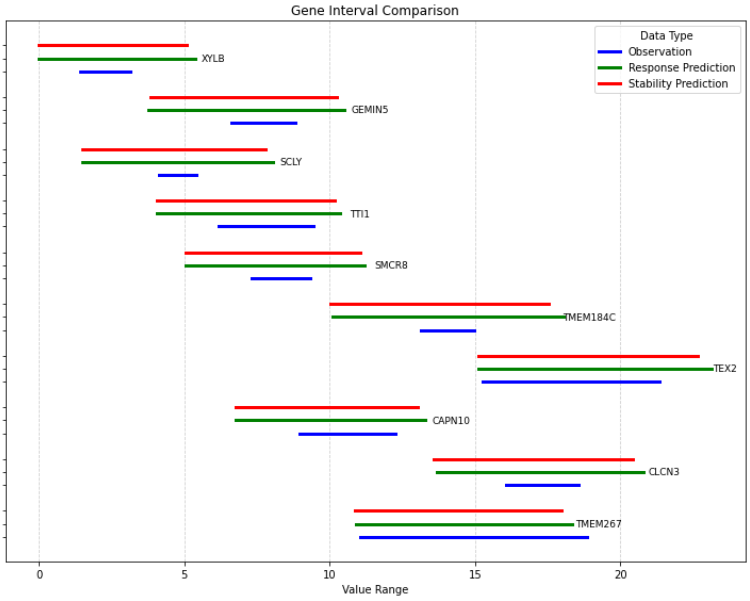

Figure 9: Inter-individual variability intervals for the Key-Response genes for Humans at 32° for the top 10 genes ranked with respect to (7). Comparison of observed intervals vs intervals predicted by trained networks. The fractional errors, RE and SE, are computed according to formulas (13) and (14) respectively.

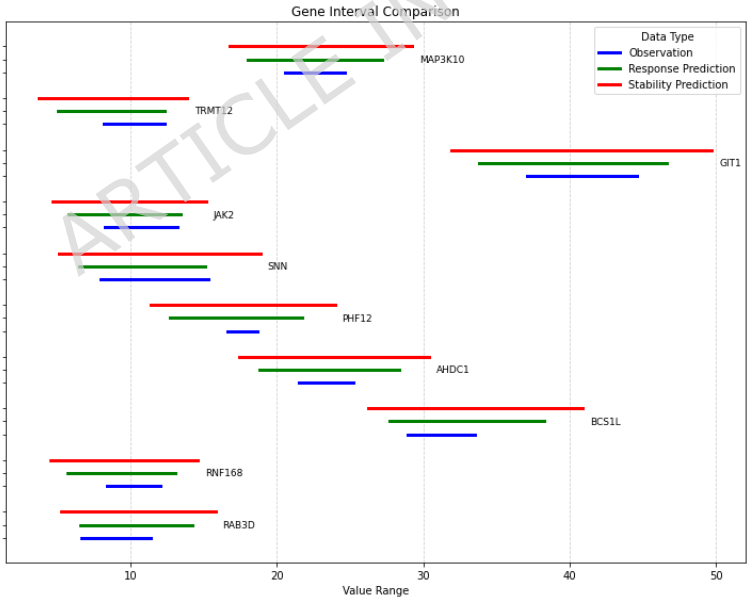

Figure 10: Inter-individual variability intervals for the Key-Response genes for Humans at 41° for the top 10 genes ranked with respect to (7). Comparison of observed intervals vs predicted by trained networks. The fractional errors, RE and SE, are computed according to formulas (13) and (14) respectively.

3.4 Measures of well-being after environmental perturbations

A robust measure of entropy in the response can be defined in terms of the network models computed using the extreme response sets. Since our models are signed graphs, we implement a modified Random Walker Shannon Entropy measure that accounts for the direction (sign) of the interactions.

The neural network is viewed as the superposition of a positive and a negative network. Positive and negative probability distributions are then defined in terms of the weights. The total entropy is calculated as the sum of the negative and positive network entropies. The entropy for each subgraph can range from 0 to 1 as in the classical case; and hence, the total value of $\mathcal{H}$ will range from 0 to 2.

Below we present the network entropy values for the response of camels and humans at the 32° and 41° treatments. For both treatments the camel is ranked higher.

Treatment	Camels	Humans
32°	1.12	1.49
41°	1.16	1.51

Table 5: Total entropy of the model for Humans and Camels at the 32° and 41° treatments.

The quantity $S_k^{(j)}$ in the computation of total entropy is the contribution of entropy from node k to the jth node. With this perspective, we define the entropy departing from the noisy genes as: $S_{G4}^{G1\cup G2}$

$$S_{G4}^{G1\cup G2} = \frac{1}{N^2 \ln(N)} \sum_{j\in G1\cup G2} \sum_{k\in G4} S_k^{(j)}. \tag{22}$$

The notation $j \in G1 \cup G2$ means: the index j for genes in the list $G1 \cup G2$; which are genes in $G1$ together with genes in $G2$ ranked according to (7).

In the following table we present these computations for camels and humans for the 32° and 41° treatments. We see that a small fraction of the entropy is coming from the noisy genes to the rest of the networks. This demonstrates that the noisy group is weakly connected to the rest of the extreme response network in the models.

Treatment	Camels	Humans
32°	0.08	0.11
41°	0.16	0.10

Table 6: Entropy from the Noisy genes on the model for Humans and Camels at the 32° and 41° treatments.

3.5 Other measures of stability of the response

We expect that for a system that is able to maintain homeostasis, small perturbations of the counts at baseline are still mapped to counts within the attractor after treatment. We also expect the system to be resilient to small perturbations of the parameters. We construct yet another measure of stability for the models based on quantifying this ideal property in terms of the parameters.

3.5.1 Assessing the effects of perturbing the parameters in terms of ratios of errors in approximating the attractors

To each matrix defining the response model, we apply a random perturbation of 10% of their norm value for a fixed number of times (i.e., 10) and compute the predicted state intervals and errors with respect to the raw data as before (See equations (13) and (14)). We then compute the average error for the 10 trials and calculate a ratio of this average and the original error for each gene. Finally, we compute the average ratio for the Key Response genes (G1) and the Treatment-Specific genes (G2) and report these in Tables 16 and 17. In both cases the camels are ranked higher than the humans.

	Camels	Humans
Response Prediction	0.98	4.99
Stability Prediction	2.33	4.60

Table 7: Average ratio of the response and stability errors after a 10% perturbation of the interaction parameters for the Key Response and the Treatment-Specific groups of genes for the 32° model.

	Camels	Humans
Response Prediction	1.11	6.72
Stability Prediction	1.26	6.03

Table 8: Average ratio of the response and stability errors after a 10% perturbation of the interaction parameters for the Key Response and the Treatment-Specific groups of genes for the 41° model.

These tables show a significantly higher error after perturbation for the human models compared to the camel models.

3.5.2 Quantifying the domain of attraction of the model

Another way of quantifying the stability of the model itself as a measure of the stability of the response is by approximating the magnitude of the deviation of the model produced by an infinitesimal perturbation of the model parameters. More precisely, for each gene except for the Noisy genes we apply a very small perturbation and retrain the networks with the same learning rate and measure the deviation from the original parameters. All original networks had converged according to the criteria explained in Section 2). Finally, we compute the average for all the model genes (ignoring the Noisy genes). With respect to this measure of well-being the camels are also ranked higher than the humans.

Treatment	Camels	Humans
32°	$7.3 * 10^{-5}$	$2.1 * 10^{-4}$
41°	$2.8 * 10^{-4}$	$1.1 * 10^{-3}$

Table 9: Average deviation of the trained model parameter after a small perturbation.

3.6 Extreme response genes enrichment analysis. Brief comparison with model based on limma selected genes for humans

We compared the key response genes to the same number of genes ranked by limma [16] using the publicly available database https://string-db.org/ and https://www.proteinatlas.org/ (default settings):

Treatment	Gene Set	PPI Enrichment P-Value
32°	Model-Selected Genes	6.2e-05
	Limma-Selected Genes	$<$ 1.0e-16
41°	Model-Selected Genes	1.7e-08
	Limma-Selected Genes	$<$ 1.0e-16

Table 10: STRING-db Results. Enrichment analysis of the modeled extreme response genes in G1 compared to the same size model of limma genes for the 32° (169 genes) and 41° (191 genes) treatments for humans.

In both cases the enrichment p-values are significant. It is worth observing that the p-values associated with the limma selected genes are considerably smaller than those from the extreme response selection possibly due to the fact that limma has been widely used for over a decade and has greatly influenced the direction/focus of the studies further strengthening their association in the databases.

We also compared the largest connected component (LCC) of the set of genes according to their association relation recorded in the database. For details regarding the algorithm see [8]. This again shows that the assumption that the selected genes form part of a mechanism of response to the stress is supported by the literature.

	Model-Selected G1	Limma-Selected
Number of genes with $\geq$ 1 known interactions in PA	155 of 169 (91.7%)	162 of 169 (95.9%)
Number of genes in LCC (1st & 2nd order)	117 (75.5%) P-value $<$ 0.00001 Mean for random: 109.7 Stdev: 4.24	135 (83.3%) P-value = 0.00001 Mean for random: 130.65 Stdev: 3.26

Table 11: Comparison of the length of the Largest Connected Component (LCC) by first and second order association for the 32° treatment for the model and limma selected genes. Protein interactions were obtained from the Human Protein Atlas (PA) (https://www.proteinatlas.org/) "Interaction" section, which aggregates data from four major sources: IntAct (high and medium confidence physical associations), BioGRID (multivalidated physical interactions), BioPlex (interactions with >75% probability), and OpenCell (significant physical interactions). We included any known interaction reported in at least one of these four major sources.

	Model-Selected G1	**Limma-Selected**
Number of genes with ≥ 1 known interactions in PA	174 of 191 (91.1%)	178 of 191 (93.2%)
Number of genes in LCC (1st & 2nd order)	129 (74.1%) P-value < 0.00887 Mean for random: 125.6 Stdev: 4.50	134 (75.3%) P-value $= 0.01634$ Mean for random: 136.7 Stdev: 5.21

Table 12: Comparison of the length of the Largest Connected Component (LCC) by first and second order association for the 41° treatment for the model and limma selected genes. Protein interactions were obtained from the Human Protein Atlas (PA) (https://www.proteinatlas.org/) "Interaction" section, which aggregates data from four major sources: IntAct (high and medium confidence physical associations), BioGRID (multivalidated physical interactions), BioPlex (interactions with >75% probability), and OpenCell (significant physical interactions). We included any known interaction reported in at least one of these four major sources.

Finally, we built a neural network with the limma selected genes using the same algorithm as for the model based on the extreme response genes. We compare the response and stability of the response networks of the two models for the 32° and 41° treatments for humans. Our first observation is that the variance of the RE error for the limma model at 41° is considerably higher than the model based on extreme response genes; however, this was not the case for the 32° treatment. The second important observation is that, as expected, the SE for the full model based on the G1, G2, and G4 genes is considerably worse than for the G1 only model and the limma model also for 41°. This shows that the full model can capture the deterioration of the state of the cells after a long period of time exposed to the new conditions. This possible behavior seems to be completely undetected by the limma model. No drastic difference is observed for RE or SE for the models for the 32° treatment. Finally, the well-being measure introduced in Section 3.5.2 shows that the extreme response models are stable as opposed to the limma models which collapse after a small perturbation. This was the case for both the 32° and 41° treatments.

Errors	**Model G1**	**Model G1G2G3**	**Model G1G2G4**	**Model Limma**
RE:(mean,variance)	(0.88, 0.60)	(0.31,0.12)	(0.45, 1.12)	(0.73, 43.08)
SE:(mean,variance)	(1.02, 0.93)	(0.47,0.33)	(19.10, 57057)	(0.25, 0.04)
Stability Sec 3.5.2	2.9e-4	2.6e-4	1.1e-3	6.0e269

Table 13: Response and Stability interval predictions for the Extreme Response models and the Limmma model for the 41° treatment. The well-being measure introduced in Section 3.5.2 is also included. The smaller this number is the more stable the model is to perturbations.

Errors	**Model G1**	**Model G1G2G3**	**Model G1G2G4**	**Model Limma**
RE:(mean,variance)	(0.84,0.25)	(0.49,0.31)	(0.63,0.26)	(0.26,0.07)
SE:(mean,variance)	(0.84,0.23)	(0.53,0.61)	(0.82,0.49)	(0.33,0.09)
Stability Sec 3.5.2	3.1e-4	2.6e-4	2.3e-4	1.3e237

Table 14: Response and Stability interval predictions for the Extreme Response models an the Limmma model for the 32° treatment. The well-being notion introduced in Section 3.5.2 is also included. The smaller this number is the more stable the model is to perturbations.

4 Discussion & Conclusions

In this paper, we identify three subsets of genes that, across mammalian species, capture the primary response of homogeneous cell cultures of skin fibroblasts to changes in temperature. These groups of genes act as a robust set of coordinates that separate the dynamics and permit the study of their interactions separately. In mathematical terms, these three classes of genes can be viewed as a coordinate system that diagonalizes the response of the species, in the same sense that diagonalization simplifies the dynamics of a matrix by isolating independent directions of variation.

The Key-Response set contains genes that appear to be most central to the response to our experimental temperature perturbations, as they maintain low inter-individual variability both before and after treatment. The Treatment-Specific genes are those for which the inter-individual variability contracts, suggesting that their regulation becomes tightly constrained in response to the treatment and that they may only become functionally active under the altered conditions. The third highlighted set, the Noisy genes, consists of those genes for which the inter-individual variability expands significantly following treatment. We hypothesize that this group captures aspects of the vulnerability of the species to the perturbation and reflects components of the response that become destabilized under stress.

The network models constructed on these extreme response sets exhibit predictive power and can be used to identify gene–gene interactions that may play important roles in species survival under changing environmental conditions. A key feature of our framework is that the set of possible models satisfying the architecture and constraints outlined in Section 2 is finite. This restriction is critical for model validation, as it allows the incorporation of prior biological knowledge—such as known gene functions and regulatory interactions—to identify the most plausible models among the admissible candidates.

Our analysis further demonstrates that even with transcript count data from a relatively small number of individuals per species, it is feasible to identify differentially expressed genes using a criterion based on activity, rather than relying on fold-change statistics or hypothesis-testing frameworks that require larger sample sizes. Activity, as defined here, is a positive quantity that measures the magnitude of transcriptional change regardless of direction. This approach allows the detection of meaningful biological responses even in datasets where classical statistical methods may lack power.

Comparing the inter-individual variability of DEGs before and after treatment provides insight into the regulatory mechanisms underlying the response of a species to a perturbation. In particular, this comparison allows us to distinguish very-well-regulated genes—those that maintain consistent behavior across individuals—from genes that respond in a less coherent or more heterogeneous manner. The Key-Response, Treatment-Specific, and Noisy groups capture the high-order structure of the species' response to treatment, while the Support genes, although also very-well-regulated, likely participate in many cellular processes and may represent broadly conserved cellular functions.

One of the most significant contributions of this work is the development of biologically plausible network models that can be constructed from a small number of individual replicates. Identifying the extreme response groups is the first step toward constructing these models. The resulting networks must satisfy the relation depicted in Figure 1, which ensures that the learned mapping semi-conjugates the homeostasis dynamics under baseline and treatment conditions. This constraint provides a natural dynamical interpretation of the response and limits the set of admissible models. Further validation using known gene functions and biological pathways can help ensure that the selected models are biologically meaningful.

We also introduce a measure of species well-being after treatment based on network entropy. The classical Random Walker Shannon Entropy was adapted to our network architecture in order to quantify the disruption of regulatory interactions induced by a perturbation. Because

the entropy measure depends on the network structure itself, it provides a standardized metric that is well suited for comparisons across species and treatments. All measures of well-being introduced in this work consistently rank camels higher than humans in terms of resilience to the 32°C and 41°C treatments (Tables 5, 7, 8, 9), in agreement with known physiological differences in temperature tolerance.

Although the present work focuses on extreme response genes, many DEGs were intentionally excluded from the network models. Incorporating additional DEGs represents an important direction for future work, as it may reveal finer regulatory interactions associated with different treatments. With larger numbers of replicates, it will also be possible to refine the network architecture, tune activation functions for each species, and improve the approximation of the attractor sets that characterize homeostasis.

In the current study, extreme response networks were constructed for humans and camels as representative examples of species exhibiting relatively strict versus flexible homeostasis. Future work will extend this comparative analysis to additional species in order to better understand how different regulatory architectures support distinct physiological strategies.

Large-scale computational analyses may also clarify the relationships among the different gene groups identified here. While the extreme response sets capture the dominant structure of the response, weaker interactions between genes in different groups likely exist. Experimental validation will be necessary to determine the extent to which such cross-group interactions contribute to the overall regulatory response. More broadly, the framework developed in this paper was intentionally formulated in general terms with applications beyond the specific biological system studied here. The essential requirement for applying the method is the availability of samples from a stable dynamical system consisting of comparable replicates, together with observations before and after a perturbation. Under these conditions, the method can be used to infer the common response mechanism of the system. In this sense, the approach provides a practical framework for inferring the dynamics of complex interacting systems from sparse observational data, a situation that frequently arises in biological experiments where the number of replicates is limited.

A key conceptual contribution of this work is the observation that the extreme response gene groups act as a low-dimensional coordinate system describing the response of the system to perturbation. Rather than modeling the behavior of thousands of variables simultaneously, the dynamics can be expressed in terms of a small number of coordinated directions corresponding to stable, inducible, and destabilized components of the response. In analogy with diagonalization in linear systems, this representation separates the dominant modes of variation and allows the regulatory dynamics to be studied in a structured and interpretable way. This perspective suggests that many biological responses to environmental changes may admit a similarly reduced description in terms of a small number of coordinated regulatory programs.

In cellular biology, for example, the framework could be applied to study the response of specific cell types to pharmacological treatments, such as cancer cells exposed to chemotherapy agents or immune cells responding to infection. More generally, the approach may be applicable to a wide range of cellular perturbation experiments, including nutrient deprivation, hypoxia, hormonal stimulation, or toxin exposure. The method could also be particularly useful in the analysis of single-cell transcriptomic data, where inter-cell variability is intrinsic to the system and distinguishing coherent regulatory programs from stochastic fluctuations remains a major challenge. Because the method does not rely on large sample sizes, it may also be valuable in experimental contexts where biological material is limited, such as rare cell populations or primary clinical samples.

Beyond transcriptomics, the same principles could be applied to other molecular measurements, including chromatin accessibility, DNA methylation, proteomic abundance, or metabolomic profiles. In these settings, the extreme response groups would identify stable regulatory pro-

grams, inducible pathways activated by the perturbation, and components of the system that become destabilized under stress. As a result, the framework may provide a unified way of interpreting multi-omics datasets describing how different regulatory layers coordinate responses to environmental change.

The methodology also naturally extends to comparative and evolutionary studies, where the goal is to understand how different organisms respond to environmental challenges. Because the network models provide quantitative measures of stability and entropy, they offer a principled way to compare the resilience of regulatory systems across species, tissues, or environmental conditions. In this context, the approach may help identify conserved regulatory programs underlying adaptation to stress, as well as species-specific mechanisms that support distinct physiological strategies.

Beyond molecular biology, the approach may also be applicable to ecological and population-level systems. In such contexts, genes could be replaced by species, and transcript counts by population abundances. The resulting framework would then describe how ecological communities reorganize in response to environmental perturbations such as climate change, habitat disturbance, or the introduction of invasive species. In this setting, the extreme response groups could reveal stable components of an ecosystem, species that respond specifically to environmental change, and populations that become destabilized during ecological stress.

More generally, the methodology may be relevant for any complex system in which the goal is to understand how the collective behavior of interacting components changes under shifts in external conditions. Examples include microbial community dynamics, neural population activity, and other large-scale biological networks in which a large number of interacting variables respond to environmental or physiological perturbations. In all such systems, identifying a reduced set of coordinates that captures the dominant response modes may provide a powerful strategy for uncovering the underlying mechanisms governing system-level behavior.

5 Appendix

$\mathcal{K}$: number of individuals in the study.

ϵ : will denote an arbitrary small number in this paper. Usually, introduced to avoid dividing by 0 in practice.

$A \subseteq B$: A is a subset of B, i.e every element of A is an element of B.

$A \cap B$: The set intersection of A and B.

$A \cup B$: The set union of A and B.

$f \circ g(x)$: the composition function f of $g(x)$, i.e $f(g(x))$.

$*$: regular matrix multiplication.

$\approx$: approximately equal as sets.

$\mathcal{N}(T, t; N_0)$: Solution in time t of the general transcript dynamics stochastic governing equation in the presence of noise with parameters T and initial condition N_0.

J_0 : Homeostasis attractor at baseline conditions T_0.

J_1 : Homeostasis attractor at treatment conditions T_1.

I_0 : Intervals of transcripts at baseline conditions T_0.

I_1 : Intervals of transcripts at treatment conditions T_1.

$D_0 = \mathcal{N}(T_0, 1; J_0)$

$D_1 = \mathcal{N}(T_1, 1; J_1)$

$\Delta(S)$: denotes the diameter of the set S for an arbitrary interval S. When S is an interval then it is simply the length of the interval.

$\|f\|$: magnitude of f in some sense.

α_i : Activity of the ith gene with respect to a given stress.

r_i : Rank of the ith gene according to level of activity with respect to a given stress.

$\sum_i$: Summation in terms of i

6 Declarations

Ethics approval and consent to participate : Not applicable

Consent for publication : Not applicable

Availability of data and materials : https://github.com/joluigonza/bio_nnets

Competing interests : No competing interests

Funding : This work was funded by an NSF Understanding the Rules of Life Collaborative Research Grant (Epigenetic pathways to regulate homeostatic resilience: Model-based discovery of rules across diverse mammals) to Valery E. Forbes (#2022050), Diane Genereux (#2022012), Allyson Hindle (#2022046), and Elinor Karlsson (#2022007). Funding for Jorge Gonzalez was provided by Florida Atlantic University.

Authors' contributions : Jorge Gonzalez (Conceptualization, Formal analysis, Methodology, Software, Validation, Writing original draft), Diane P. Genereux (Funding acquisition, Conceptualization, Writing – review and editing), Kristin Crouse (Conceptualization, Writing – review and editing), Bradley Frishman (Formal analysis, Methodology, Writing – review and editing), Allyson Hindle (Funding acquisition, Conceptualization, Writing – review and editing), Carla Madelaire (Data acquisition, Writing – review and editing), Elinor Karlsson (Funding acquisition, Conceptualization, Writing – review and editing), Lucas Moreira (Formal analysis, Methodology, Writing - review and editing), Valery Forbes (Funding acquisition, Conceptualization, Project administration, Supervision, Writing – review and editing). All authors read and approved the final manuscript.

Acknowledgments : We would like to thank Ines Haberle (Florida Atlantic University) for the insightful discussions and suggestions during the preparation of this manuscript. We thank members of the Hindle lab (Janessa Montenegro, Amy Klink, TJ Crippen, and Sebastiano Cupani) for their essential contributions to the collection of cell culture data that were used in model development.

7 Supplementary Information

7.1 Estimating α and the Power of the method of selecting DEGs and comparing with Limma modulated t-test

In the following tables $R := \frac{1}{\mathcal{K}}(r_i^0 + r_i^1)$ as in Definition 2.2.

$\mathcal{K}$	Normal	Log-normal	Lévy
5	0.024667	0.129400	0.545067
10	0.000000	0.009067	0.410533
15	0.000000	0.000800	0.344333
20	0.000000	0.000067	0.304267
25	0.000000	0.000133	0.263533
30	0.000000	0.000000	0.250667
35	0.000000	0.000000	0.229000
40	0.000000	0.000000	0.220067
45	0.000000	0.000000	0.205000
50	0.000000	0.000000	0.196467

Table 15: $P(R > 2)$ for iid X, Y with different marginal distributions.

$\mathcal{K}$	Normal	Lognormal	Levy
5	0.055400	0.156975	0.344788
10	0.000737	0.035112	0.271150
15	0.000025	0.009350	0.233600
20	0.000000	0.002550	0.207100
25	0.000000	0.000700	0.191362
30	0.000000	0.000175	0.174200
35	0.000000	0.000087	0.161312
40	0.000000	0.000013	0.152300
45	0.000000	0.000025	0.145150
50	0.000000	0.000000	0.139263

Table 16: Estimated probabilities $P(\frac{r_i^0}{\mathcal{K}} > 1)$ for iid X, Y with different marginal distributions.

t	$(\mathcal{K} = 5)$	$(\mathcal{K} = 10)$	$(\mathcal{K} = 15)$
0.000	0.02450	0.00002	0.00000
1.111	0.16122	0.00770	0.00026
2.222	0.44240	0.11310	0.02498
3.333	0.67888	0.38126	0.19144
4.444	0.82580	0.64882	0.48872
5.556	0.90356	0.82682	0.74150
6.667	0.94676	0.91688	0.88806
7.778	0.96968	0.96366	0.95534
8.889	0.98108	0.98244	0.98214
10.000	0.98818	0.99160	0.99312

Table 17: $P(R > 2)$ with $Y \sim N(0, 1)$ fixed and $X \sim N(t, 1 + t)$.

t	$(\mathcal{K} = 5)$	$(\mathcal{K} = 10)$	$(\mathcal{K} = 15)$
0.000	0.05504	0.00094	0.00000
1.111	0.40886	0.12402	0.03502
2.222	0.75538	0.57042	0.41078
3.333	0.90926	0.86770	0.82164
4.444	0.96380	0.96562	0.96342
5.556	0.98404	0.99102	0.99318
6.667	0.99310	0.99774	0.99888
7.778	0.99646	0.99920	0.99968
8.889	0.99796	0.99974	0.99986
10.000	0.99882	0.99998	0.99996

Table 18: $P(\frac{r_i^0}{\mathcal{K}} > 1)$ with $X \sim N(0, 1)$ fixed and $Y \sim N(t, 1 + t)$.

$\mathcal{K}$ **(per group)**	**Moderated df**	**Power**
2	12	0.053
3	14	0.072
4	16	0.088
5	18	0.104
8	24	0.153
10	28	0.187
15	38	0.263
20	48	0.339
30	68	0.480
50	108	0.697

Table 19: Estimated power of a limma-style moderated two-sample t-test (two-sided, $\alpha = 0.05$) for a true mean difference $\delta = 0.5$ with $\sigma = 1$. Equal sample sizes per group. Empirical Bayes variance moderation with prior degrees of freedom $d_0 = 10$ and prior variance $s_0^2 = 1$. Power estimated via simulation (1000 genes per replicate, 300 replicates).

7.2 Distributions

The following distributions serve as reference for the location of the peaks:

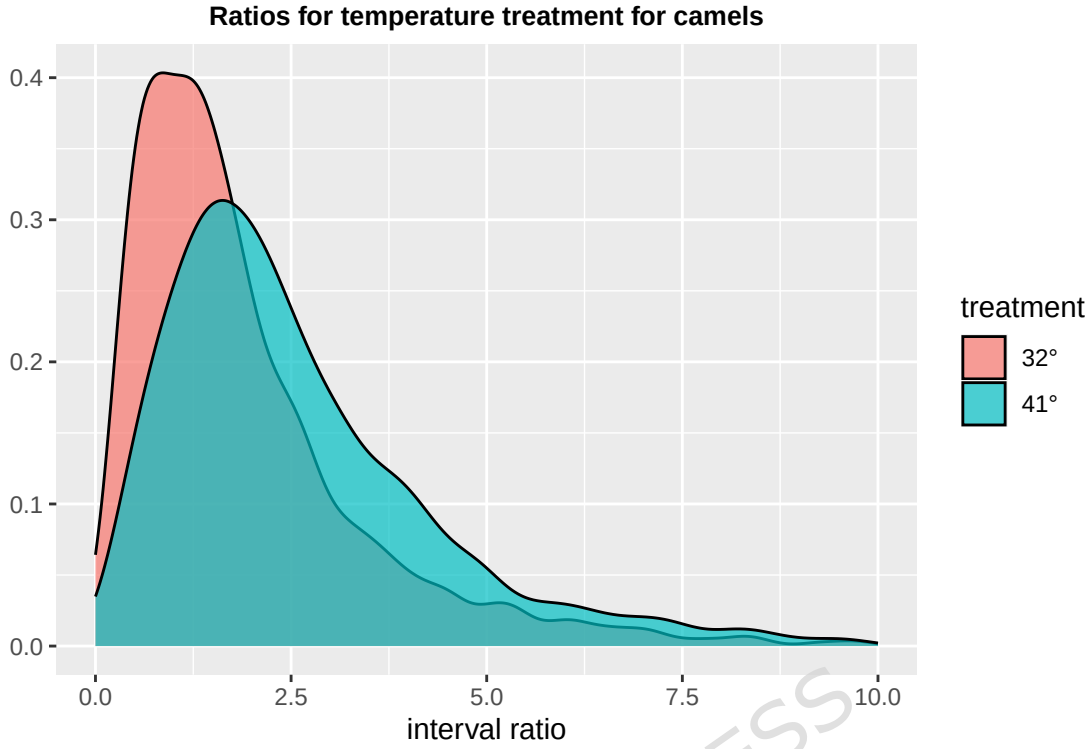

Figure 11: Distributions of the ratios of inter-individual variability before and after treatment for camels under the 32° and 41° treatments for all DEGs.

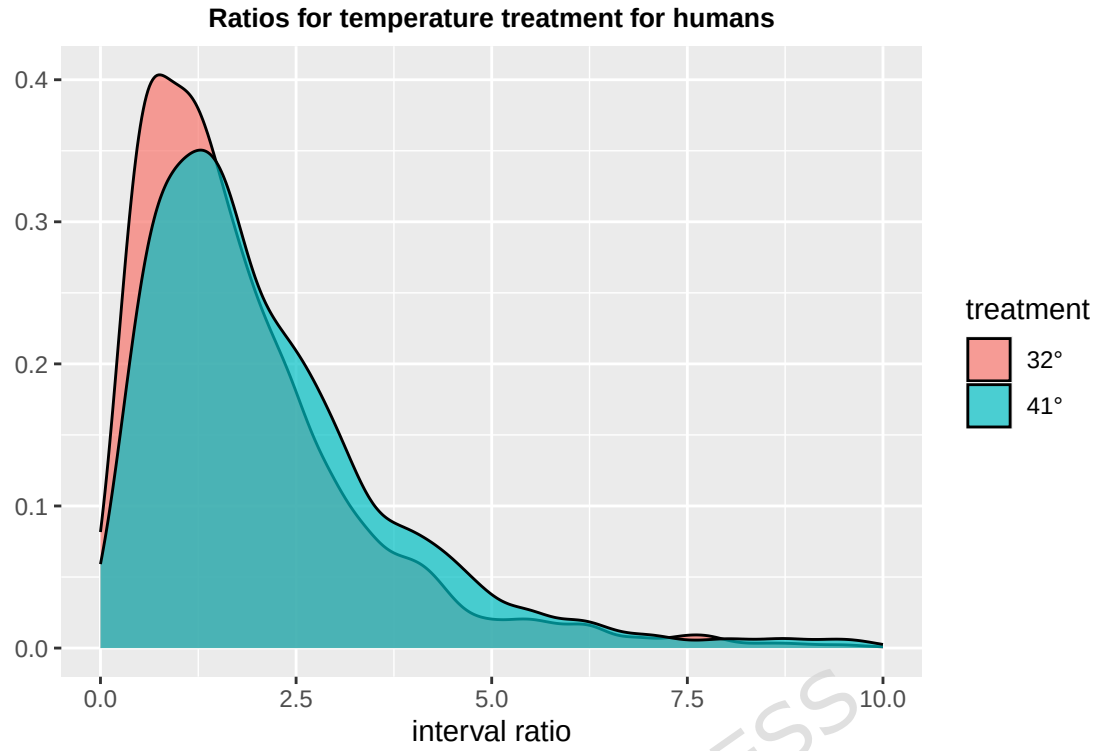

Figure 12: Distributions of the ratios of inter-individual variability before and after treatment for humans under the 32° and 41° treatments for all DEGs.

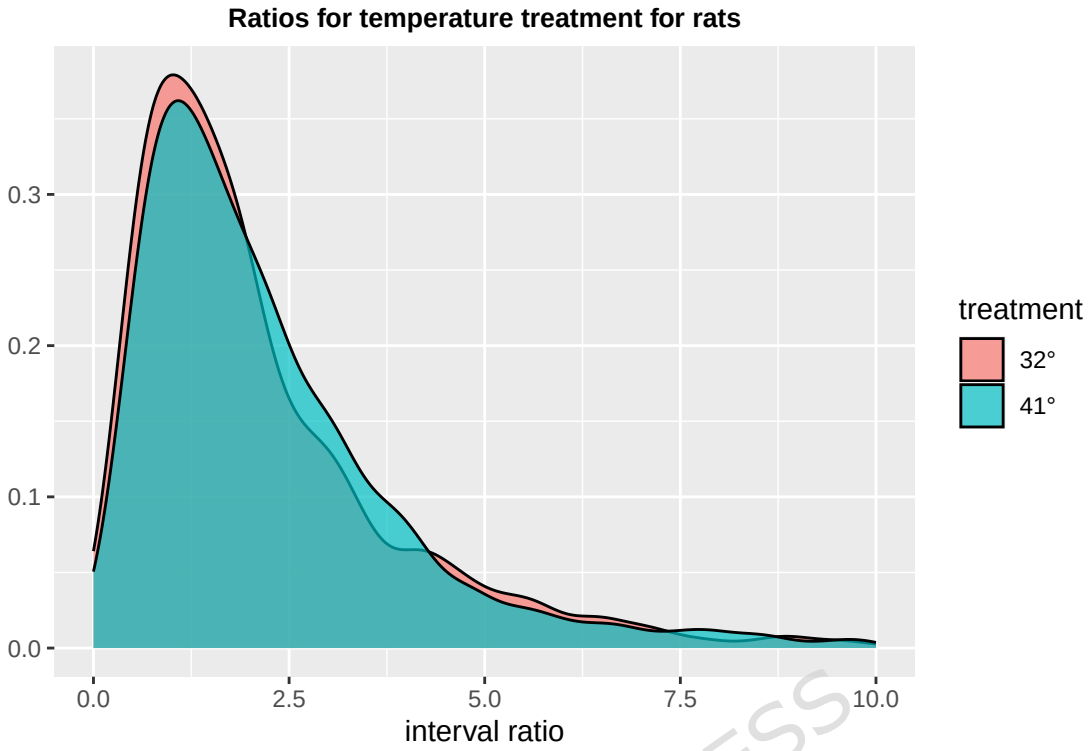

Figure 13: Distributions of the ratios of inter-individual variability before and after treatment for rats under the 32° and 41° treatments for all DEGs.

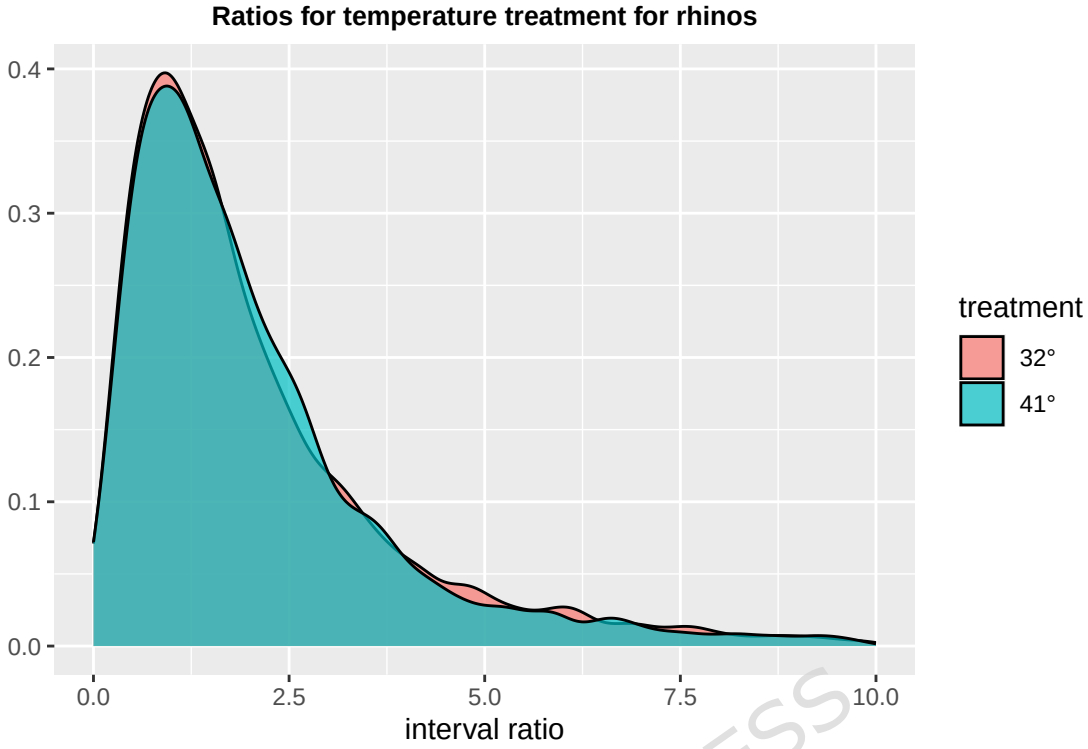

Figure 14: Distributions of the ratios of inter-individual variability before and after treatment for rhinos under the 32° and 41° treatments for all DEGs.

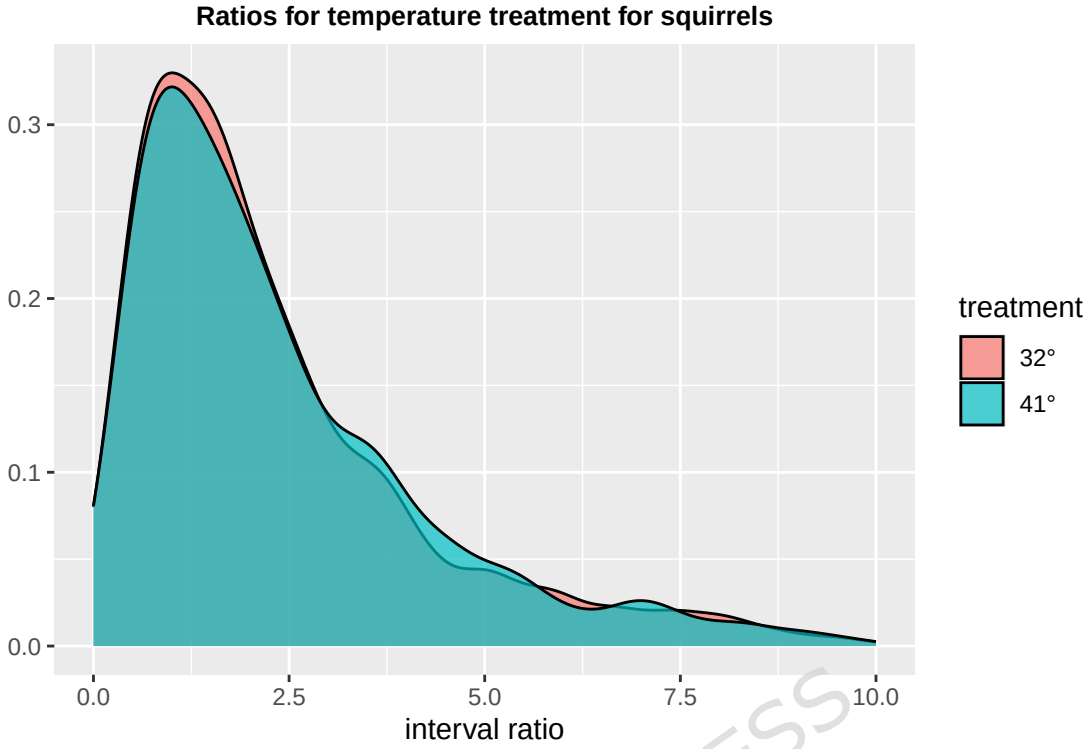

Figure 15: Distributions of the ratios of inter-individual variability before and after treatment for squirrels under the 32° and 41° treatments for all DEGs.

The figures below are useful for visualizing the peaks used to define the **extreme response sets**. Recall that the Extreme response sets are defined in terms of their relative position in the distributions of inter-individual variability at baseline and after treatment:

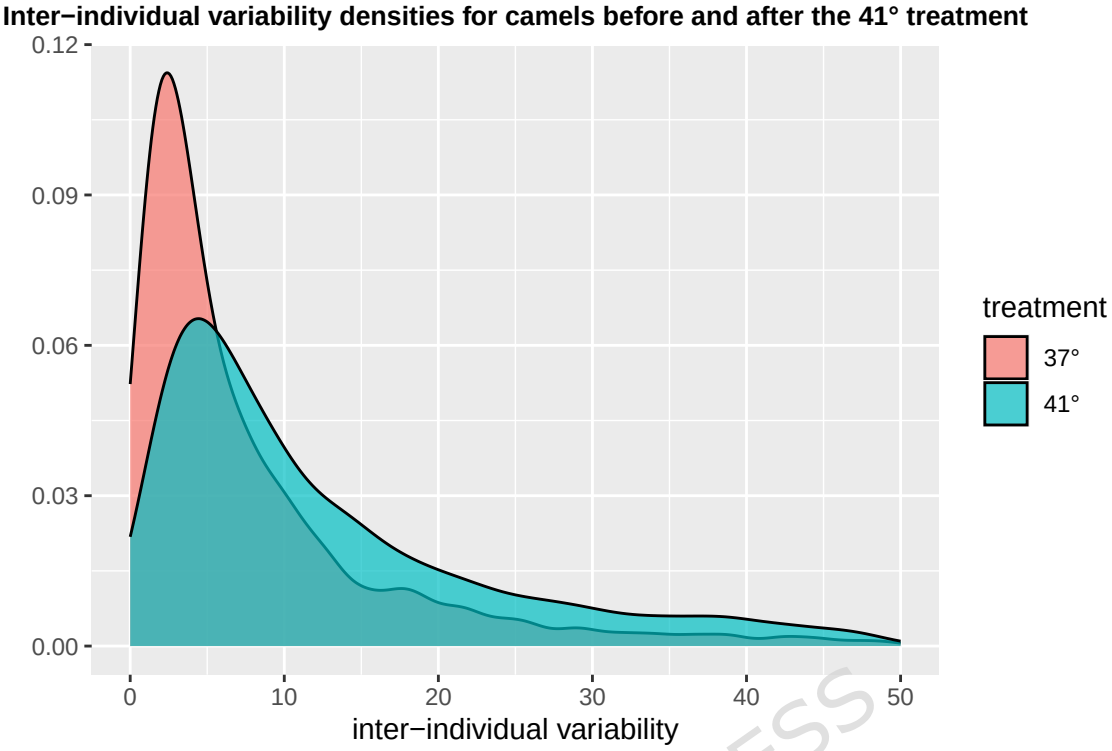

Figure 16: Distributions of the inter-individual variability for camels at 37°(baseline) and the 41° treatment for all DEGs.

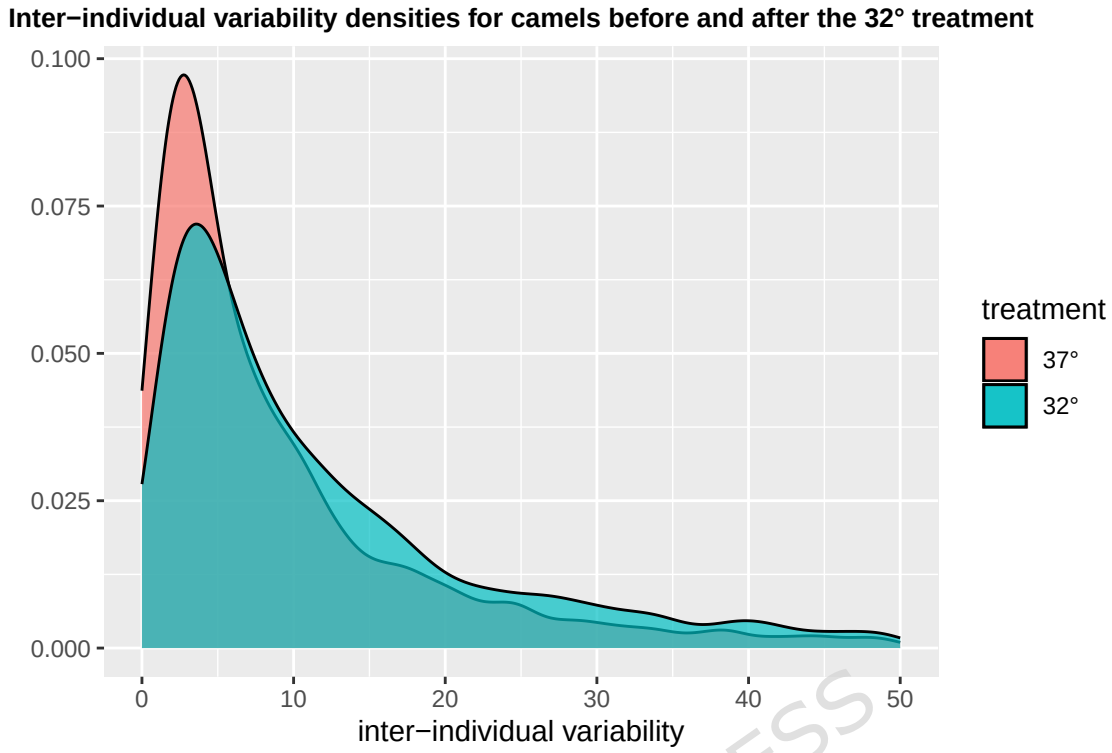

Figure 17: Distributions of the inter-individual variability for camels at 37°(baseline) and the 32° treatment for all DEGs.

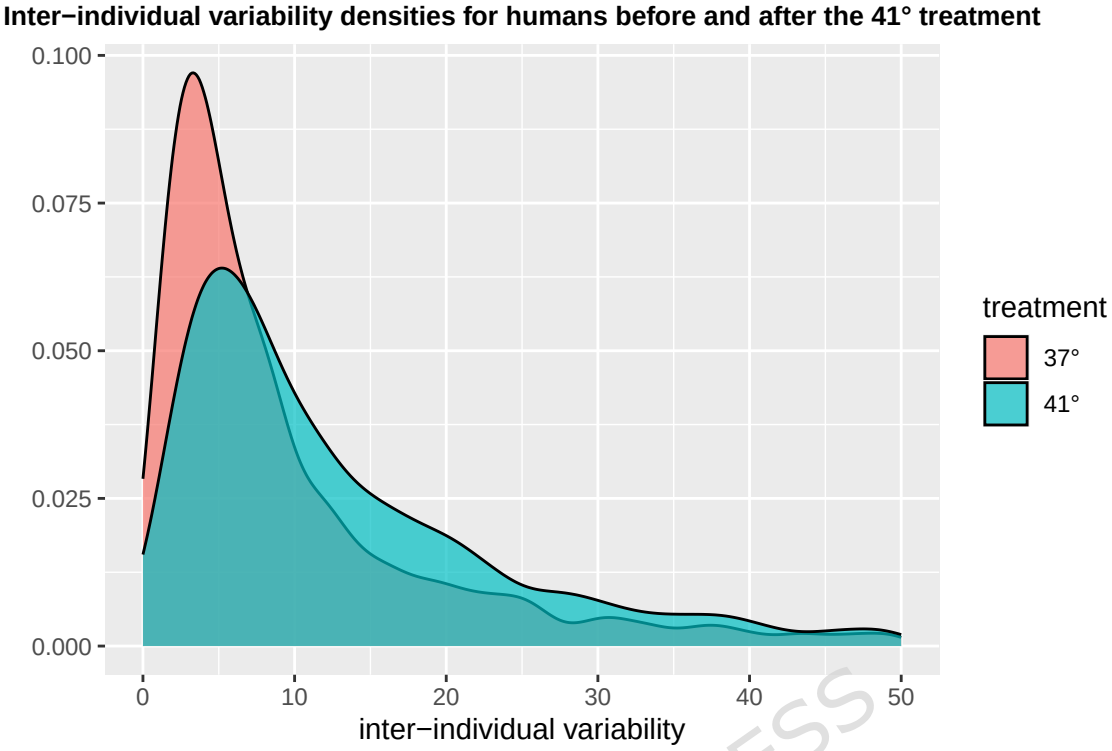

Figure 18: Distributions of the inter-individual variability for humans at 37°(baseline) and the 41° treatment for all DEGs.

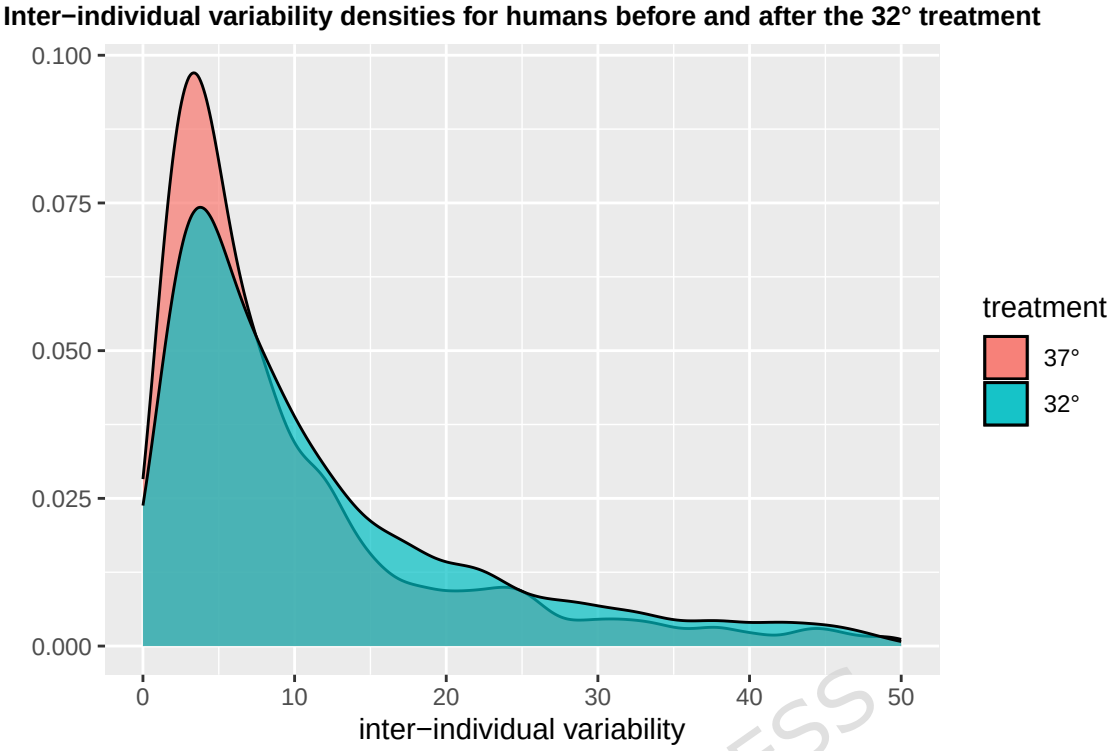

Figure 19: Distributions of the inter-individual variability for humans at 37°(baseline) and the 32° treatment for all DEGs.

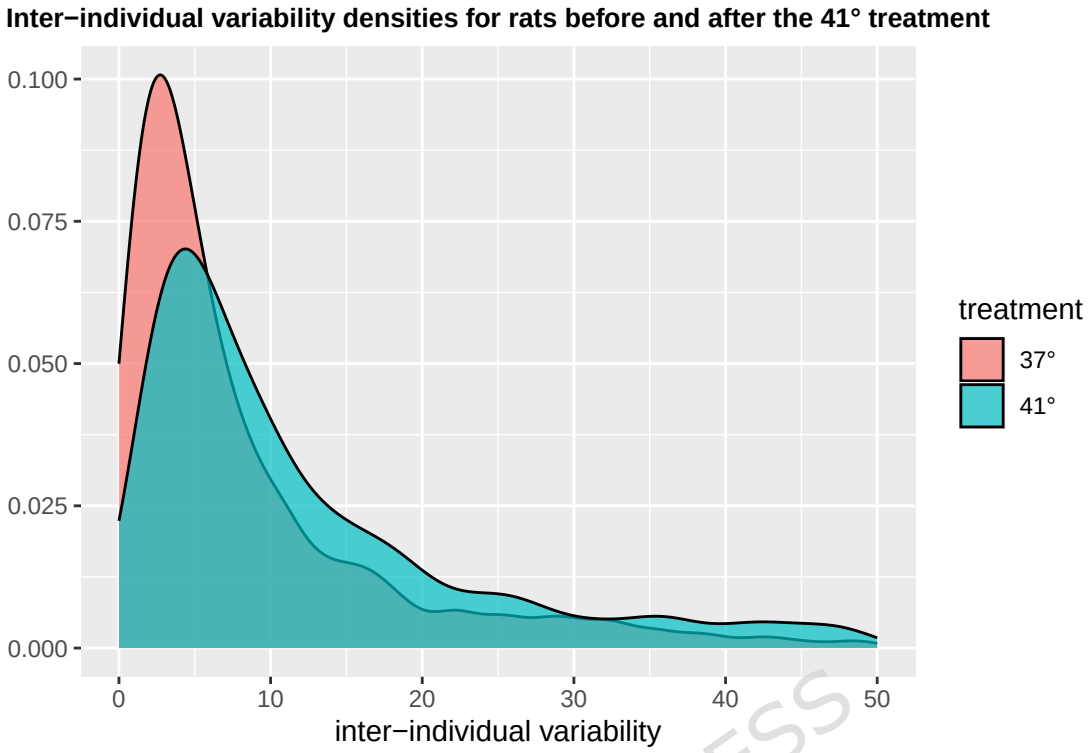

Figure 20: Distributions of the inter-individual variability for rats at 37°(baseline) and the 41° treatment for all DEGs.

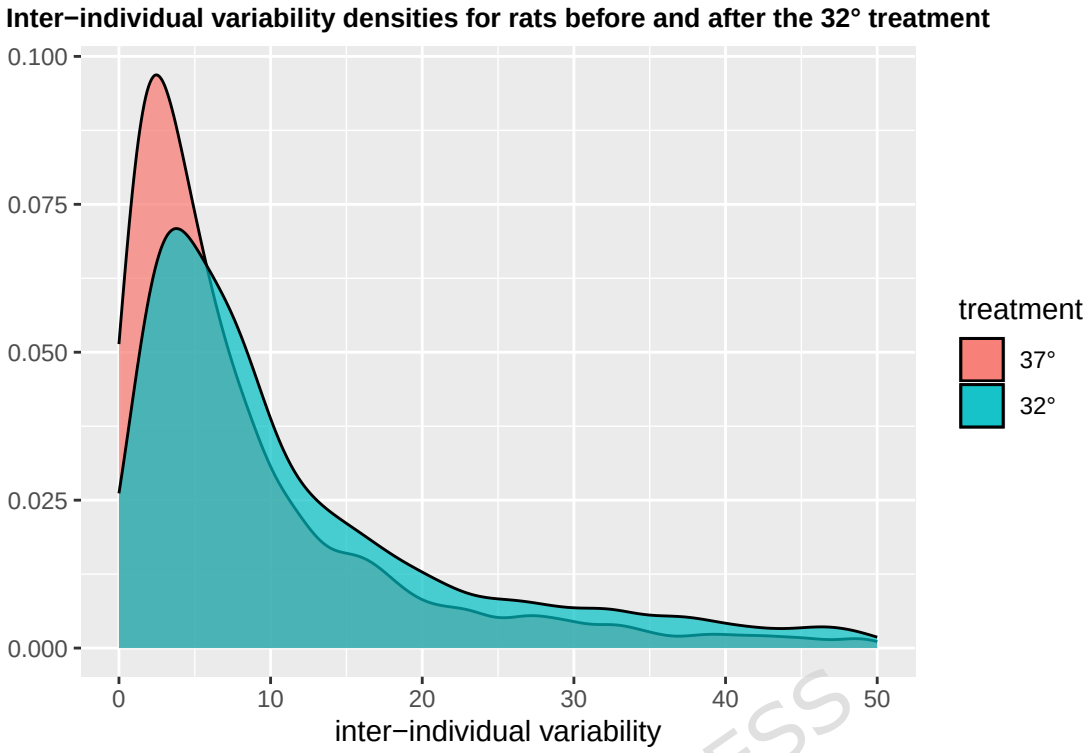

Figure 21: Distributions of the inter-individual variability for rats at 37°(baseline) and the 32° treatment for all DEGs.

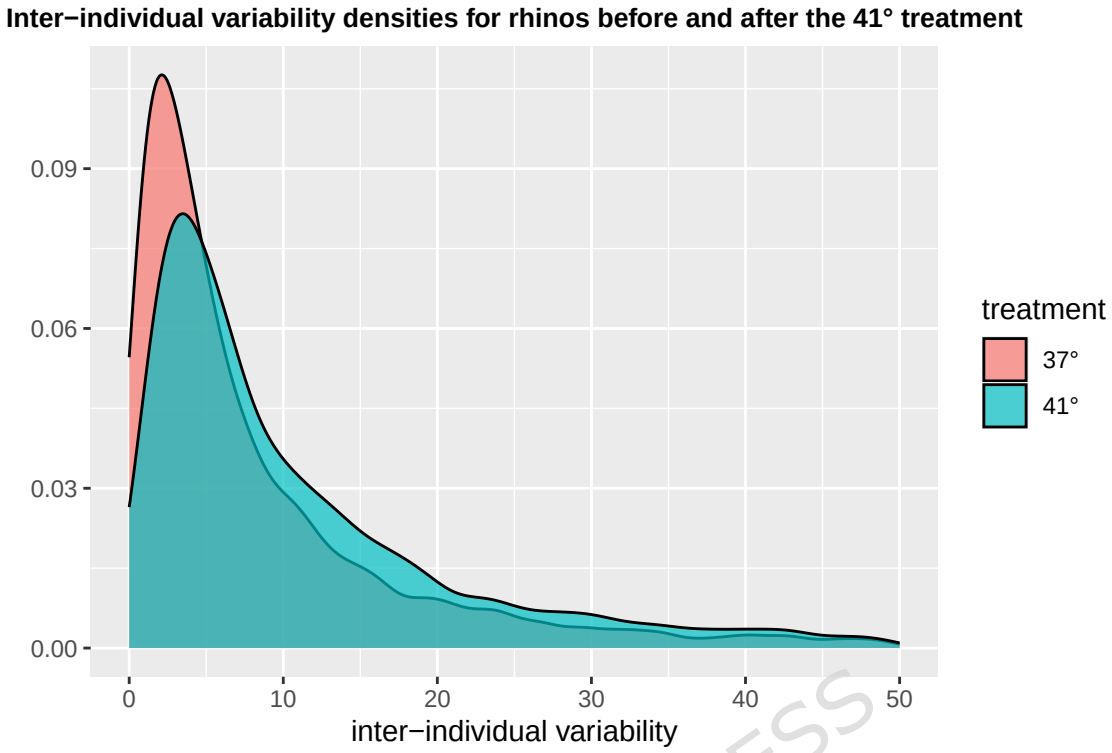

Figure 22: Distributions of the inter-individual variability for rhinos at 37°(baseline) and the 41° treatment for all DEGs.

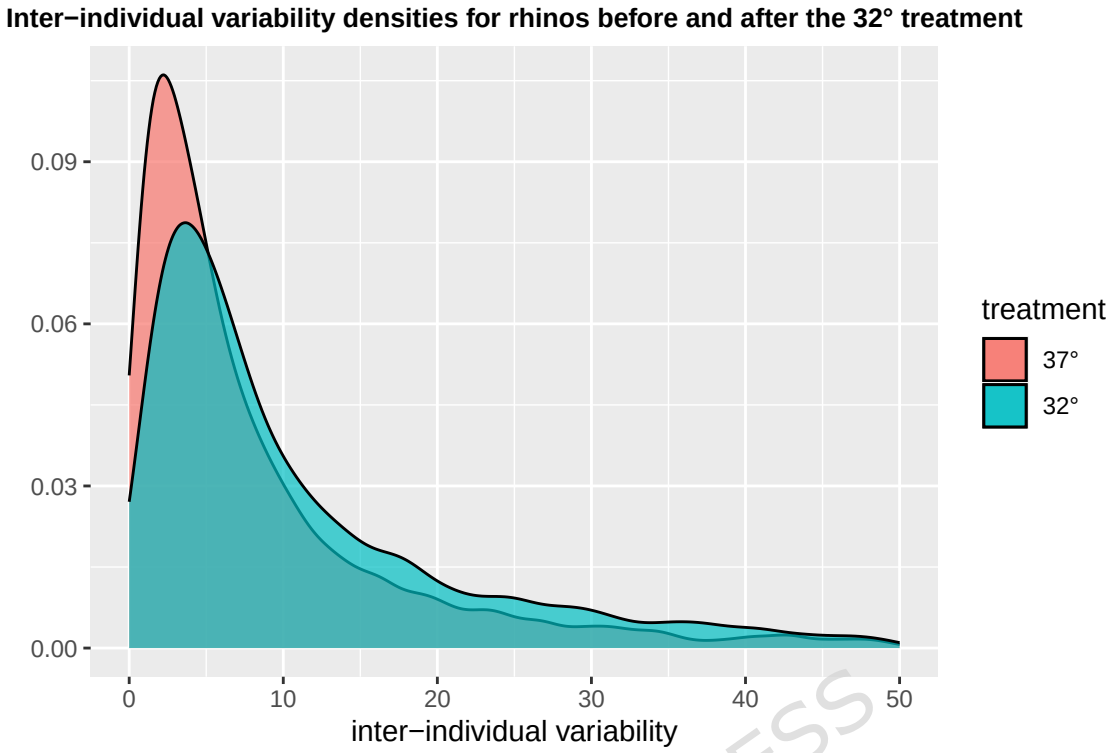

Figure 23: Distributions of the inter-individual variability for rhinos at 37°(baseline) and the 32° treatment for all DEGs.

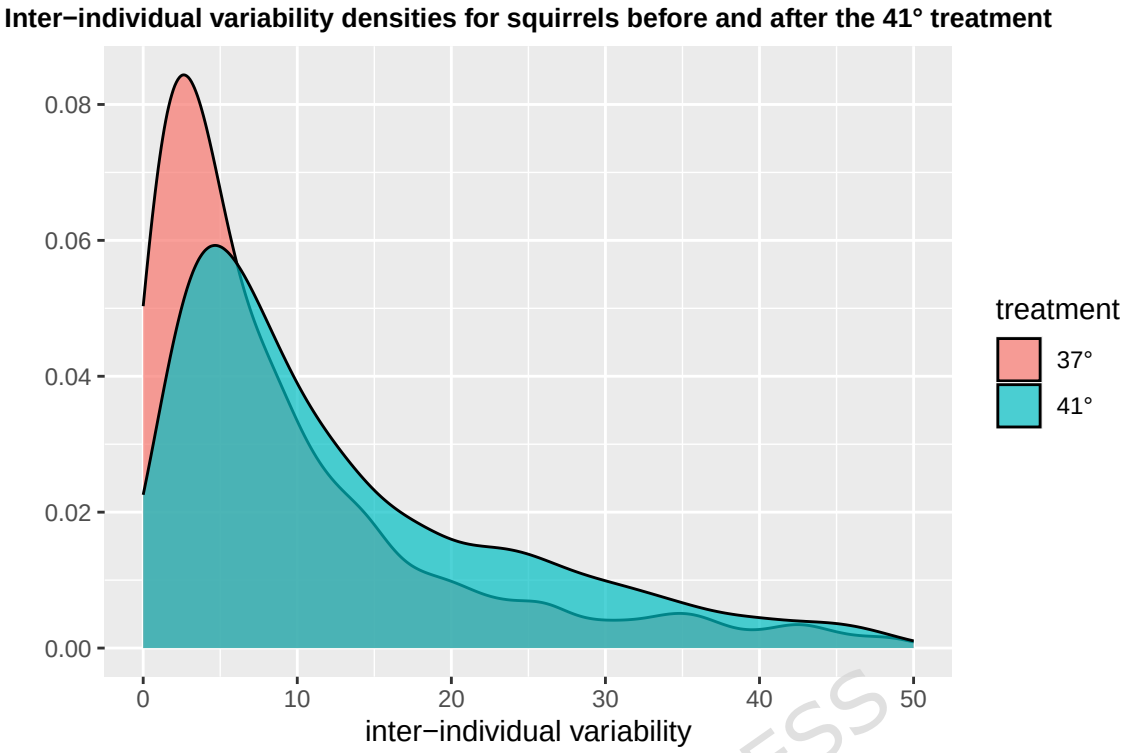

Figure 24: Distributions of the inter-individual variability for squirrels at 37°(baseline) and the 41° treatment for all DEGs.

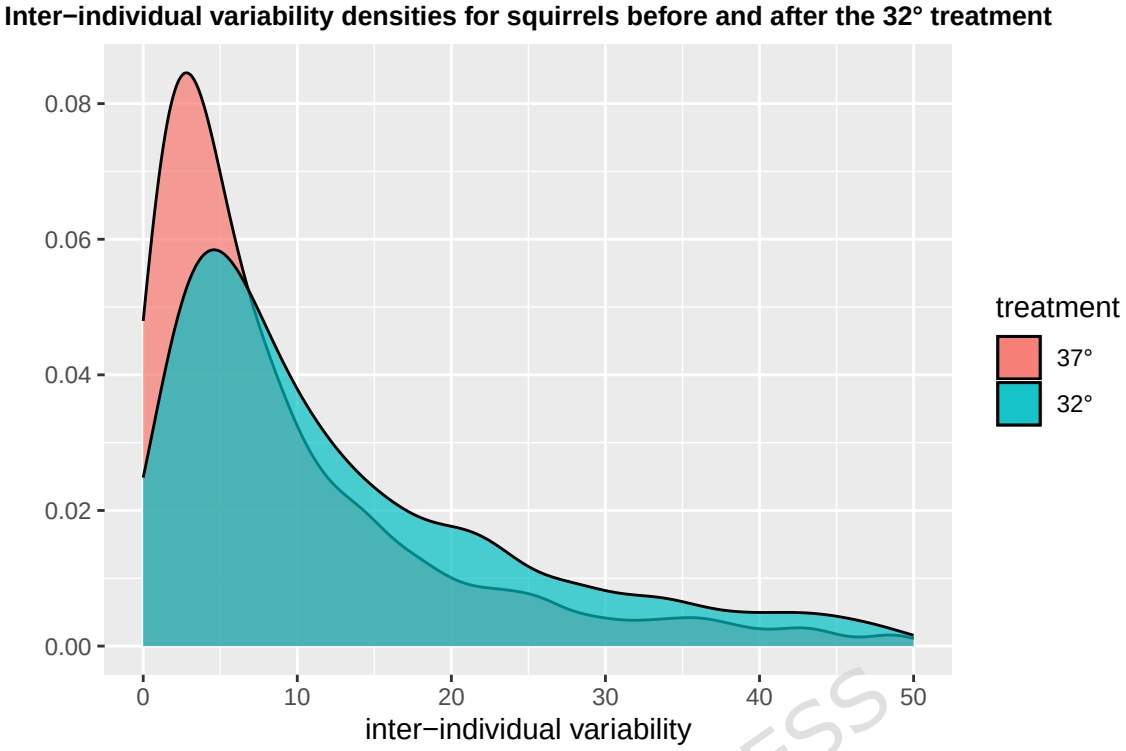

Figure 25: Distributions of the inter-individual variability for squirrels at 37°(baseline) and the 32° treatment for all DEGs.

7.3 Boxplots

For camels:

Quantiles	50%	95%
32°	0.3904	1.9444
41°	0.7574	2.2680

Table 20: Log quantiles for the 32° and 41° treatments for all DEGs according to the activity norm (6) for camels. The upper quantiles provide bounds for the ratios of the inter-individual variability of the DEGs.

The 95 percentile, for camels, for the 32° treatment is significantly smaller than for the 41° treatment.

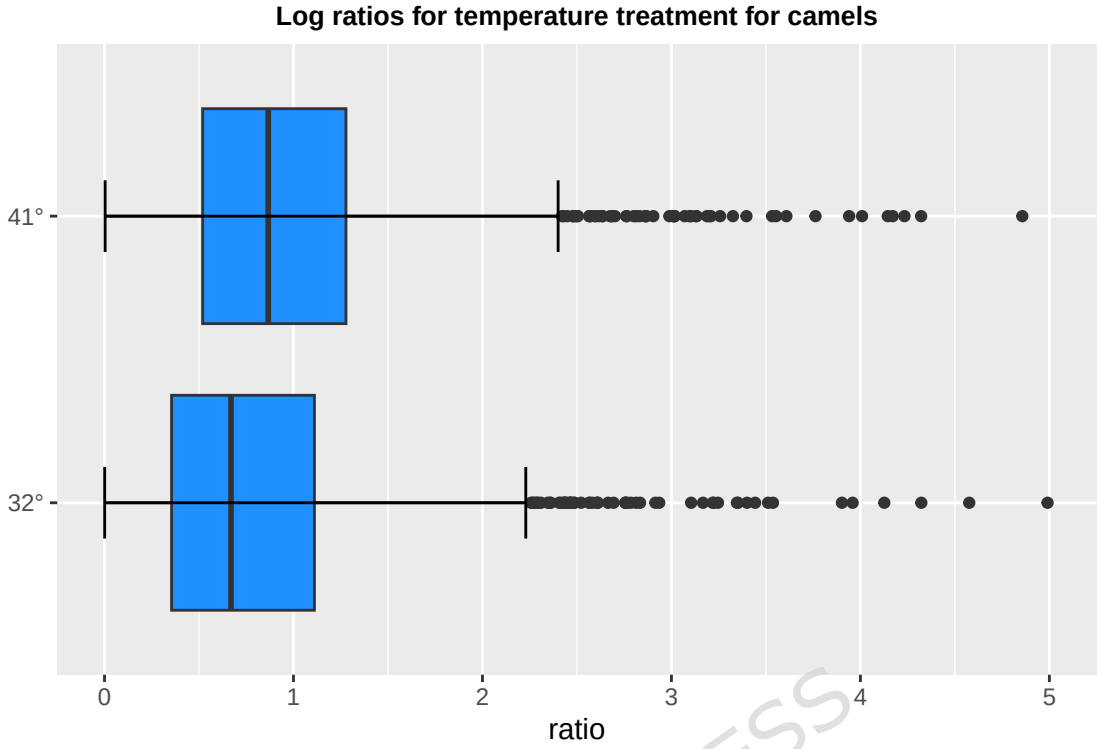

Figure 26: Boxplots of log ratios of inter-individual variability before and after treatment for camels under the 32° and 41° treatments for all DEGs. The 32° distribution is visibly more shifted to the left.
D = 0.217, p-value <2e-16
W = 2577087, p-value <2e-16

935 For humans:

Quantiles	50%	95%
32°	0.3638	1.5797
41°	0.5373	1.7092

Table 21: Log quantiles for the 32° and 41° treatments for all DEGs according to the activity norm (6) for humans. The upper quantiles provide bounds for the ratios of the inter-individual variability of the DEGs.

936 The ratios for humans are significantly smaller for the 32° than for the 41° treatment.

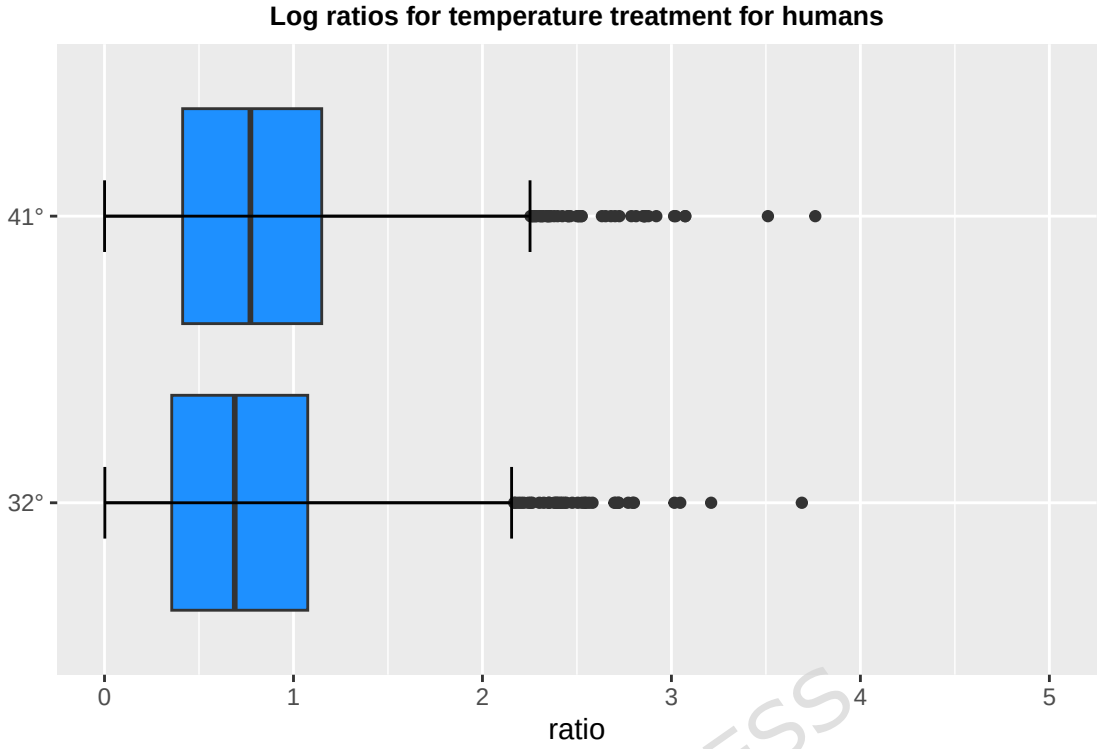

Figure 27: Boxplots of log ratios of inter-individual variability before and after treatment for humans under the 32° and 41° treatments for all DEGs. The 32° distribution is visibly more shifted to the left.
D = 0.477, p-value <2e-16
W = 3398677, p-value <2e-16

937 For rats:

Quantiles	50%	95%
32°	0.5377	2.8549
41°	0.5980	2.7749

Table 22: Log quantiles for the 32° and the 41° treatment for all DEGs according to the activity norm (6) for rats. The upper quantiles provide bounds for the ratios of the inter-individual variability of the DEGs.

938 For rats the 95 percentile, for the 32° treatment is larger than for the 41° treatment, indicating
939 the possibility that rats are better acclimated to the latter treatment.

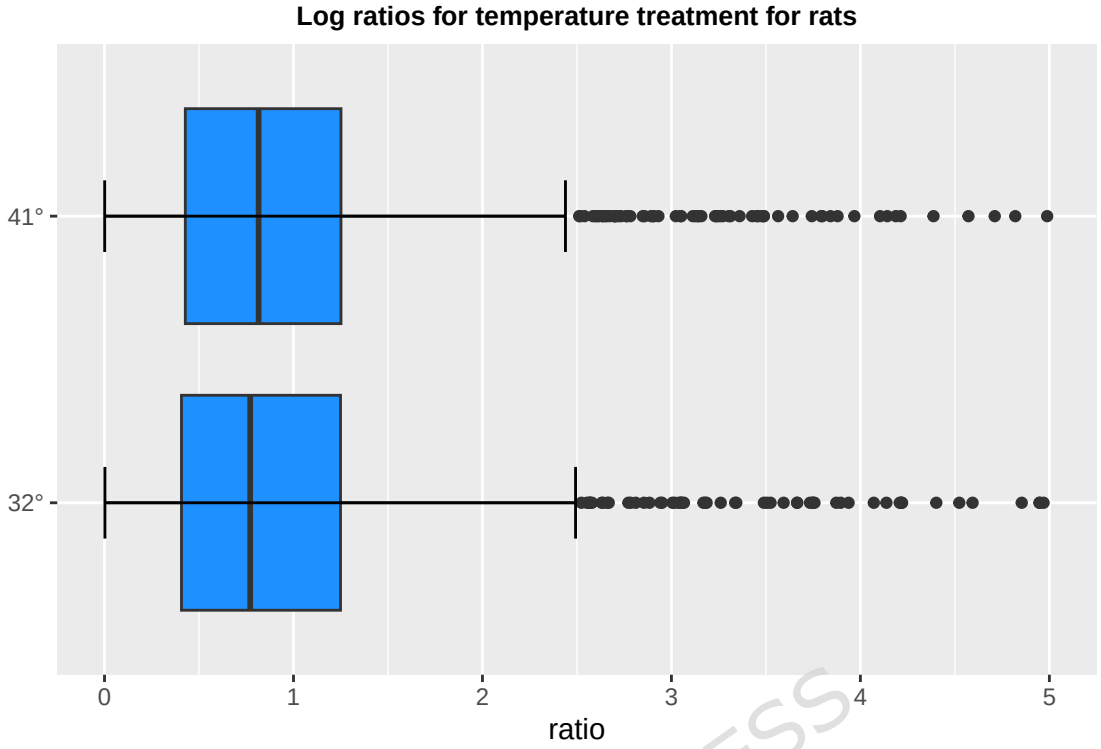

Figure 28: Boxplots of log ratios of inter-individual variability before and after treatment for rats under the 32° and 41° treatments for all DEGs.
D = 0.515, p-value <2e-16
W = 1299915, p-value <2e-16

940 For rhinos:

Quantiles	50%	95%
32°	0.4538	2.1447
41°	0.5016	2.2095

Table 23: Log quantiles for the 32° and 41° treatments for all active genes according to the activity norm (6) for rhinos. The upper quantiles provide bounds for the ratios of the inter-individual variability of the DEGs.

941 For rhinos, the ratios for the 32° treatment are again less than for the 41° treatment.

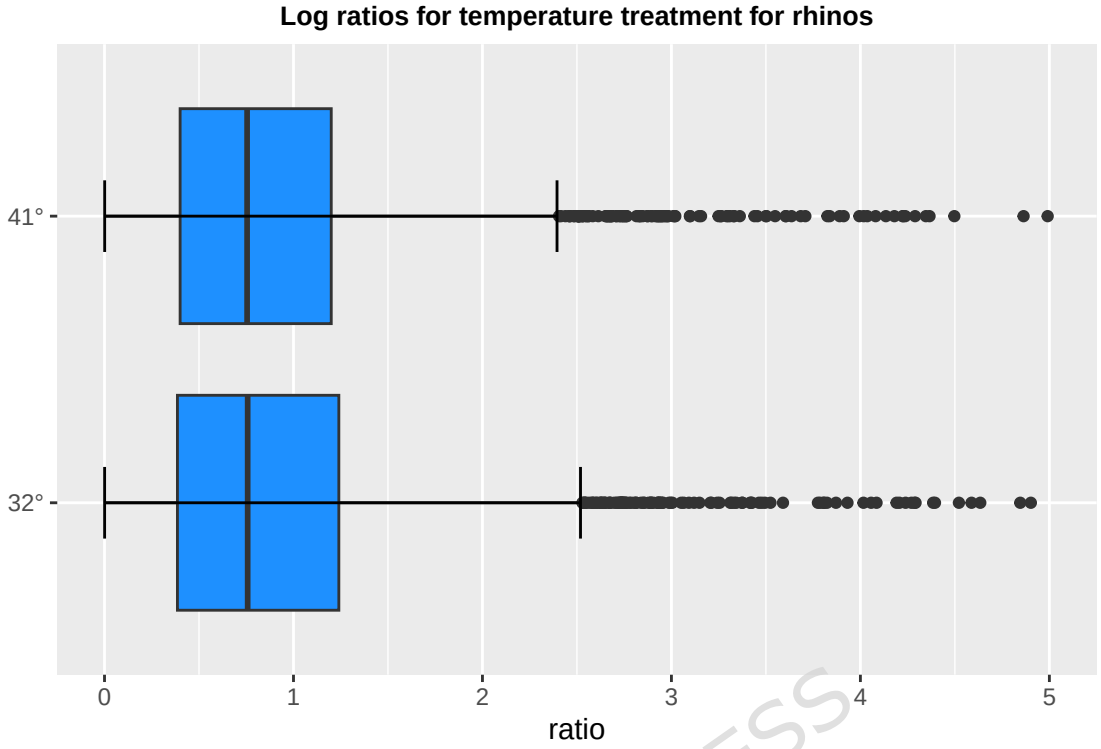

Figure 29: Boxplots of log ratios of inter-individual variability before and after treatment for rhinos under the 32° and 41° treatments for all DEGs.
D = 0.497, p-value <2e-16
W = 4090204, p-value <2e-16

7.4 Common DEGs

Below is the diagram of the common DEGs for the high temperature (41°) treatment listed according to their rank (7) for humans.

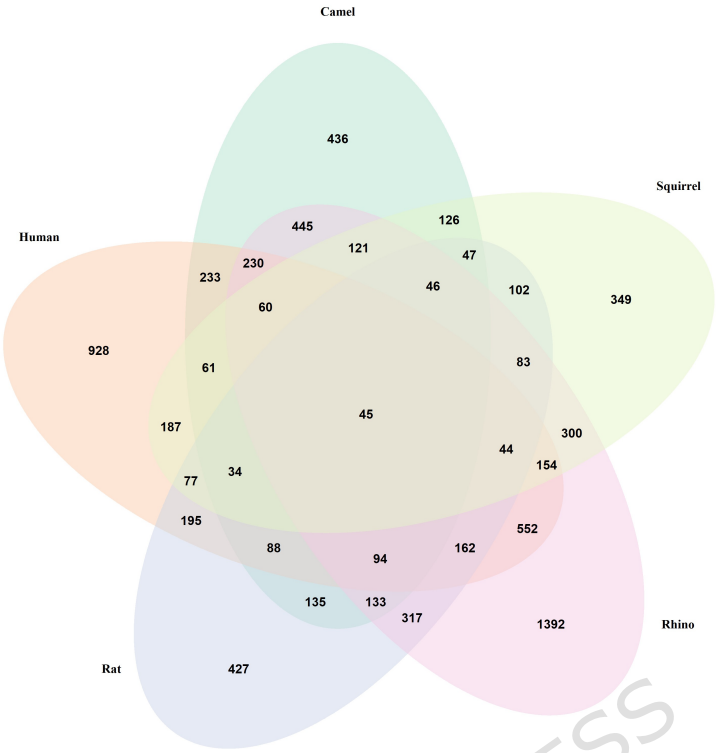

Figure 30: Diagram constructed from all DEGs for the 41° treatment.

The genes in the intersection (i.e., DEGs common to all species) are listed according to their rank (ordering) by (7) for humans: [1] "ENSG00000130724" "ENSG00000100591" "ENSG00000186480" "ENSG00000169710" "ENSG00000076067" [6] "ENSG00000102317" "ENSG00000120656" "ENSG00000167772" "ENSG00000124587" "ENSG00000088986" [11] "ENSG00000011451" "ENSG00000092199" "ENSG00000155660" "ENSG00000149257" "ENSG00000004478" [16] "ENSG00000068745" "ENSG00000110921" "ENSG00000122884" "ENSG00000144647" "ENSG00000109919" [21] "ENSG00000145919" "ENSG00000160752" "ENSG00000221821" "ENSG00000117500" "ENSG00000141002" [26] "ENSG00000007392" "ENSG00000137288" "ENSG00000120437" "ENSG00000272047" "ENSG00000086061" [31] "ENSG00000167508" "ENSG00000171148" "ENSG00000130638" "ENSG00000134262" "ENSG00000198146" [36] "ENSG00000100982" "ENSG00000198911" "ENSG00000265491" "ENSG00000188706" "ENSG00000107669" [41] "ENSG00000170345" "ENSG00000052841" "ENSG00000184557" "ENSG00000117394" "ENSG00000141013"

Below is the diagram of the common DEGs for the 32° treatment according to their rank (7) for humans.

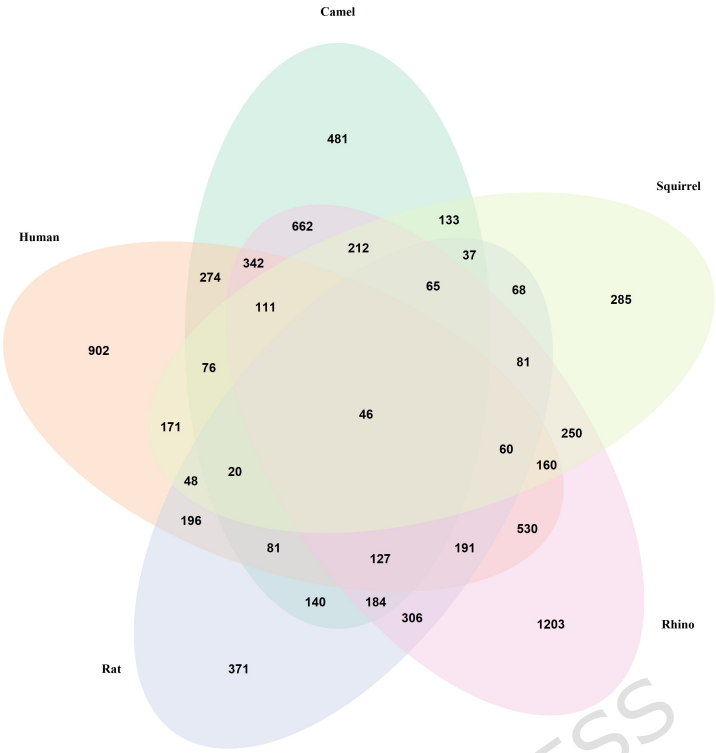

Figure 31: Diagram constructed from the active genes for the 32° treatment.

The genes in the intersection for the 32° treatment are listed according to their rank (7) for humans: [1] "ENSG00000139613" "ENSG00000112685" "ENSG00000198642" "ENSG00000241973" "ENSG00000105576" [6] "ENSG00000138413" "ENSG00000186480" "ENSG00000139514" "ENSG00000115486" "ENSG00000169710" [11] "ENSG00000070423" "ENSG00000163156" "ENSG00000114956" "ENSG00000196284" "ENSG00000103544" [16] "ENSG00000198001" "ENSG00000126249" "ENSG00000113070" "ENSG00000161920" "ENSG00000136100" [21] "ENSG00000108528" "ENSG00000158019" "ENSG00000145029" "ENSG00000001630" "ENSG00000121058" [26] "ENSG00000198911" "ENSG00000117758" "ENSG00000012061" "ENSG00000175467" "ENSG00000145919" [31] "ENSG00000172725" "ENSG00000102317" "ENSG00000131475" "ENSG00000185115" "ENSG00000120129" [36] "ENSG00000137207" "ENSG00000117505" "ENSG00000142039" "ENSG00000104549" "ENSG00000113845" [41] "ENSG00000166295" "ENSG00000136146" "ENSG00000136485" "ENSG00000160310" "ENSG00000187024" [46] "ENSG00000115226"

7.5 Extreme response sets

Below we present the number genes in each of the extreme sets for Camels, Humans, Rats, Rhinos, and Squirrels, including different criteria for "large" in the definitions of the extreme response groups :

	Camels	Humans	Rats	Rhinos	Squirrels
DEGs	2334	3144	2029	4178	1836
Key-Response	352	412	296	518	245

Table 24: Numbers of active genes belonging to the Key-Response set at 41° for camels, humans, rats, rhinos, squirrels.

	Camels	Humans	Rats	Rhinos	Squirrels
DEGs	2334	3144	2029	4178	1836
Treatment-specific 50%	46	82	55	104	38
Treatment-specific 60%	23	45	22	53	19
Treatment-specific 70%	6	22	10	28	4
Treatment-specific 80%	0	10	6	8	0
Treatment-specific 90%	0	1	2	3	0

Table 25: Numbers of active genes belonging to the Treatment-Specific set at 41° for camels, humans, rats, rhinos, and squirrels.

	Camels	Humans	Rats	Rhinos	Squirrels
DEGs	2334	3144	2029	4178	1836
Support 50%	298	334	176	333	140
Support 60%	237	257	135	244	140
Support 70%	166	186	98	180	59
Support 80%	104	124	59	109	38
Support 90%	48	59	24	52	18

Table 26: Numbers of active genes belonging to the Support set at 41° for camels, humans, rats, rhinos, and squirrels.

	Camels	Humans	Rats	Rhinos	Squirrels
DEGs	2334	3144	2029	4178	1836
Noisy 50%	69	77	62	112	63
Noisy 60%	40	33	36	78	47
Noisy 70%	23	10	24	44	33
Noisy 80%	13	1	9	21	13
Noisy 90%	5	0	4	6	5

Table 27: Numbers of active genes belonging to the Noisy set at 41° for camels, humans, rats, rhinos, and squirrels.

	Camels	Humans	Rats	Rhinos	Squirrels
DEGs	2991	3335	2021	4530	1462
Key-Response	406	426	264	548	149

Table 28: Numbers of active genes belonging to the Key-Response set at 32° for camels, humans, rats, rhinos, and squirrels.

	Camels	Humans	Rats	Rhinos	Squirrels
DEGs	2991	3335	2021	4530	1462
Treatment-specific 50%	73	97	42	136	52
Treatment-specific 60%	37	47	23	64	25
Treatment-specific 70%	12	20	12	27	10
Treatment-specific 80%	1	9	3	7	6
Treatment-specific 90%	0	1	1	1	1

Table 29: Numbers of active genes belonging to the Treatment-Specific set at 32° for camels, humans, rats, rhinos, and squirrels.

	Camels	Humans	Rats	Rhinos	Squirrels
DEGs	2991	3335	2021	4530	1462
Support 50%	234	266	167	330	100
Support 60%	166	189	124	234	77
Support 70%	114	129	85	159	54
Support 80%	63	76	41	87	39
Support 90%	35	28	17	38	14

Table 30: Numbers of active genes belonging to the Support set at 32° for camels, humans, rats, rhinos, and squirrels.

	Camels	Humans	Rats	Rhinos	Squirrels
DEGs	2991	3335	2021	4530	1462
Noisy 50%	98	102	68	129	72
Noisy 60%	59	44	44	73	46
Noisy 70%	35	15	26	35	23
Noisy 80%	17	3	15	20	13
Noisy 90%	9	0	8	8	8

Table 31: Numbers of active genes belonging to the Noisy set at 32° for camels, humans, rats, rhinos, and squirrels.

7.6 Network predictions

In the tables below we show the results from training neural networks with the Key-Response group, the Treatment-Specific group, and the Noisy group for humans and camels for the 32° and 41° treatments. Humans and camels are chosen as representatives for the strict and flexible homeostasis mammals respectively, in order to compare their networks. The Response Prediction column shows the intervals containing the output of the trained networks with baseline conditions as input. The Stability Prediction column shows the intervals containing the output of the trained networks with observations after treatment used as the input conditions. Response Prediction assesses how well the networks represent the response of the species, whereas Stability Prediction measures how well homeostasis is approximated after treatment. In particular, in the case of the Treatment-Specific group and the Noisy group Stability Prediction indicates whether the intervals continue to contract, expand, or are stable.

Gene	Observation	Response Prediction	Error 1	Stability Prediction	Error 2
ENSG00000151881	[11.063, 18.834]	[10.9, 18.325]	0.022	[10.874, 17.957]	0.036
ENSG00000109572	[16.057, 18.547]	[13.671, 20.802]	0.134	[13.57, 20.441]	0.127
ENSG00000142330	[8.972, 12.256]	[6.751, 13.272]	0.152	[6.77, 13.012]	0.139
ENSG00000136478	[15.246, 21.338]	[15.118, 23.135]	0.053	[15.13, 22.665]	0.039
ENSG00000164168	[13.155, 14.962]	[10.081, 18.052]	0.219	[10.023, 17.527]	0.203
ENSG00000176994	[7.299, 9.314]	[5.028, 11.205]	0.251	[5.043, 11.035]	0.239
ENSG00000101407	[6.193, 9.446]	[4.051, 10.357]	0.195	[4.071, 10.168]	0.182
ENSG00000132330	[4.142, 5.417]	[1.485, 8.045]	0.553	[1.479, 7.778]	0.526
ENSG00000082516	[6.613, 8.814]	[3.749, 10.486]	0.294	[3.824, 10.245]	0.274
ENSG00000093217	[1.421, 3.127]	[-0.0, 5.355]	0.802	[-0.0, 5.071]	0.74

Table 32: Inter-individual variability intervals for the Key-Response genes for Humans at 32° for the top 10 genes. Comparison of observed intervals vs predicted by trained networks. The fractional errors, Error 1 and Error 2, are computed according to formulas (13) and (14).

Gene	Observation	Response Prediction	Error 1	Stability Prediction	Error 2
ENSG00000133104	[19.197, 26.009]	[21.748, 27.212]	0.083	[18.763, 19.921]	0.144
ENSG00000127948	[38.091, 50.447]	[38.619, 50.449]	0.006	[37.843, 40.558]	0.114
ENSG00000154803	[16.398, 19.8]	[16.843, 18.817]	0.039	[16.388, 16.79]	0.083
ENSG00000117614	[72.455, 89.65]	[70.811, 91.606]	0.022	[58.198, 62.925]	0.253
ENSG00000138801	[45.56, 52.936]	[47.068, 54.114]	0.027	[35.259, 38.842]	0.248
ENSG00000075420	[55.156, 57.33]	[50.535, 60.568]	0.07	[44.3, 46.467]	0.193
ENSG00000052802	[16.91, 24.462]	[19.96, 24.564]	0.076	[17.87, 18.876]	0.158
ENSG00000134108	[12.002, 23.902]	[17.734, 21.301]	0.232	[18.503, 19.595]	0.301
ENSG00000102032	[0.594, 2.675]	[0.54, 1.079]	0.505	[0.749, 0.875]	0.598
ENSG00000138078	[5.105, 9.103]	[5.699, 6.531]	0.223	[5.941, 6.154]	0.266

Table 33: Inter-individual variability intervals for the Treatment-Specific genes for Humans at 32° for the top 10 genes. Comparison of observed intervals vs predicted by trained networks. The fractional errors, Error 1 and Error 2, are computed according to formulas (13) and (14).

Gene	Observation	Response Prediction	Error 1	Stability Prediction	Error 2
ENSG00000113812	[25.157, 44.798]	[31.714, 34.901]	0.235	[29.651, 37.985]	0.162
ENSG00000182872	[19.306, 29.141]	[19.871, 21.947]	0.16	[18.17, 23.896]	0.132
ENSG00000109220	[50.979, 78.179]	[56.321, 65.479]	0.14	[51.152, 74.007]	0.034
ENSG00000011007	[14.222, 40.918]	[21.593, 30.927]	0.315	[17.16, 37.803]	0.11
ENSG00000221821	[15.52, 34.153]	[19.618, 23.446]	0.298	[16.893, 26.558]	0.181
ENSG00000227057	[66.175, 79.663]	[66.426, 76.097]	0.026	[62.21, 83.848]	0.056
ENSG00000124875	[1.414, 21.149]	[8.017, 11.235]	0.732	[7.025, 14.177]	0.558
ENSG00000026559	[6.352, 23.306]	[15.13, 18.696]	0.451	[13.307, 21.808]	0.285
ENSG00000181915	[12.845, 24.9]	[16.838, 18.832]	0.267	[15.283, 20.472]	0.182
ENSG00000182180	[23.254, 41.483]	[22.966, 25.855]	0.246	[21.329, 28.605]	0.229

Table 34: Inter-individual variability intervals for the Noisy genes for Humans at 32° for the top 10 genes. Comparison of observed intervals vs predicted by trained networks. The fractional errors, Error 1 and Error 2, are computed according to formulas (13) and (14).

Gene	Observation	Response Prediction	Error 1	Stability Prediction	Error 2
ENSG00000105514	[6.644, 11.372]	[6.578, 14.253]	0.164	[5.267, 15.789]	0.322
ENSG00000163961	[8.362, 11.999]	[5.722, 13.086]	0.183	[4.56, 14.611]	0.315
ENSG00000074582	[28.946, 33.559]	[27.674, 38.276]	0.096	[26.269, 40.869]	0.16
ENSG00000126705	[21.513, 25.189]	[18.777, 28.376]	0.127	[17.427, 30.402]	0.199
ENSG00000109118	[16.651, 18.682]	[12.711, 21.758]	0.199	[11.344, 23.946]	0.299
ENSG00000184602	[7.984, 15.332]	[6.509, 15.098]	0.073	[5.129, 18.87]	0.274
ENSG00000096968	[8.278, 13.187]	[5.791, 13.416]	0.127	[4.658, 15.144]	0.26
ENSG00000108262	[37.114, 44.58]	[33.797, 46.668]	0.066	[31.951, 49.704]	0.126
ENSG00000183665	[8.19, 12.351]	[5.043, 12.331]	0.154	[3.749, 13.855]	0.289
ENSG00000130758	[20.569, 24.657]	[17.984, 27.186]	0.113	[16.739, 29.251]	0.186

Table 35: Inter-individual variability intervals for the Key-Response genes for Humans at 41° for the top 10 genes. Comparison of observed intervals vs predicted by trained networks. The fractional errors, Error 1 and Error 2, are computed according to formulas (13) and (14).

Gene	Observation	Response Prediction	Error 1	Stability Prediction	Error 2
ENSG00000230124	[17.656, 22.366]	[17.652, 19.115]	0.081	[17.838, 18.321]	0.106
ENSG00000118960	[21.334, 26.062]	[22.183, 25.127]	0.038	[22.029, 22.884]	0.082
ENSG00000154803	[17.802, 26.947]	[21.818, 25.741]	0.117	[21.099, 22.22]	0.179
ENSG00000139428	[6.516, 11.384]	[8.482, 9.58]	0.211	[8.887, 9.266]	0.251
ENSG00000102032	[0.39, 1.142]	[0.406, 1.203]	0.05	[0.645, 0.9]	0.325
ENSG00000145390	[7.972, 11.553]	[9.129, 10.78]	0.099	[9.053, 9.608]	0.155
ENSG00000090487	[62.85, 71.837]	[61.308, 74.283]	0.03	[58.458, 62.224]	0.104
ENSG00000179604	[36.008, 41.285]	[35.822, 40.411]	0.014	[34.882, 36.136]	0.081
ENSG00000126767	[44.606, 52.648]	[43.758, 51.118]	0.024	[42.489, 44.51]	0.105
ENSG00000103353	[32.337, 44.014]	[38.679, 44.338]	0.087	[36.99, 38.459]	0.134

Table 36: Inter-individual variability intervals for the Treatment-Specific genes for Humans at 41° for the top 10 genes. Comparison of observed intervals vs predicted by trained networks. The fractional errors, Error 1 and Error 2, are computed according to formulas (13) and (14).

Gene	Observation	Response Prediction	Error 1	Stability Prediction	Error 2
ENSG00000026559	[19.335, 34.83]	[28.121, 31.471]	0.224	[26.056, 36.131]	0.148
ENSG00000116685	[65.525, 95.388]	[69.489, 79.099]	0.126	[65.347, 94.424]	0.007
ENSG00000175387	[18.342, 69.288]	[17.06, 52.976]	0.201	[17.996, 103.054]	0.389
ENSG00000176454	[34.389, 56.251]	[36.215, 40.38]	0.195	[34.832, 45.981]	0.118
ENSG00000182872	[49.825, 61.927]	[49.244, 55.647]	0.061	[45.435, 59.332]	0.063
ENSG00000171497	[45.237, 70.254]	[50.874, 60.913]	0.13	[51.963, 78.545]	0.13
ENSG00000182180	[19.797, 36.477]	[20.725, 22.189]	0.27	[19.371, 23.995]	0.229
ENSG00000122965	[18.576, 34.204]	[19.232, 20.576]	0.271	[18.126, 22.397]	0.232
ENSG00000136478	[24.664, 39.739]	[26.498, 28.654]	0.201	[25.353, 31.968]	0.131
ENSG00000163320	[63.244, 86.488]	[68.261, 79.704]	0.079	[66.656, 87.734]	0.031

Table 37: Inter-individual variability intervals for the Noisy genes for Humans at 41° for the top 10 genes. Comparison of observed intervals vs predicted by trained networks. The fractional errors, Error 1 and Error 2, are computed according to formulas (13) and (14).

Gene	Observation	Response Prediction	Error 1	Stability Prediction	Error 2
ENSG00000113240	[5.587, 8.642]	[4.316, 11.119]	0.263	[3.442, 12.002]	0.387
ENSG00000204843	[-0.0, 3.113]	[-0.0, 4.148]	0.333	[-0.0, 4.963]	0.594
ENSG00000055332	[-0.0, 2.198]	[-0.0, 4.733]	1.153	[-0.0, 5.62]	1.557
ENSG00000025772	[23.283, 27.519]	[21.23, 29.87]	0.087	[20.047, 30.518]	0.123
ENSG00000174437	[1.098, 1.512]	[-0.0, 5.33]	1.883	[-0.0, 6.577]	2.36
ENSG00000156502	[6.732, 10.555]	[6.232, 12.775]	0.157	[5.238, 13.572]	0.261
ENSG00000122033	[7.142, 7.78]	[4.377, 10.71]	0.382	[3.593, 11.678]	0.499
ENSG00000130021	[15.477, 20.038]	[14.431, 21.223]	0.063	[13.671, 22.048]	0.107
ENSG00000143373	[15.629, 18.579]	[13.093, 21.015]	0.145	[11.998, 22.007]	0.206
ENSG00000113272	[11.956, 15.628]	[9.703, 17.366]	0.145	[8.779, 18.197]	0.208

Table 38: Inter-individual variability intervals for the Key-Response genes for Camels at 32° for the top 10 genes. Comparison of observed intervals vs predicted by trained networks. The fractional errors, Error 1 and Error 2, are computed according to formulas (13) and (14).

Gene	Observation	Response Prediction	Error 1	Stability Prediction	Error 2
ENSG00000118816	[56.735, 61.825]	[53.014, 65.81]	0.065	[50.367, 56.01]	0.103
ENSG00000100417	[10.271, 14.917]	[10.59, 13.399]	0.073	[10.68, 11.997]	0.132
ENSG00000100403	[35.349, 47.615]	[37.143, 48.337]	0.03	[37.397, 42.177]	0.09
ENSG00000126545	[17.886, 22.241]	[17.915, 21.573]	0.017	[17.828, 19.372]	0.073
ENSG00000048828	[62.446, 66.18]	[58.171, 72.008]	0.079	[54.749, 60.813]	0.102
ENSG00000185761	[26.272, 29.618]	[25.798, 30.112]	0.017	[25.906, 27.761]	0.04
ENSG00000180354	[13.18, 16.621]	[13.116, 15.44]	0.042	[13.386, 14.338]	0.083
ENSG00000135521	[32.671, 41.319]	[35.503, 44.021]	0.075	[33.596, 37.359]	0.066
ENSG00000164062	[12.921, 16.589]	[13.317, 17.066]	0.03	[13.183, 14.912]	0.066
ENSG00000285025	[36.267, 45.838]	[40.404, 46.728]	0.061	[36.082, 41.169]	0.059

Table 39: Inter-individual variability intervals for the Treatment-Specific genes for Camels at 32° for the top 10 genes. Comparison of observed intervals vs predicted by trained networks. The fractional errors, Error 1 and Error 2, are computed according to formulas (13) and (14).

Gene	Observation	Response Prediction	Error 1	Stability Prediction	Error 2
ENSG00000060762	[-0.0, 224.047]	[-0.0, 250.247]	0.117	[-0.0, 253.88]	0.133
ENSG00000127922	[-0.0, 160.942]	[-0.0, 169.151]	0.051	[-0.0, 188.016]	0.168
ENSG00000205581	[-0.0, 107.072]	[-0.0, 108.682]	0.015	[-0.0, 108.216]	0.011
ENSG00000023734	[-0.0, 63.777]	[-0.0, 65.249]	0.023	[-0.0, 64.476]	0.011
ENSG00000149428	[-0.0, 58.468]	[-0.0, 75.264]	0.287	[-0.0, 84.724]	0.449
ENSG00000179889	[-0.0, 40.623]	[-0.0, 42.074]	0.036	[-0.0, 41.422]	0.02
ENSG00000204628	[-0.0, 1157.682]	[-0.0, 1157.733]	0.0	[-0.0, 1157.926]	0.0
ENSG00000100568	[47.771, 61.505]	[45.326, 62.156]	0.028	[43.88, 67.474]	0.09
ENSG00000122705	[-0.0, 61.838]	[-0.0, 80.188]	0.297	[-0.0, 89.969]	0.455
ENSG00000011478	[45.341, 68.772]	[45.273, 66.225]	0.023	[44.857, 72.788]	0.039

Table 40: Inter-individual variability intervals for the Noisy genes for Camels at 32° for the top 10 genes. Comparison of observed intervals vs predicted by trained networks. The fractional errors, Error 1 and Error 2, are computed according to formulas (13) and (14).

Gene	Observation	Response Prediction	Error 1	Stability Prediction	Error 2
ENSG00000109654	[-0.0, 4.083]	[0.874, 4.77]	0.382	[-0.0, 6.019]	0.474
ENSG00000065883	[-0.0, 3.747]	[-0.0, 3.768]	0.006	[-0.0, 5.194]	0.386
ENSG00000143776	[-0.0, 3.774]	[-0.0, 3.238]	0.142	[-0.0, 4.661]	0.235
ENSG00000137817	[10.446, 12.86]	[8.884, 12.86]	0.067	[7.552, 14.233]	0.183
ENSG00000125818	[0.149, 3.982]	[-0.0, 3.568]	0.136	[-0.0, 5.137]	0.316
ENSG00000175387	[19.807, 29.375]	[25.45, 30.669]	0.141	[24.034, 32.629]	0.152
ENSG00000110013	[5.446, 10.195]	[5.84, 10.406]	0.039	[4.311, 12.009]	0.188
ENSG00000132604	[24.061, 28.816]	[24.279, 29.794]	0.023	[22.428, 31.705]	0.086
ENSG00000041988	[9.143, 14.735]	[10.495, 14.746]	0.057	[9.21, 16.315]	0.069
ENSG00000100023	[0.0, 2.189]	[-0.0, 2.302]	0.052	[-0.0, 3.379]	0.544

Table 41: Inter-individual variability intervals for the Key-Response genes for Camels at 41° for the top 10 genes. Comparison of observed intervals vs predicted by trained networks. The fractional errors, Error 1 and Error 2, are computed according to formulas (13) and (14).

Gene	Observation	Response Prediction	Error 1	Stability Prediction	Error 2
ENSG00000168710	[70.823, 85.673]	[73.771, 84.688]	0.025	[71.678, 77.537]	0.057
ENSG00000156875	[37.437, 43.681]	[39.589, 42.485]	0.041	[39.486, 41.181]	0.056
ENSG00000110921	[14.585, 21.737]	[19.7, 20.327]	0.18	[19.799, 20.131]	0.188
ENSG00000179163	[74.041, 93.539]	[80.193, 90.545]	0.055	[76.907, 83.382]	0.078
ENSG00000104976	[25.445, 29.776]	[27.518, 28.775]	0.056	[27.501, 28.198]	0.066
ENSG00000120137	[11.298, 14.705]	[12.637, 13.043]	0.115	[12.678, 12.892]	0.123
ENSG00000156535	[30.0, 41.923]	[34.046, 37.924]	0.112	[34.657, 36.848]	0.135
ENSG00000182973	[24.9, 34.438]	[29.353, 30.435]	0.143	[29.206, 29.83]	0.15
ENSG00000198912	[43.092, 47.649]	[44.01, 46.862]	0.019	[44.069, 45.515]	0.034
ENSG00000160803	[25.443, 31.457]	[27.357, 28.587]	0.084	[27.341, 28.015]	0.094

Table 42: Inter-individual variability intervals for the Treatment-Specific genes for Camels at 41° for the top 10 genes. Comparison of observed intervals vs predicted by trained networks. The fractional errors, Error 1 and Error 2, are computed according to formulas (13) and (14).

Gene	Observation	Response Prediction	Error 1	Stability Prediction	Error 2
ENSG00000127922	[-0.0, 162.926]	[122.398, 163.831]	0.757	[95.797, 166.951]	0.613
ENSG00000114850	[-0.0, 148.288]	[27.22, 190.509]	0.468	[25.599, 337.806]	1.451
ENSG00000122705	[-0.0, 58.442]	[22.292, 56.732]	0.411	[5.203, 60.34]	0.122
ENSG00000168883	[-0.0, 21.301]	[10.275, 14.524]	0.801	[9.508, 14.819]	0.751
ENSG00000137710	[-0.0, 43.779]	[-0.0, 28.836]	0.341	[-0.0, 32.468]	0.258
ENSG00000100650	[15.445, 44.225]	[27.732, 34.748]	0.365	[25.906, 37.494]	0.288
ENSG00000087502	[0.607, 34.171]	[6.165, 9.84]	0.859	[5.491, 11.146]	0.803
ENSG00000165410	[-0.0, 19.264]	[4.616, 6.294]	0.913	[3.744, 7.078]	0.827
ENSG00000127415	[28.815, 57.777]	[42.181, 46.376]	0.286	[38.914, 50.334]	0.203
ENSG00000143436	[-0.0, 20.913]	[11.281, 14.486]	0.847	[9.896, 17.035]	0.659

Table 43: Inter-individual variability intervals for the Noisy genes for Camels at 41° for the top 10 genes. Comparison of observed intervals vs predicted by trained networks. The fractional errors, Error 1 and Error 2, are computed according to formulas (13) and (14).

7.7 Strong interactions

We can visualize and compare the strengths of the interactions by graphing the ordered interaction profile for all the DEGs. Explicitly, we compute the interaction for all genes on a fixed jth gene, order them from smallest to largest, and graph these values as a curve. To demonstrate how DEG interaction strengths vary among treatments and species, we plot curves for Key-Response genes for humans and camels at 32°C and 41°C.

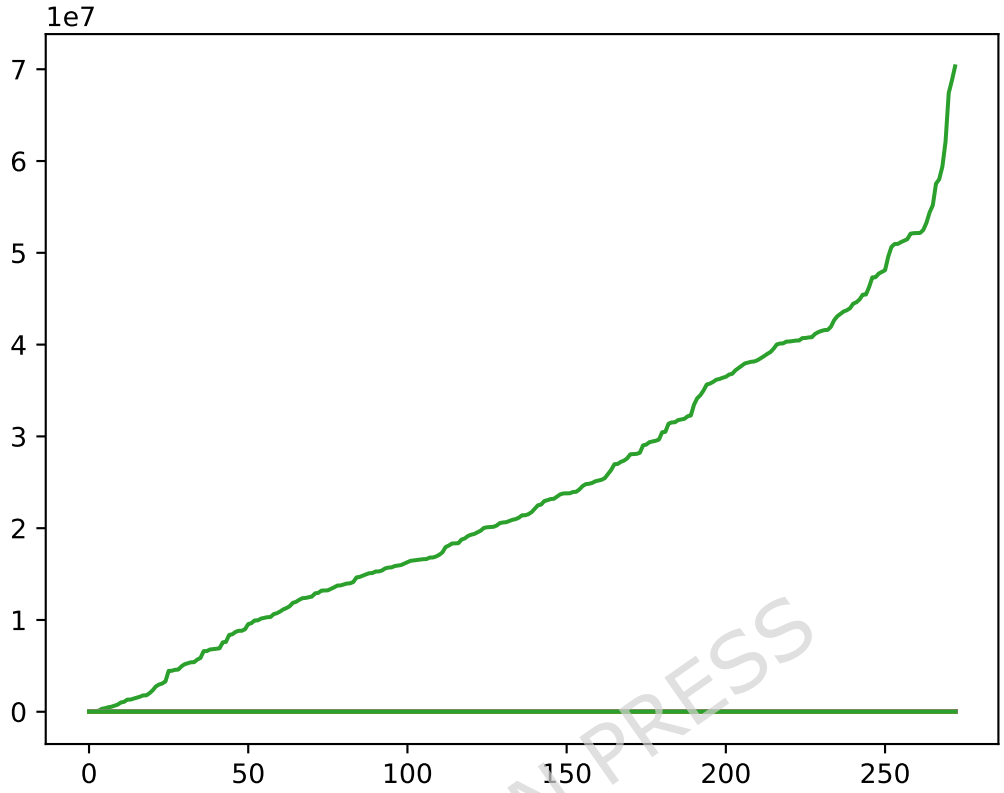

Figure 32: Interaction profiles for Key-Response genes for humans at 32°. Each profile has been sorted. The x axis denotes the rank of the interaction. The y axis denotes the relative strength of the interaction.

At this scale only two groups of profiles are distinguishable for humans at 32°. We present below the strongest pairs of interacting genes.

ENSG00000204138	ENSG00000104728
ENSG00000152620	"ENSG00000104728
ENSG00000188277	ENSG00000104728
ENSG00000099822	ENSG00000104728
ENSG00000165312	ENSG00000104728
ENSG00000185220	ENSG00000104728
ENSG00000135945	ENSG00000104728
ENSG00000124523	ENSG00000104728
ENSG00000211454	ENSG00000164944
ENSG00000104728	ENSG00000104728

Table 44: Top 10 interaction pairs among Key-Response genes for humans at 32°.

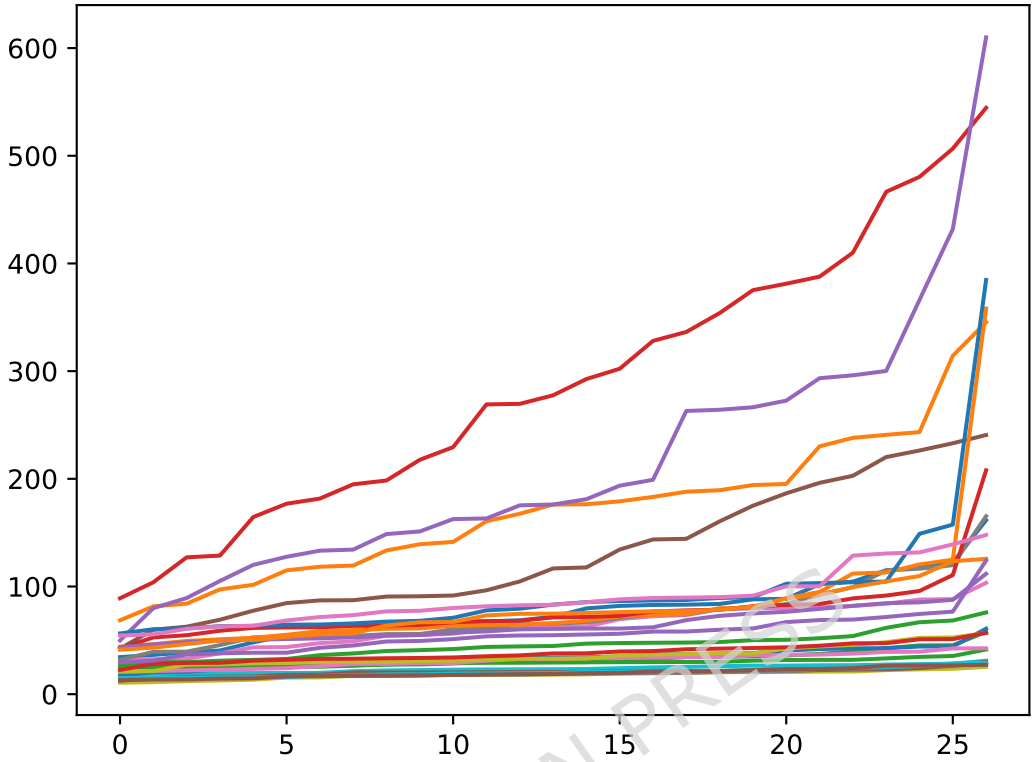

Figure 33: Interaction profiles for Treatment-Specific genes for humans at 32°. Each profile has been sorted. The x axis denotes the rank of the interaction. The y axis denotes the relative strength of the interaction.

ENSG00000138801	ENSG00000052802
ENSG00000117614	ENSG00000117614
ENSG00000099949	ENSG00000052802
ENSG00000177868	ENSG00000052802
ENSG00000127948	ENSG00000134108
ENSG00000075420	ENSG00000117614
ENSG00000119048	ENSG00000052802
ENSG00000134108	ENSG00000052802
ENSG00000133104	ENSG00000052802
"ENSG00000241839	ENSG00000154803

Table 45: Top 10 interaction pairs among Treatment-Specific genes for humans at 32°.

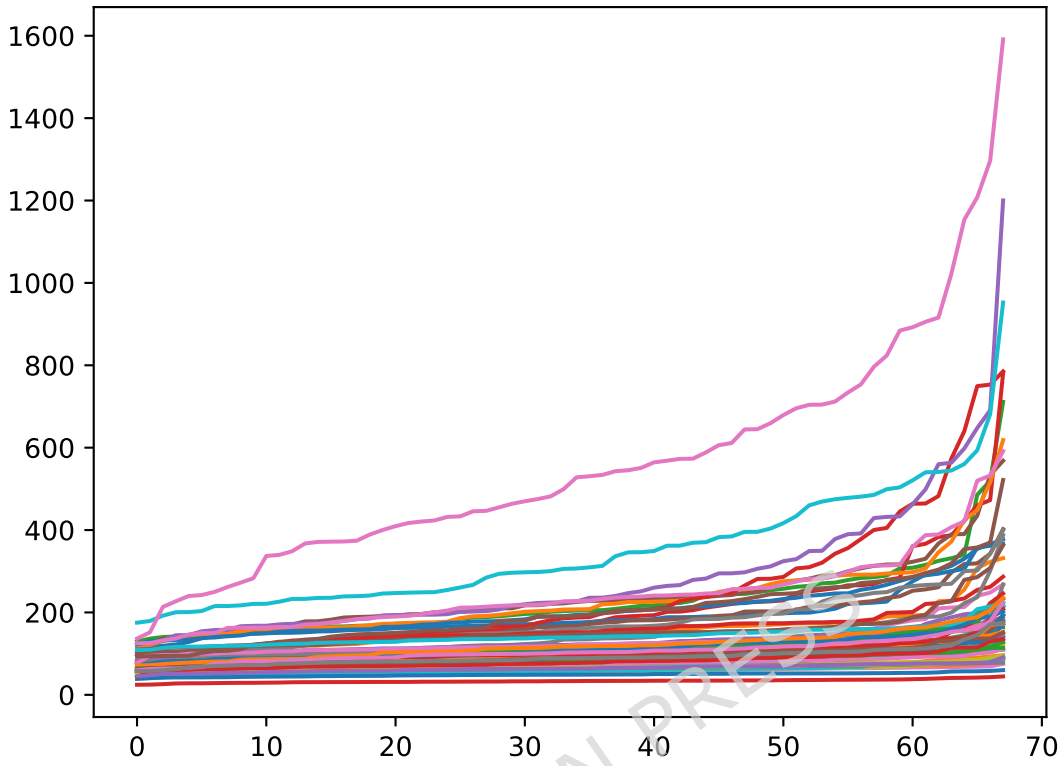

Figure 34: Interaction profiles for Noisy genes for humans at 32°. Each profile has been sorted. The x axis denotes the rank of the interaction. The y axis denotes the relative strength of the interaction.

ENSG00000100029	ENSG00000100029
ENSG00000187678	ENSG00000109111
ENSG00000168002	ENSG00000100029
ENSG00000130304	ENSG00000168002
ENSG00000011007	ENSG00000109111
ENSG00000109220	ENSG00000109111
ENSG00000184557	ENSG00000109111
ENSG00000109111	ENSG00000168002
ENSG00000227057	ENSG00000109111
ENSG00000150760	ENSG00000100029

Table 46: Top 10 interaction pairs among Noisy genes for humans at 32°.

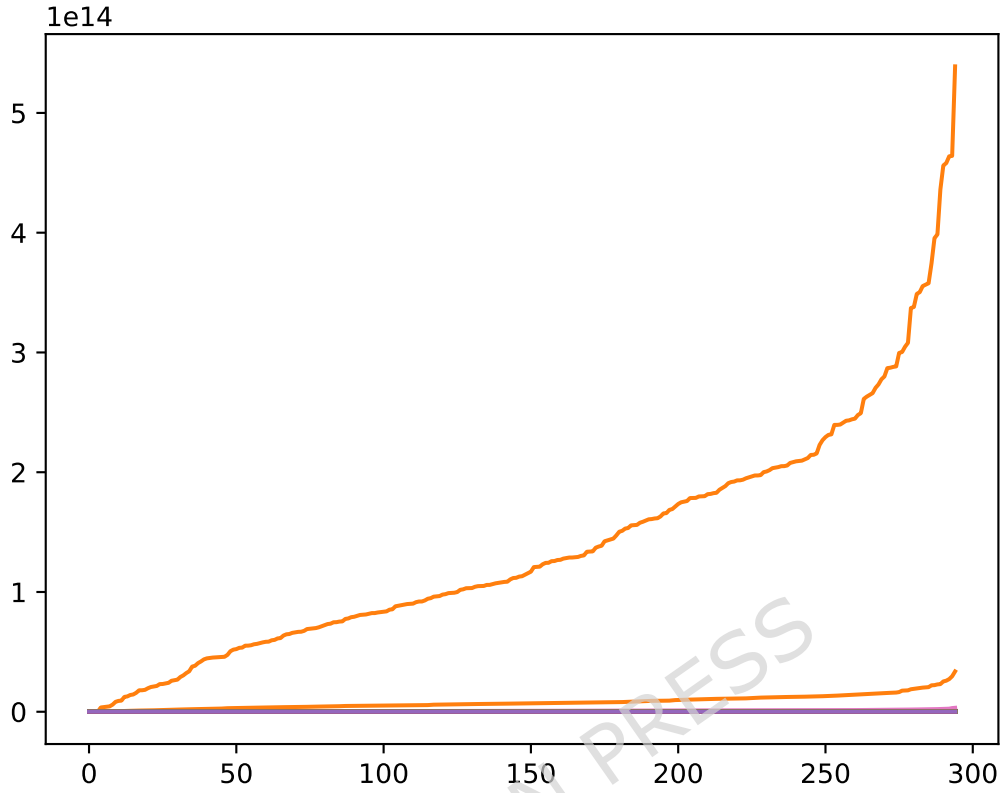

Figure 35: Interaction profiles for Key-Response genes for humans at 41°. Each profile has been sorted. The x axis denotes the rank of the interaction. The y axis denotes the relative strength of the interaction.

ENSG00000078403"	"ENSG00000136451
"ENSG00000127870"	"ENSG00000127870"
"ENSG00000100426"	"ENSG00000127870"
"ENSG00000204228"	"ENSG00000127870"
"ENSG00000181915"	"ENSG00000127870"
"ENSG00000198794"	"ENSG00000127870"
"ENSG00000167625"	"ENSG00000127870"
"ENSG00000165312"	"ENSG00000127870"
"ENSG00000126705"	"ENSG00000136451"
"ENSG00000221995"	"ENSG00000136451"

Table 47: Top 10 interaction pairs among Key-Response genes for humans at 41°.

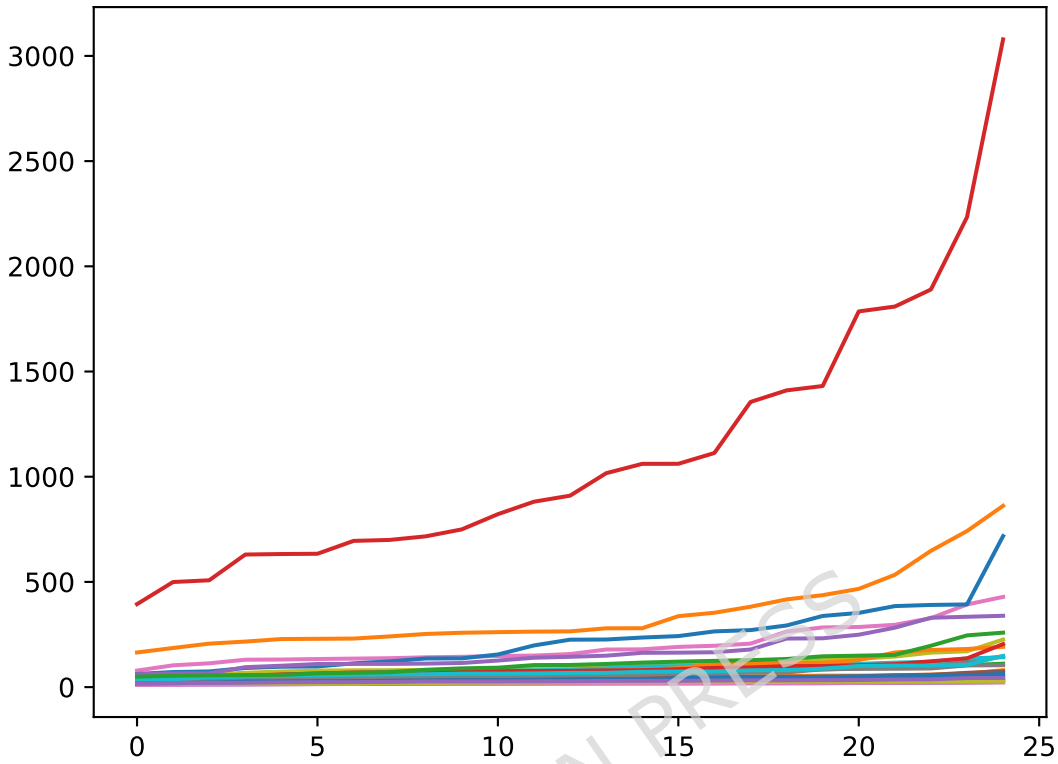

Figure 36: Interaction profiles for Treatment-Specific genes for humans at 41°. Each profile has been sorted. The x axis denotes the rank of the interaction. The y axis denotes the relative strength of the interaction.

ENSG00000117298	ENSG00000117298
ENSG00000178913	ENSG00000117298
ENSG00000159461	ENSG00000117298
ENSG00000090487	ENSG00000090487
ENSG00000117448	ENSG00000121769
ENSG00000119986	ENSG00000117298
ENSG00000126767	ENSG00000117298
ENSG00000103249	ENSG00000117298
ENSG00000083099	ENSG00000178913
ENSG00000141447	ENSG00000117298

Table 48: Top 10 interaction pairs among Treatment-Specific genes for humans at 41°.

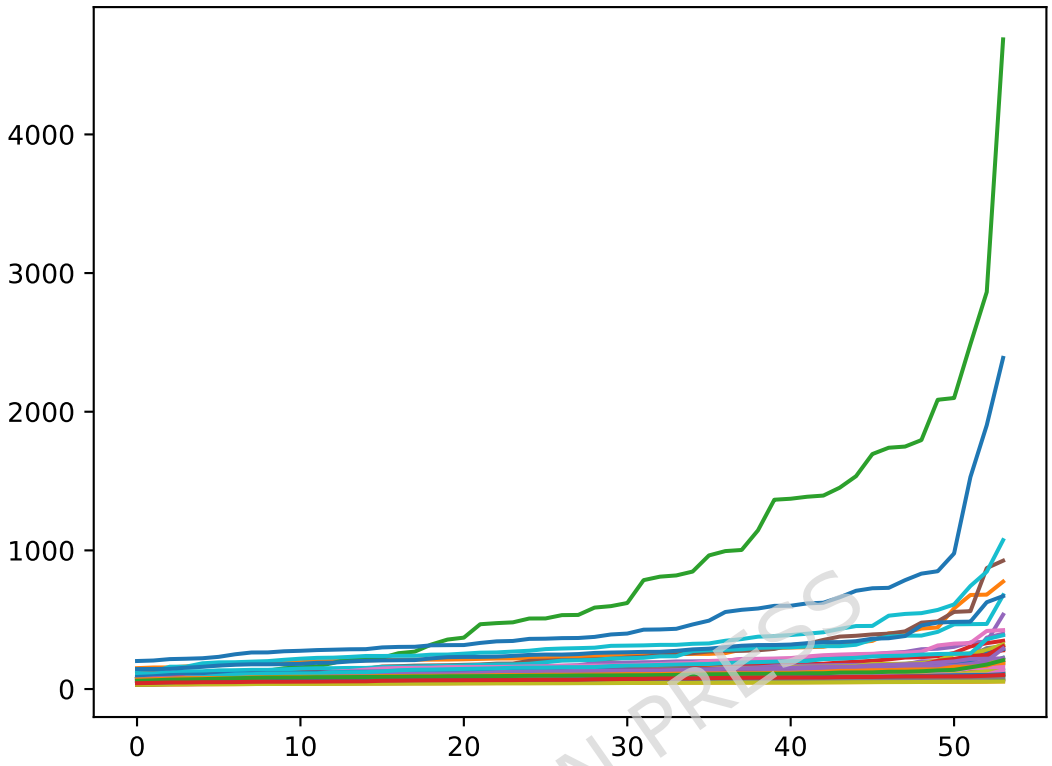

Figure 37: Interaction profiles for Noisy genes for humans at 41°. Each profile has been sorted. The x axis denotes the rank of the interaction. The y axis denotes the relative strength of the interaction.

ENSG00000175387	ENSG00000182180
ENSG00000100029	ENSG00000120963
ENSG00000163320	ENSG00000168002
ENSG00000116685	ENSG00000100029
ENSG00000116685	ENSG00000100029
ENSG00000154545	ENSG00000182180
ENSG00000168002	ENSG00000168002
ENSG00000182872	ENSG00000100029
ENSG00000163512	ENSG00000163320
ENSG00000147852	ENSG00000120963

Table 49: Top 10 interaction pairs among Noisy genes for humans at 41°.

In the case of Camels the pictures are considerably different, and there is more spread in the profiles.

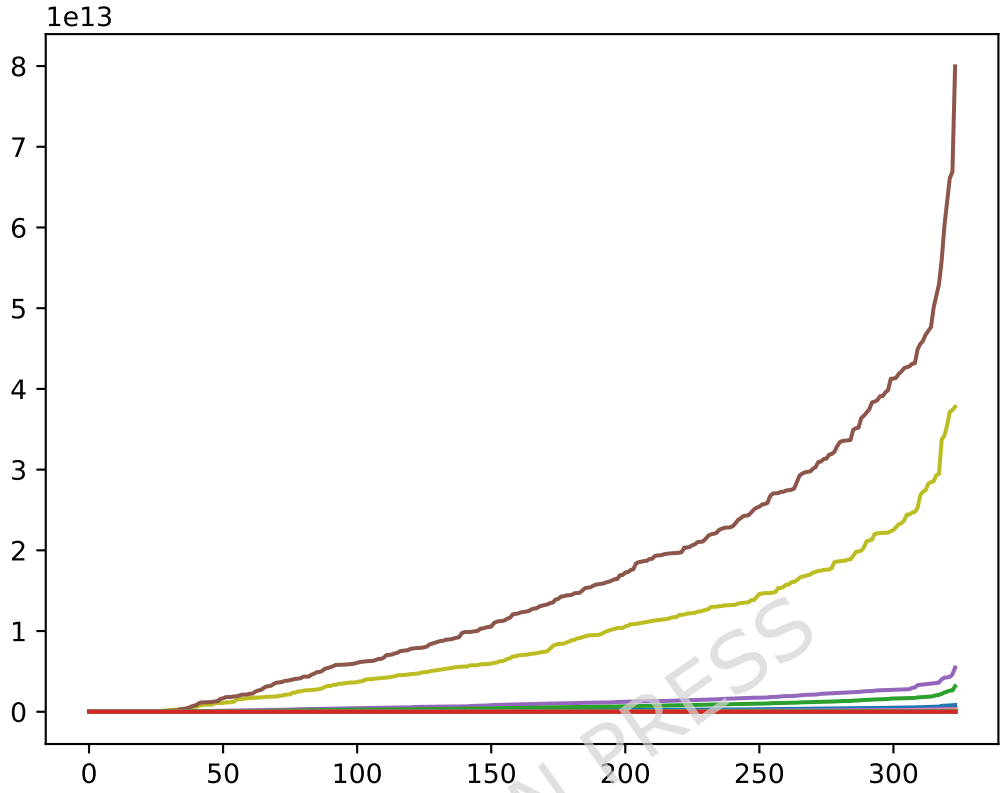

Figure 38: Interaction profiles for Key-Response genes for Camels at 32°. Each profile has been sorted and the x axis denotes the rank of the interaction. The y axis denotes the relative strength of the interaction.

"ENSG00000151151"	"ENSG00000100151"
"ENSG00000182224"	"ENSG00000167202"
"ENSG00000196155"	"ENSG00000100151"
"ENSG00000170502"	"ENSG00000100151"
"ENSG00000109686"	"ENSG00000167202"
"ENSG00000138231"	"ENSG00000100151"
"ENSG00000145331"	"ENSG00000167202"
"ENSG00000105323"	"ENSG00000100151"
"ENSG00000121481"	"ENSG00000100151"
"ENSG00000048028"	"ENSG00000167202"

Table 50: Top 10 interaction pairs among Key-Response genes for camels at 32°.

In the case of Camels the pictures are considerably different, and there is more spread in the profiles.

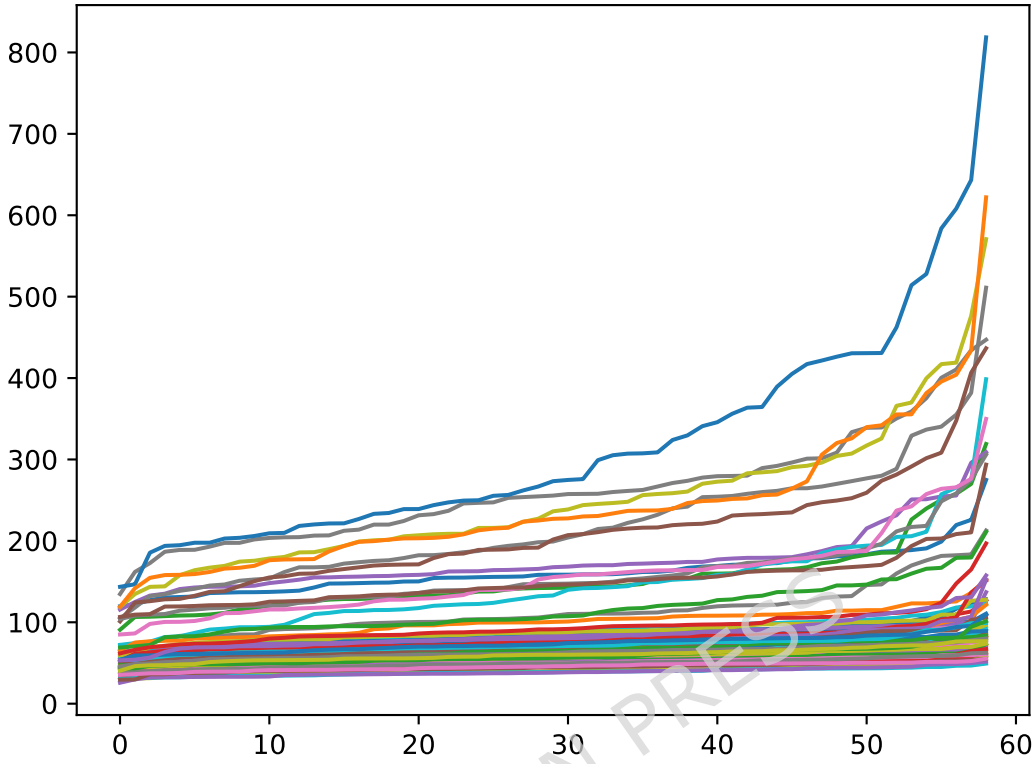

Figure 39: Interaction profiles for Treatment-Specific genes for Camels at 32°. Each profile has been sorted and the x axis denotes the rank of the interaction. The y axis denotes the relative strength of the interaction.

ENSG00000134330	ENSG00000118816
ENSG00000100811	ENSG00000118816
ENSG00000135441	ENSG00000118816
ENSG00000147471	ENSG00000118816
ENSG00000239789	ENSG00000118816
ENSG00000060971	ENSG00000118816
ENSG00000285025	ENSG00000118816
ENSG00000125734	ENSG00000118816
ENSG00000100403	ENSG00000048828
ENSG00000048828	ENSG00000118816

Table 51: Top 10 interaction pairs among Treatment-Specific genes for camels at 32°.

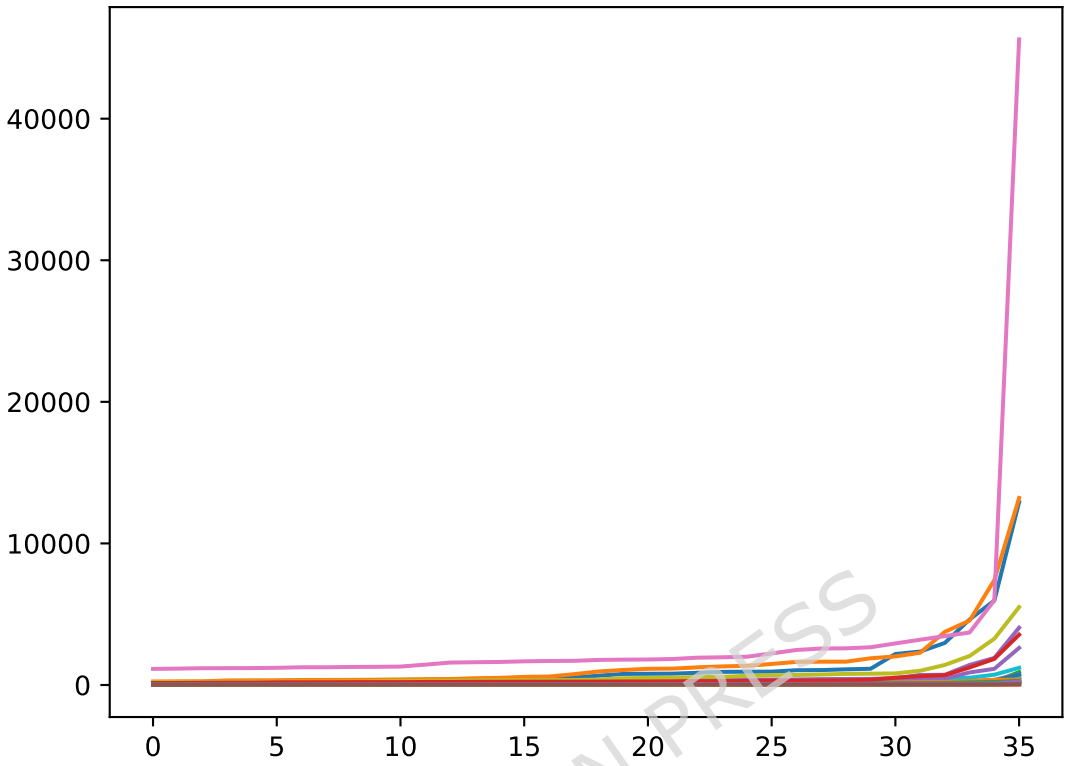

Figure 40: Interaction profiles for Noisy genes for Camels at 32°. Each profile has been sorted and the x axis denotes the rank of the interaction. The y axis denotes the relative strength of the interaction.

ENSG00000204628	ENSG00000204628
ENSG00000127922	ENSG00000205581
ENSG00000060762	ENSG00000205581
ENSG00000122705	ENSG00000205581
ENSG00000149428	ENSG00000205581
ENSG00000165410	ENSG00000205581
ENSG00000170445	ENSG00000205581
ENSG00000011478	ENSG00000205581
ENSG00000205581	ENSG00000204628
ENSG00000100568	ENSG00000205581

Table 52: Top 10 interaction pairs among Noisy genes for camels at 32°.

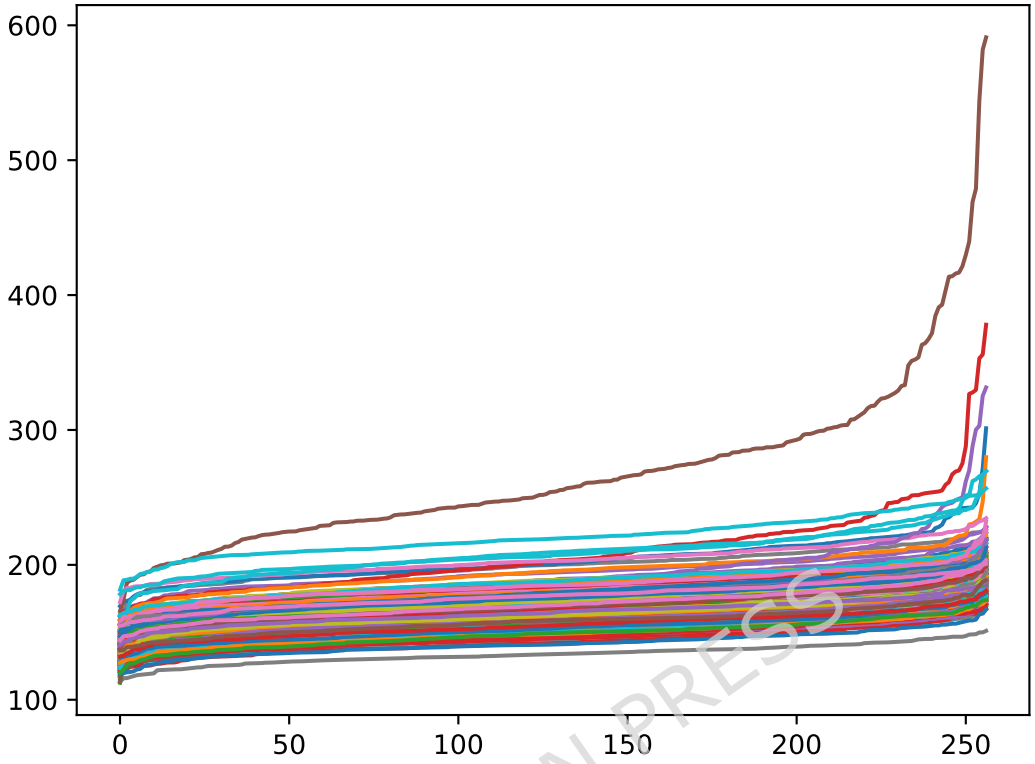

Figure 41: Interaction profiles for Key-Response genes for Camels at 41°. Each profile has been sorted and the x axis denotes the rank of the interaction. The y axis denotes the relative strength of the interaction.

"ENSG00000164190"	"ENSG00000086232"
"ENSG00000164291"	"ENSG00000134882"
"ENSG00000106089"	"ENSG00000134882"
"ENSG00000100151"	"ENSG00000134882"
"ENSG00000142733"	"ENSG00000134882"
"ENSG00000197024"	"ENSG00000134882"
"ENSG00000086232"	"ENSG00000164920"
"ENSG00000134882"	"ENSG00000134882"
"ENSG00000033011"	"ENSG00000099875"
"ENSG00000136159"	"ENSG00000255072"

Table 53: Top 10 interaction pairs among Response genes for camels at 41°.

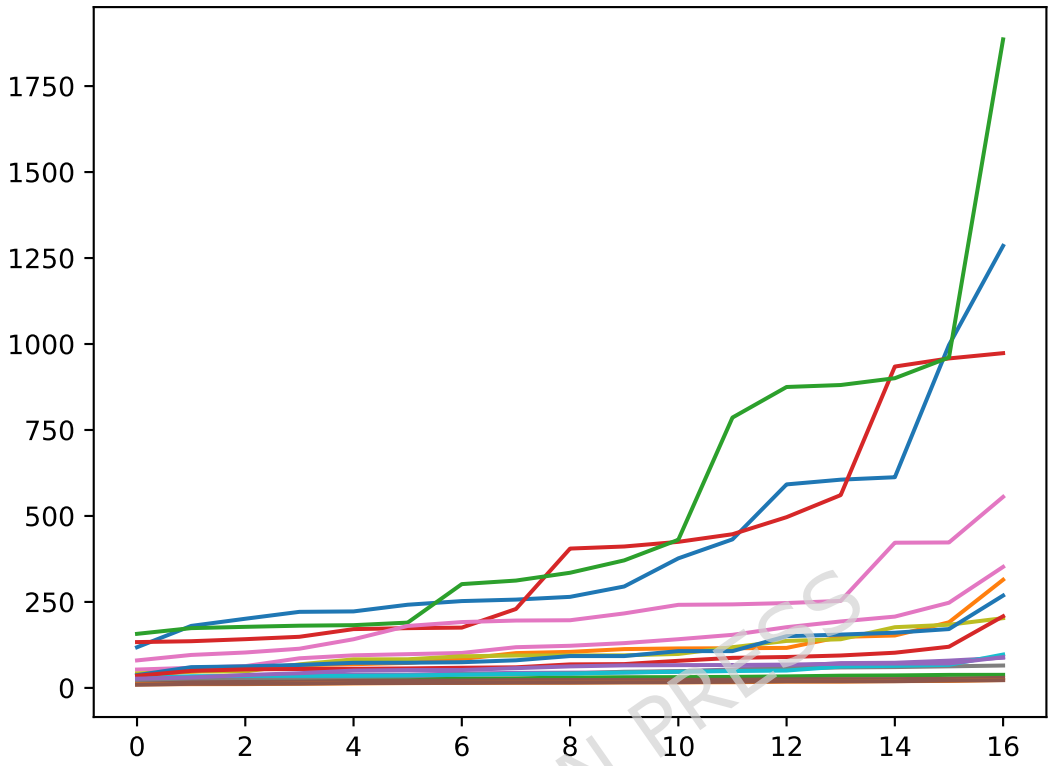

Figure 42: Interaction profiles for Treatment-Specific genes for Camels at 41°. Each profile has been sorted and the x axis denotes the rank of the interaction. The y axis denotes the relative strength of the interaction.

ENSG00000101152	ENSG00000168710
ENSG00000168710	ENSG00000101152
ENSG00000179163	ENSG00000179163
ENSG00000084652	ENSG00000101152
ENSG00000156535	ENSG00000168710
ENSG00000156875	ENSG00000101152
ENSG00000101473	ENSG00000168710
ENSG00000168303	ENSG00000101152
ENSG00000198912	ENSG00000101152
ENSG00000160803	ENSG00000101152

Table 54: Top 10 interaction pairs among Treatment-Specific genes for camels at 41°.

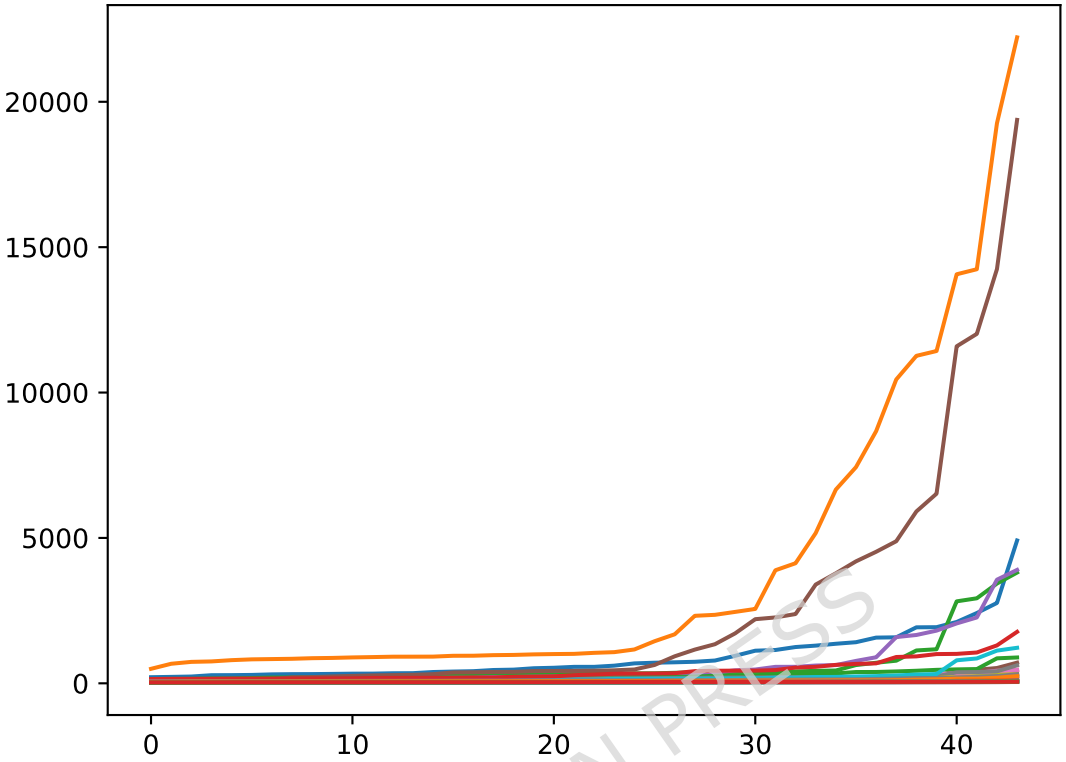

Figure 43: Interaction profiles for Noisy genes for Camels at 41°. Each profile has been sorted and the x axis denotes the rank of the interaction. The y axis denotes the relative strength of the interaction.

ENSG00000114850	ENSG00000146278
ENSG00000265972	ENSG00000146278
ENSG00000127922	ENSG00000100650
ENSG00000137710	ENSG00000146278
ENSG00000122705	ENSG00000100650
ENSG00000100568	ENSG00000100568
ENSG00000141295	ENSG00000100650
ENSG00000227057	ENSG00000146278
ENSG00000100650	ENSG00000100650
ENSG00000146278	ENSG00000100650

Table 55: Top 10 interaction pairs among Noisy genes for camels at 41°.

7.8 Network Entropy

	G1	G2	G4
Humans	0.621	-8.528	1.082
Camels	-4912.596	1.247	-0.382

Table 56: Network entropy for humans and camels at 32°.

	G1	G2	G4
Humans	-20514.161	-20.082	0.348
Camels	1.558	-35.239	-5.492

Table 57: Network entropy for humans and camels at 41°.

References

[1] Á. Bartha and B. Győrffy. Tnmplot. com: a web tool for the comparison of gene expression in normal, tumor and metastatic tissues. *International journal of molecular sciences*, 22(5):2622, 2021.

[2] L. Benet and D. P. Sanders. Intervalarithmetic.jl. `https://github.com/JuliaIntervals/IntervalArithmetic.jl`, 2022.

[3] A. M. Bolger, M. Lohse, and B. Usadel. Trimmomatic: a flexible trimmer for illumina sequence data. *Bioinformatics*, 30(15):2114–2120, 2014.

[4] A. P. Bustamante, A. Celletti, and C. Lhotka. Breakdown of rotational tori in 2d and 4d conservative and dissipative standard maps. *Physica D: Nonlinear Phenomena*, 453:133790, 2023.

[5] A. Celletti and L. Chierchia. Kam tori for n-body problems: a brief history. In *Periodic, Quasi-Periodic and Chaotic Motions in Celestial Mechanics: Theory and Applications: Selected papers from the Fourth Meeting on Celestial Mechanics, CELMEC IV San Martino al Cimino (Italy), 11–16 September 2005*, pages 117–139. Springer, 2006.

[6] G. Cybenko. Approximation by superpositions of a sigmoidal function. *Mathematics of control, signals and systems*, 2(4):303–314, 1989.

[7] J. Da-Anoy, N. Posadas, and C. Conaco. Interspecies differences in the transcriptome response of corals to acute heat stress. *PeerJ*, 12:e18627, 2024.

[8] B. A. Frishman, J. L. Gonzalez, and V. E. Forbes. A context-specific, literature-supported framework for validating stress response models in mammals. *bioRxiv*, pages 2025–12, 2025.

[9] J. Gonzalez. bio_nnets.jl. `https://github.com/joluigonza/bio\_nnets`, 2025.

[10] J. Huang, X. Zhao, and J. Chory. The arabidopsis transcriptome responds specifically and dynamically to high light stress. *Cell reports*, 29(12):4186–4199, 2019.

[11] D. Kim, J. Paggi, D. Park, C. Bennett, and S. Salzberg. hisat2, 2021.

[12] B. M. Kirilenko, C. Munegowda, E. Osipova, D. Jebb, V. Sharma, M. Blumer, A. E. Morales, A.-W. Ahmed, D.-G. Kontopoulos, L. Hilgers, et al. Integrating gene annotation with orthology inference at scale. *Science*, 380(6643):eabn3107, 2023.

[13] W. Pan. A comparative review of statistical methods for discovering differentially expressed genes in replicated microarray experiments. *Bioinformatics*, 18(4):546–554, 2002.

[14] M. Pertea, G. M. Pertea, C. M. Antonescu, T.-C. Chang, J. T. Mendell, and S. L. Salzberg. Stringtie enables improved reconstruction of a transcriptome from rna-seq reads. *Nature biotechnology*, 33(3):290–295, 2015.

[15] P. D. Price, D. H. Palmer Droguett, J. A. Taylor, D. W. Kim, E. S. Place, T. F. Rogers, J. E. Mank, C. R. Cooney, and A. E. Wright. Detecting signatures of selection on gene expression. *Nature Ecology & Evolution*, 6(7):1035–1045, 2022.

[16] M. E. Ritchie, B. Phipson, D. Wu, Y. Hu, C. W. Law, W. Shi, and G. K. Smyth. limma powers differential expression analyses for rna-sequencing and microarray studies. *Nucleic acids research*, 43(7):e47–e47, 2015.

[17] Y. D. Shaul, B. Yuan, P. Thiru, A. Nutter-Upham, S. McCallum, C. Lanzkron, G. W. Bell, and D. M. Sabatini. Merav: a tool for comparing gene expression across human tissues and cell types. *Nucleic acids research*, 44(D1):D560–D566, 2016.

[18] S. W. Wingett and S. Andrews. Fastq screen: A tool for multi-genome mapping and quality control. *F1000Research*, 7:1338, 2018.

[19] L. Yang, S. Wang, M. Zhou, X. Chen, Y. Zuo, D. Sun, and Y. Lv. Comparative analysis of housekeeping and tissue-selective genes in human based on network topologies and biological properties. *Molecular genetics and genomics*, 291:1227–1241, 2016.

[20] Y. Yang, G. Li, Y. Zhong, Q. Xu, B.-J. Chen, Y.-T. Lin, R. S. Chapkin, and J. J. Cai. Gene knockout inference with variational graph autoencoder learning single-cell gene regulatory networks. *Nucleic Acids Research*, 51(13):6578–6592, 2023.

[21] L. Yu, J. Zhang, G. Brock, and S. Fernandez. Fully moderated t-statistic in linear modeling of mixed effects for differential expression analysis. *BMC bioinformatics*, 20:1–9, 2019.

[22] J. Zhu, F. He, S. Hu, and J. Yu. On the nature of human housekeeping genes. *Trends in genetics*, 24(10):481–484, 2008.